arXiv:1803.10178v1 [hep-ex] 27 Mar 2018

EUROPEAN ORGANISATION FOR NUCLEAR RESEARCH (CERN)

Submitted to: PRD

CERN-EP-2018-024
July 2, 2022

Search for top squarks decaying to tau sleptons in pp collisions at $\sqrt{s} = 13$ TeV with the ATLAS detector

The ATLAS Collaboration

A search for direct pair production of top squarks in final states with two tau leptons, b-jets, and missing transverse momentum is presented. The analysis is based on proton–proton collision data at $\sqrt{s} = 13$ TeV corresponding to an integrated luminosity of 36.1 fb^{-1} recorded with the ATLAS detector at the Large Hadron Collider in 2015 and 2016. Two exclusive channels with either two hadronically decaying tau leptons or one hadronically and one leptonically decaying tau lepton are considered. No significant deviation from the Standard Model predictions is observed in the data. The analysis results are interpreted in terms of model-independent limits and used to derive exclusion limits on the masses of the top squark $\tilde{t}_1$ and the tau slepton $\tilde{\tau}_1$ in a simplified model of supersymmetry with a nearly massless gravitino. In this model, masses up to $m(\tilde{t}_1) = 1.16$ TeV and $m(\tilde{\tau}_1) = 1.00$ TeV are excluded at 95% confidence level.

© 2022 CERN for the benefit of the ATLAS Collaboration.
Reproduction of this article or parts of it is allowed as specified in the CC-BY-4.0 license.

Contents

1 Introduction **2**

2 ATLAS detector **4**

3 Dataset and simulation **4**

4 Event reconstruction **6**
4.1 Analysis variables 7

5 Event selection **8**
5.1 Preselection 8
5.2 Signal selections 9

6 Background estimation **9**
6.1 Lep-had channel 10
6.2 Had-had channel 13
6.3 Common control regions 14

7 Systematic uncertainties **17**

8 Results **19**
8.1 Interpretation 21

9 Conclusion **24**

1 Introduction

Supersymmetry (SUSY) [1–6] (see Ref. [7] for a review) extends the Standard Model (SM) with an additional symmetry that connects bosons and fermions, thereby providing answers to several of the open questions in the SM. It predicts the existence of new particles that have the same mass and quantum numbers as their SM partners but differ in spin by one half-unit. Since no such particles have yet been observed, SUSY, if realized in nature, must be a broken symmetry, allowing the supersymmetric partner particles to have higher masses than their SM counterparts. In the model considered in this work, the conservation of R-parity is assumed [8], so that the supersymmetric particles (sparticles) are produced in pairs, and the lightest supersymmetric particle (LSP) is stable, providing a viable candidate for dark matter.

This article describes a search for SUSY in a benchmark scenario motivated by gauge-mediated SUSY breaking [9–11] and natural gauge mediation [12]. In this scenario, only three sparticles are assumed to be sufficiently light to be relevant for phenomenology at the Large Hadron Collider (LHC): the lightest scalar partner of the top quark (top squark, $\tilde{t}_1$), the lightest scalar partner of the tau lepton (tau slepton, $\tilde{\tau}_1$), and a nearly massless gravitino $\tilde{G}$.

The search strategy is optimized using a simplified model [13, 14] with this limited sparticle content. The relevant parameters are the sfermion masses $m(\tilde{t}_1)$ and $m(\tilde{\tau}_1)$. The process is illustrated in Figure 1. The top squark is assumed to be light [15, 16] and directly pair-produced through the strong interaction. Each

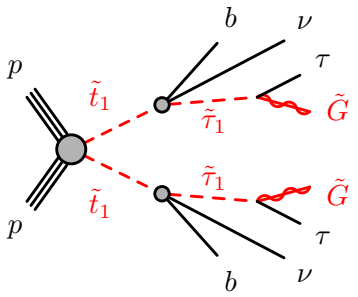

Figure 1: The simplified model for production and decay of supersymmetric particles considered in this analysis. The branching ratios are assumed to be 100% in the decay mode shown, both for the decay of the top squark as well as for the decay of the tau slepton. All sparticles not appearing in this diagram are assumed to be too massive to be relevant for LHC phenomenology. The top-squark decay vertex is drawn as a blob to indicate that the three-body decay is assumed to happen through an off-shell chargino.

top squark decays to a b-quark, a tau neutrino, and a tau slepton which in turn decays to a tau lepton and a gravitino. The branching ratios for these decays are set to 100%, and the decays are assumed to be prompt. The tau-slepton mixing matrix is chosen such that the tau slepton is an equal mix of the superpartners of the left- and the right-handed tau lepton. Alternative scenarios with a neutralino $\tilde{\chi}_1^0$ as the LSP, which would suggest a high branching ratio of direct decays $\tilde{t}_1 \to t\tilde{\chi}_1^0$, have been studied elsewhere [17–21].

The search uses proton–proton (pp) collision data collected with the ATLAS detector at a center-of-mass energy of $\sqrt{s} = 13$ TeV in 2015 and 2016, with a combined integrated luminosity of 36.1 fb^{-1}. A previous analysis considering the same three-body decay mode of the top squark to the tau slepton based on 20 fb^{-1} of ATLAS data at $\sqrt{s} = 8$ TeV set lower limits on the mass of the top squark $\tilde{t}_1$ of up to 650 GeV [22]. The combined LEP lower limit on the mass of the tau slepton, derived from searches for $\tilde{\tau} \to \tau\tilde{\chi}_1^0$ decays and assuming the unification of gaugino masses, ranges between 87 GeV and 96 GeV depending on the assumed mass of the lightest neutralino [23]. Models with small mass differences between the tau slepton and the lightest neutralino of up to approximately 10 GeV are not excluded by the LEP experiments. For a branching ratio $\tilde{\tau} \to \tau\tilde{\chi}_1^0$ of 100% and a massless $\tilde{\chi}_1^0$, the lower limit on the tau-slepton mass is around 90 GeV. The limits published by the LHC experiments [24, 25] obtained from models with direct production of tau sleptons are not more stringent than those provided by LEP.

Final states with two tau leptons can be classified into one of three channels, depending on the decay modes of the tau leptons. If both tau leptons decay hadronically, events belong to the "had-had" channel. The "lep-had" channel refers to events in which one of the tau leptons decays leptonically and the other hadronically. Final states where both tau leptons decay leptonically have the smallest branching ratio and are not considered, as studies showed that they would not contribute significantly to the sensitivity of the analysis.

This article is structured as follows. Section 2 gives a brief description of the ATLAS detector. Section 3 describes the recorded and simulated events used in the analysis, while Section 4 summarizes the reconstruction of physics objects such as leptons and jets and the kinematic variables used in the event selection. In Section 5, the selection used to obtain a signal-enriched event sample is described. The background determination is described in Section 6, followed by a discussion of the methods used to derive the corresponding systematic uncertainties in Section 7. Section 8 presents the analysis results and their interpretation. The article concludes with a brief summary in Section 9.

2 ATLAS detector

The ATLAS detector [26] is a multipurpose particle detector with a forward–backward symmetric cylindrical geometry and nearly 4π coverage in solid angle. [1] It consists of, starting from the interaction point and moving outwards, an inner tracking detector, electromagnetic and hadronic calorimeters, and a muon spectrometer. The inner tracking detector covers the pseudorapidity range $|\eta| < 2.5$ and consists of silicon pixel, silicon microstrip, and transition radiation detectors, immersed in a 2 T axial magnetic field provided by a thin superconducting solenoid. The insertable B-layer, the innermost layer of the silicon pixel detector, was added before the $\sqrt{s} = 13$ TeV data-taking and provides high-resolution hits to improve the tracking and b-tagging performance [27, 28]. The calorimeter system covers pseudorapidities $|\eta| < 4.9$. Electromagnetic energy measurements with high granularity are provided by lead/liquid-argon sampling calorimeters in the region $|\eta| < 3.2$. Hadronic calorimetry is provided by sampling calorimeters with scintillator tiles and steel absorbers within $|\eta| < 1.7$ and with copper/liquid-argon for $1.5 < |\eta| < 3.2$. The forward regions are instrumented with sampling calorimeters using liquid-argon as the active medium for both the electromagnetic and hadronic calorimetry. The muon spectrometer features three large superconducting toroid magnets with eight coils each, precision-tracking detectors in the region $|\eta| < 2.7$, and fast, dedicated chambers for triggering in the region $|\eta| < 2.4$. Collision events are selected for recording by a two-stage trigger system, which has been upgraded for the run at $\sqrt{s} = 13$ TeV [29]. It consists of a hardware-based trigger as the first level, followed by the software-based high-level trigger, which is able to run reconstruction and calibration algorithms similar to those used offline, reducing the event rate to about 1 kHz.

3 Dataset and simulation

The dataset analyzed in this article was recorded with the ATLAS detector from pp collisions delivered by the Large Hadron Collider at CERN in 2015 and 2016 at a center-of-mass energy of $\sqrt{s} = 13$ TeV [30]. Collision events are selected with triggers on electrons or muons in the lep-had channel, and missing transverse momentum or two hadronic tau leptons in the had-had channel. The total integrated luminosity of the dataset after the application of data-quality requirements that ensure that all subdetectors are functioning normally is 36.1 fb^{-1} with an uncertainty of 3.2%. The uncertainty was derived, following a methodology similar to that detailed in Ref. [31], from a preliminary calibration of the luminosity scale using x–y beam-separation scans performed in August 2015 and May 2016.

Monte Carlo (MC) simulation was used to generate samples of collision events, which model the expected kinematics of the supersymmetric signal and allow the prediction of the contributions from the various SM background processes. The MC generators, parton distribution function (PDF) sets and parameters used to simulate the Standard Model background processes and the supersymmetric signal process of the simplified model are summarized in Table 1. Additional MC samples are used to estimate systematic uncertainties, as described in Section 7. Data-driven methods are used to augment the accuracy of the simulation-based estimates for the major background processes (cf. Section 6).

[1] ATLAS uses a right-handed coordinate system with its origin at the nominal interaction point (IP) in the center of the detector and the z-axis along the beam pipe. The x-axis points from the IP to the center of the LHC ring, and the y-axis points upward. Cylindrical coordinates (r, ϕ) are used in the transverse plane, ϕ being the azimuthal angle around the z-axis. The pseudorapidity is defined in terms of the polar angle θ as $\eta = -\ln\tan(\theta/2)$. When the mass of a particle cannot be neglected, the rapidity $y = 0.5 \ln[(E + p_z)/(E - p_z)]$ is used instead of the pseudorapidity η to specify its direction.

Process	Matrix element	PDF set	Parton shower	PDF set	Tune
$t\bar{t}$	Powheg-Box v2	CT10	Pythia 6.428	CTEQ6L1	Perugia 2012
Single-top	Powheg-Box v1	CT10	Pythia 6.428	CTEQ6L1	Perugia 2012
$t\bar{t}H$	MG5aMC 2.2.2	CT10	Herwig++ 2.7.1	CTEQ6L1	UE-EE-5
$t\bar{t}V$	MG5aMC 2.3.3	NNPDF3.0 NLO	Pythia 8.210	NNPDF2.3 LO	A14
tWZ	MG5aMC 2.3.2	NNPDF3.0 NLO	Pythia 8.210	NNPDF2.3 LO	A14
tZ	MG5aMC 2.2.1	CTEQ6L1	Pythia 6.428	CTEQ6L1	Perugia 2012
Multi-top	MG5aMC 2.2.2	NNPDF2.3 LO	Pythia 8.186	NNPDF2.3 LO	A14
V + jets	Sherpa 2.2.1	NNPDF3.0 NNLO			
VV (1)	Sherpa 2.2.1	NNPDF3.0 NNLO			
VV (2)	Sherpa 2.1.1	CT10			
VVV	Sherpa 2.2.2	NNPDF3.0 NNLO			
SUSY	MG5aMC 2.2.3 and 2.3.3	NNPDF2.3 LO	Pythia 8.186, 8.205 or 8.210	NNPDF2.3 LO	A14

Table 1: Overview of the simulation codes, parton distribution function (PDF) sets and parameters used to simulate the Standard Model background processes and the supersymmetric signal process. MadGraph5_aMC@NLO is abbreviated as MG5aMC. Corresponding references are given in the text.

Signal samples were generated from leading-order (LO) matrix elements (ME) with MadGraph5-aMC@NLO v2.2.3 and v2.3.3 [32] interfaced to Pythia 8.186, 8.205 or 8.210 [33, 34] with the ATLAS 2014 (A14) [35] set of tuned parameters (tune) for the modeling of the parton showering (PS), hadronization and underlying event. The matrix element calculation was performed at tree level and includes the emission of up to two additional partons. The PDF set used for the generation was NNPDF2.3 LO [36]. The ME–PS matching was done using the CKKW-L [37] prescription, with the matching scale set to one quarter of the top-squark mass. Signal cross sections were calculated to next-to-leading order (NLO) in the strong coupling constant, adding the resummation of soft gluon emission at next-to-leading logarithmic accuracy [38–40].

Production of top-quark pairs and of single top quarks in the s- and t-channel or associated with W bosons was simulated at NLO with Powheg-Box [41–45] interfaced to Pythia 6.428 [46] for the parton shower, hadronization, and underlying event, using the CT10 PDF set [47] in the matrix element calculations and the CTEQ6L1 PDF set [48] with the Perugia 2012 tune [49] for the parton shower and underlying event. Associated production of top-quark pairs and Higgs bosons was simulated at NLO with MadGraph5_aMC@NLO [32] interfaced to Herwig++ 2 [50, 51], using the UE-EE-5 tune [52]. For $t\bar{t}+V$, where V is a W or Z boson, and tWZ production at NLO, MadGraph5_aMC@NLO with the NNPDF3.0 NLO PDF set [53] and Pythia 8.210 [34] were used. Finally, production of tZ and three or four top quarks (multi-top) was simulated at LO with MadGraph5_aMC@NLO and Pythia. The EvtGen program [54] was used for all samples with top quarks and the signal samples to model the properties of the bottom- and charm-hadron decays.

Drell–Yan production of charged and neutral leptons, $Z/\gamma^* \to \ell^+\ell^-$ and $Z \to \nu\bar{\nu}$, and leptonic decays of W bosons, $W \to \ell\nu$, in association with jets (V + jets) were simulated [55] with Sherpa [56], using the Sherpa parton shower [57] and a dedicated tuning developed by the Sherpa authors. Sherpa was also used for the simulation of diboson production (VV) and leptonic decays of triboson production (VVV) [58]. The diboson samples include one set of tree-induced processes with dileptonic and semileptonic decays,

VV (1), and a second set with electroweak $VVjj$ production and loop-induced production with leptonic decays, VV (2).

All simulated background events were passed through a full GEANT4 [59] simulation of the ATLAS detector [60]. For signal events, a fast detector simulation was used, which is based on a parameterization of the performance of the electromagnetic and hadronic calorimeters [61] and on GEANT4 for all other detector components. The same algorithms were used for the reconstruction of physics objects in simulated signal and background events and in collision data. Agreement between simulated events and collision data is improved by weighting the simulated events to account for differences in the lepton trigger, reconstruction, identification and isolation efficiencies, b-tagging efficiency, and jet-vertex-tagging efficiency, using correction factors derived in dedicated studies.

The effect of additional pp interactions in the same and nearby bunch crossings ("pileup") was taken into account by overlaying the hard-scattering process with soft pp interactions generated with PYTHIA 8.186 using the A2 tune [62] and the MSTW2008LO PDF set [63]. Simulated events were reweighted to make the distribution of the average number of simultaneous pp collisions match that of the recorded dataset.

4 Event reconstruction

The data recorded in collision events are processed to reconstruct and identify physics objects needed for the event selection, and to reject events of insufficient quality. Candidate events are required to have a reconstructed vertex [64] with at least two associated tracks with a transverse momentum $p_{\mathrm{T}} > 400\,\mathrm{MeV}$. If there are several such vertices, the one with the largest scalar sum of p_{T}^2 of its associated tracks is used as the primary collision vertex.

Jets are reconstructed from topological energy clusters in the calorimeters [65, 66] using the anti-k_t algorithm [67] with radius parameter $R = 0.4$ and are calibrated to the hadronic scale, accounting for the impact of pileup in the event. The calibration is improved with the global sequential correction scheme [68]. Jets with $p_{\mathrm{T}} > 20\,\mathrm{GeV}$ and $|\eta| < 2.8$ are retained. In addition, jets need to fulfill basic quality criteria; an event is discarded if any selected jet does not meet these criteria [69]. Pileup is suppressed further by rejecting jets with $p_{\mathrm{T}} < 60\,\mathrm{GeV}$ and $|\eta| < 2.4$ if the output of a jet-vertex-tagging algorithm [70] shows their origin is not compatible with the primary vertex.

A multivariate discriminant based on track impact parameters and reconstructed secondary vertices [71, 72] is employed to identify jets with $|\eta| < 2.5$ resulting from the hadronisation of b-quarks (b-jets). The chosen working point has a b-tagging efficiency of 77% and rejection factors of 134, 6, and 22, for light-quark and gluon jets, c-quark jets, and hadronically decaying tau leptons, τ_{had}, respectively, as evaluated on a simulated sample of $t\bar{t}$ events.

A dedicated algorithm is used to reconstruct τ_{had} candidates and match them to a primary vertex. This is seeded from jets reconstructed with the anti-k_t algorithm with a radius parameter $R = 0.4$ and fulfilling $p_{\mathrm{T}} > 10\,\mathrm{GeV}$ and $|\eta| < 2.5$ [73]. Only the visible part of the τ_{had} decay is reconstructed. An energy calibration derived independently of the jet energy scale is applied to the reconstructed τ_{had} [74]. The analysis uses τ_{had} candidates with $p_{\mathrm{T}} > 20\,\mathrm{GeV}$ and $|\eta| < 2.5$, excluding the calorimeter transition region $1.37 < |\eta| < 1.52$ because of its larger uncertainty in jet direction measurements. The τ_{had} candidates are required to have one or three associated tracks (prongs) and a total track charge of ± 1. A discriminant obtained from a boosted decision tree is used to reject jets that do not originate from a hadronically decaying tau lepton, with a working point yielding a combined tau reconstruction and identification efficiency of

55% (40%) for 1-prong (3-prong) τ_{had} [75]. A looser set of identification criteria, called "AntiID", are used for the background estimate using the fake-factor method, as described in Section 6.1.

Two sets of identification criteria are defined for electrons and muons: the *baseline* criteria are used for lepton vetoes and the overlap removal procedure described below, while *signal* criteria are used when the event selection requires the presence of a lepton.

Electron candidates are reconstructed from energy clusters in the electromagnetic calorimeter matched to tracks in the inner tracking detector. Baseline electrons must satisfy a loose likelihood-based identification [76, 77] and have $|\eta_{\text{cluster}}| < 2.47$ and $p_{\text{T}} > 10\,\text{GeV}$. Signal electrons must have $p_{\text{T}} > 25\,\text{GeV}$ and satisfy the tight likelihood-based quality criteria. In addition, they must fulfill requirements on the track and calorimetric isolation, the transverse impact parameter significance ($|d_0|/\sigma(d_0) < 5$) and the longitudinal impact parameter ($|z_0 \sin(\theta)| < 0.5\,\text{mm}$).

The muon reconstruction combines tracks recorded in the muon system with those reconstructed in the inner tracking detector. Baseline muons must have $p_{\text{T}} > 10\,\text{GeV}$ and $|\eta| < 2.7$ and fulfill medium quality criteria [78]. Signal muons must also be isolated and satisfy $p_{\text{T}} > 25\,\text{GeV}$ and $|\eta| < 2.5$ as well as requirements on the track impact parameters ($|d_0|/\sigma(d_0) < 3$ and $|z_0 \sin(\theta)| < 0.5$ mm).

The jet and lepton reconstruction algorithms described above work independently of each other and may therefore assign the same detector signature to multiple objects. A sequence of geometrical prescriptions is applied to resolve ambiguities by removing objects. In particular, τ_{had} candidates near electrons or muons ($\Delta R_y \equiv \sqrt{(\Delta\phi)^2 + (\Delta y)^2} < 0.2$) are discarded as part of this procedure. No jet is allowed near an electron or a muon: for $\Delta R_y < 0.2$, the jet is removed, while for $0.2 < \Delta R_y < 0.4$, the lepton is removed instead.

The missing transverse momentum $\vec{p}_{\text{T}}^{\,\text{miss}}$ is defined as the negative vector sum of the transverse momenta of all identified physics objects (electrons, photons, muons, tau leptons, jets) and an additional soft term. The soft term is constructed from all tracks that are not associated with any reconstructed physics object but are associated with the identified primary collision vertex [79, 80]. In this way, the missing transverse momentum benefits from the calibration of the identified physics objects, and remaining energy deposits are included in a pileup-insensitive manner. Frequently, only the magnitude $E_{\text{T}}^{\text{miss}} \equiv |\vec{p}_{\text{T}}^{\,\text{miss}}|$ is used.

4.1 Analysis variables

Besides basic kinematic quantities, the variables described below are used in the event selection.

The transverse mass m_{T} is computed from the transverse momentum of a lepton ℓ and the missing transverse momentum in the event:

$$m_{\text{T}} = \sqrt{2\,E_{\text{T}}^{\text{miss}}\,p_{\text{T},\ell} \cdot \left(1 - \cos\left(\Delta\phi\left(\vec{p}_{\text{T}}^{\,\text{miss}}, \vec{p}_{\text{T},\ell}\right)\right)\right)},$$

where $p_{\text{T},\ell}$ is the lepton's transverse momentum. In W+jets events, the m_{T} distribution has a cutoff near the W-boson mass $m(W)$.

The stransverse mass m_{T2} [81–83] is employed in this analysis to reject the top-pair background. It is a generalization of the transverse mass for final states with two invisible particles. It assumes two identical particles that decay to one visible and one invisible product each, and provides an upper bound on the mother particle's mass. This is achieved by considering all possible ways to distribute the measured $\vec{p}_{\text{T}}^{\,\text{miss}}$ between the invisible particles of the assumed decay.

In dileptonic events, m_{T2} is constructed using the leptons as the visible particles. The $\vec{p}_{\mathrm{T}}^{\,\mathrm{miss}}$ is assumed to stem from a pair of neutrinos. The resulting variable is a powerful discriminant against background events from $t\bar{t}$ or WW production, as it is bounded from above by $m(W)$ for these, while signal events do not respect this bound.

Furthermore, the invariant mass $m(\ell_1, \ell_2)$ of the two reconstructed leptons (including τ_{had}), as well as H_{T}, defined as the scalar sum of the p_{T} of the two leading jets, is used.

5 Event selection

The event selection starts from preselections that are similar for the lep-had and had-had channels, differing only in the choice of event triggers and the required numbers of reconstructed tau leptons and light leptons, i.e. electrons and muons. Prompt light leptons are not distinguished from light leptons originating from decays of tau leptons. Therefore, in the background estimates, processes with prompt light leptons contribute in the same way as processes with leptonic decays of tau leptons. The event selections for the two channels are mutually exclusive. The channels can therefore be statistically combined in the interpretation of the results.

5.1 Preselection

Preselection	lep-had	had-had
Trigger	single-electron or single-muon trigger	$E_{\mathrm{T}}^{\mathrm{miss}}$ or di-tau trigger
Leptons	exactly one τ_{had} + one signal electron or muon no additional baseline electron or muon or τ_{had}	exactly two τ_{had} no baseline electron or muon
Trigger-related requirements	$p_{\mathrm{T}}(e, \mu) > 27\,\mathrm{GeV}$	$E_{\mathrm{T}}^{\mathrm{miss}} > 180\,\mathrm{GeV}$ or $p_{\mathrm{T}}(\tau_{1,2}, \mathrm{jet}_1) > 50, 40, 80\,\mathrm{GeV}$
$p_{\mathrm{T}}(\mathrm{jet}_2)$	$> 26\,\mathrm{GeV}$	$> 20\,\mathrm{GeV}$
$p_{\mathrm{T}}(\tau_{\mathrm{had}})$	$> 70\,\mathrm{GeV}$	$> 70\,\mathrm{GeV}$
$n_{b\text{-jet}}$	≥ 1	≥ 1

Table 2: Preselections in the lep-had and had-had channel. The leading (subleading) objects are referred to using indices, e.g. jet_1 (jet_2), and τ_1 (τ_2) refers to the leading (subleading) τ_{had}.

The preselection requirements for the two channels are summarized in Table 2. In the lep-had channel, events selected by single-electron or single-muon triggers are used. The had-had channel uses a logical OR of an $E_{\mathrm{T}}^{\mathrm{miss}}$ trigger and a combined trigger selecting events with two tau leptons and one additional jet at the first trigger level. The preselection adds suitable requirements to avoid working in the turn-on regime of the trigger efficiency. For events selected by the single-lepton triggers, the p_{T} of the light lepton is required to be at least 27 GeV. For events selected by the $E_{\mathrm{T}}^{\mathrm{miss}}$ trigger, $E_{\mathrm{T}}^{\mathrm{miss}}$ needs to exceed 180 GeV, and for events selected by the combined trigger, the requirements are at least 50 GeV (40 GeV) for the p_{T} of the leading (subleading) τ_{had}, and $p_{\mathrm{T}} > 80\,\mathrm{GeV}$ for the leading jet, where leading refers to the object with the largest transverse momentum. The trigger efficiencies, which are used to compute scale factors that correct for small differences between simulation and collision data, are measured as a function of the

properties of leptons reconstructed offline, so these leptons are matched to the leptons reconstructed in the trigger.

All candidate events must have at least two jets with p_{T} larger than 26 GeV (20 GeV) in the lep-had (had-had) channel. For the lep-had channel, the preselection requires exactly one τ_{had}, exactly one signal electron or muon, and no further baseline leptons. For the had-had channel, exactly two τ_{had} are required, and no baseline light leptons must be present. No requirement on the electric charge of the leptons is applied in the preselection, as both events with opposite-charge and events with same-charge lepton pairs are used in the analysis. In all regions of both the lep-had and had-had channels, the leading hadronically decaying tau lepton must have $p_{\mathrm{T}} > 70$ GeV. In addition, events are required to have at least one b-tagged jet ($n_{b\text{-jet}} \geq 1$).

5.2 Signal selections

Two signal regions (SRs) are defined, one for the lep-had channel and one for the had-had channel. Both SR selections are based on the preselection described above, where in addition the lepton pair has to have opposite electric charge, as same-charge lepton pairs are not predicted by the signal model. They were optimized to give the largest sensitivity to the targeted signal model in terms of the discovery p-value computed using a ratio of Poisson means [84, 85].

The variables with the best discrimination power between signal and background are the missing transverse momentum and stransverse mass. The optimal selection thresholds for these two variables are different in the two channels. In the lep-had (had-had) channel, the signal selection requires $m_{\mathrm{T2}} > 100$ GeV (80 GeV) and $E_{\mathrm{T}}^{\mathrm{miss}} > 230$ GeV (200 GeV); the lep-had selection needs slightly higher thresholds to achieve the same discrimination power between signal and background. A summary of the SR definitions is included in the last column of Tables 3 and 4 for the lep-had and had-had channels, respectively.

6 Background estimation

The general strategy for estimating the SM background in this analysis is to develop dedicated control regions (CRs) for the most important background contributions. These CRs provide data-driven constraints on the overall normalization of the respective background processes, whereas the shape of the kinematic distributions is taken from simulation. A maximum-likelihood fit is performed for all control-region yields simultaneously in order to obtain the normalization factors. The normalization factors from this background fit are then extrapolated using simulation to obtain the expected yields in the signal region. Therefore, all control-region selections must be mutually exclusive, with respect to each other as well as to the signal regions. The correctness of the extrapolation is checked in additional selections called validation regions (VRs), which cover the intermediate range in m_{T2} between the control and the signal regions, without overlapping either.

The targeted final state has two tau leptons, two b-quarks and missing transverse momentum. The dominant SM background process with this signature is pair production of top quarks. This background process can contribute in two different ways. In the first case, the objects from the top-quark decays are correctly reconstructed. One of the W bosons from the top-quark decays yields a hadronically decaying tau lepton; the other W boson decays to a light lepton in the lep-had channel, either directly or through a tau-lepton decay, or to a second hadronically decaying tau lepton in the had-had channel. In the second case, the

background events contain a fake tau lepton, i.e. an object which is not a tau lepton, most often a jet or an electron, but reconstructed as a hadronically decaying tau lepton. The probability of falsely identifying a jet or an electron as a tau lepton is only of the order of a few percent, but the branching ratio of W bosons to jets or electrons is larger than that to hadronically decaying tau leptons. Moreover, the requirement on m_{T2} is more efficient in rejecting $t\bar{t}$ events with real tau leptons. Therefore, $t\bar{t}$ events with fake tau leptons dominate after applying the signal-region selection requirements. As the nature and quality of the modeling in simulation of these two background components from $t\bar{t}$ events may be very different, they are treated as separate background components in the following. The CRs and methods used to estimate the background from $t\bar{t}$ events are introduced in Sections 6.1 and 6.2. The contribution of events with a real tau lepton and a fake light lepton is expected to be negligible due to the small misidentification probabilities for light leptons.

Subdominant contributions to the SM background come from diboson production, where often a jet is falsely identified as originating from a b-hadron decay, or $t\bar{t}$ production in association with a vector boson, where most often the additional vector boson is a Z boson that decays to neutrinos. The CRs for these background processes are based on a selection of events with light leptons rather than hadronically decaying tau leptons, in order to obtain good purity and enough events in the CRs. A common normalization factor for the lep-had and had-had channels is derived. These CRs are defined in Section 6.3.

Finally, smaller contributions come from vector-boson production ($W+$jets and $Z+$jets, collectively denoted by $V+$jets) and single-top production. Multi-top, triboson production, and $t\bar{t}$ production in association with a Higgs boson contribute very little to the signal regions and are therefore summarized under the label "others" in the following. The contributions of all of these are estimated directly from simulation and normalized to the generator cross section for triboson production [86] and multi-top production, and higher-order cross-section calculations for $V+$jets, $t\bar{t}H$ and single-top production [55, 87–92]. Contributions from multi-jet events are not relevant for the analysis, as was verified using data-driven methods. The multi-jet background is therefore neglected.

One signal benchmark point was chosen to illustrate the behavior of the signal in comparison to the background processes in kinematic distributions. The mass parameters for this benchmark point are $m(\tilde{t}_1) = 1100\,\mathrm{GeV}$ and $m(\tilde{\tau}_1) = 590\,\mathrm{GeV}$. A larger mass-splitting between the top squark and the tau slepton yields more-energetic b-tagged jets in the final state, whereas a higher tau-slepton mass yields tau leptons with higher transverse momentum. As both the top squark and the tau slepton have invisible particles among their decay products, the $E_{\mathrm{T}}^{\mathrm{miss}}$ spectrum does not depend strongly on the mass of the intermediate particle, the tau slepton.

6.1 Lep-had channel

The contribution of background events with real hadronically decaying tau leptons in the lep-had channel is estimated from simulation. For top-quark pair production, the shape of the distribution of the observables is taken from simulation but the overall normalization is derived from a dedicated CR. For events with fake tau leptons, it is difficult to design a CR with sufficiently high event yields and purity. Moreover, the estimate of this background from simulation does not agree with the observed data in the VRs. Therefore, the background estimate for events with fake tau leptons is derived using a data-driven method called the fake-factor method, which is discussed below.

The CR and three VRs enriched in top-quark events or events with fake tau leptons are defined in Table 3. As explained above, the CR and VRs cover a lower m_{T2} range, with the VRs located between the CR and

Variable	CR LH $t\bar{t}$-real	VR LH $t\bar{t}$-real	VR LH $t\bar{t}$-fake (OS)	VR LH $t\bar{t}$-fake (SS)	SR LH
Charge(ℓ,τ_{had})	opposite	opposite	opposite	same	opposite
$m_{\text{T2}}(\ell, \tau_{\text{had}})$	< 60 GeV	[60, 100] GeV	[60, 100] GeV	> 60 GeV	> 100 GeV
$E_{\text{T}}^{\text{miss}}$	> 210 GeV	> 210 GeV	> 150 GeV	> 150 GeV	> 230 GeV
$m_{\text{T}}(\ell)$	> 100 GeV	> 100 GeV	< 100 GeV	—	—
$m(\ell, \tau_{\text{had}})$	—	—	> 60 GeV	—	—

Table 3: Definitions of the $t\bar{t}$ control and validation regions and the signal region in the lep-had channel. A dash means that no requirement on this variable is applied. The brackets indicate an allowed range for the variable. A common preselection as given in Table 2 for the lep-had channel is applied.

the SR to check the extrapolation in this variable. In all of these regions, the preselection requirements for the lep-had channel from Table 2 are applied.

In the opposite-charge regions, the transverse mass $m_{\text{T}}(\ell)$ of the light lepton and the missing transverse momentum is used to separate $t\bar{t}$ events with real tau leptons from those with fake tau leptons. Events with top-quark pairs, where one of the top quarks decays to a light lepton and the other decays hadronically, and a jet from the hadronic W-boson decay is misidentified as the tau lepton, yield mostly small values of m_{T}. In these events, there is only one neutrino (from the leptonic W-boson decay), so the transverse mass has an endpoint near the W-boson mass. Events where both the light lepton and the hadronically decaying tau lepton are real involve more neutrinos, leading to tails of the m_{T} distribution that go beyond this endpoint. The extrapolation from the control region to the signal region is performed in m_{T2}, which is correlated with m_{T}, but the validation regions cover the full m_{T} range so that any potential bias from the correlation of m_{T} and m_{T2} would be visible there. The requirement on $m(\ell, \tau_{\text{had}})$ is added to improve the purity of the VR.

As the purity of VR LH $t\bar{t}$-fake (OS) in $t\bar{t}$ events with fake tau leptons is low, an additional validation region, VR LH $t\bar{t}$-fake (SS), with a same-charge requirement is defined. The same-charge requirement is very efficient in rejecting events where both leptons are real and originate from the W bosons in a $t\bar{t}$ event. The correlation between the charge of a jet misidentified as a tau lepton and the charge of the light lepton in $t\bar{t}$ events is much smaller; thus, events with fake tau leptons are more likely to pass the same-charge selection.

Distributions of the main discriminating variables $m_{\text{T2}}(\ell, \tau_{\text{had}})$ and $E_{\text{T}}^{\text{miss}}$ in the CR and the three VRs of the lep-had channel are shown in Figure 2. The normalization obtained from the background fit (cf. Table 8) is used for $t\bar{t}$ production with real tau leptons, $t\bar{t} + V$ and diboson production. For single-top production and V + jets, the theory prediction for the cross section is used. All contributions from events with fake tau leptons (labeled "fake $\tau_{\text{had}} + e/\mu$" in the legend) are estimated using the fake-factor method. All other processes, which are expected to give only small contributions, are merged into one distribution ("others"). All selection requirements are applied in all plots, with the exception of the top left plot, where the requirement on $m_{\text{T2}}(\ell, \tau_{\text{had}})$ is not applied, but indicated by a vertical line instead. The predicted Standard Model background and the observed data are in good agreement. The largest differences are found in the top left plot at $m_{\text{T2}}(\ell, \tau_{\text{had}}) = 70$ GeV and in the first bin in the top right plot of $E_{\text{T}}^{\text{miss}}$. They correspond to the small excess in VR LH $t\bar{t}$-real, which is discussed in Section 8.

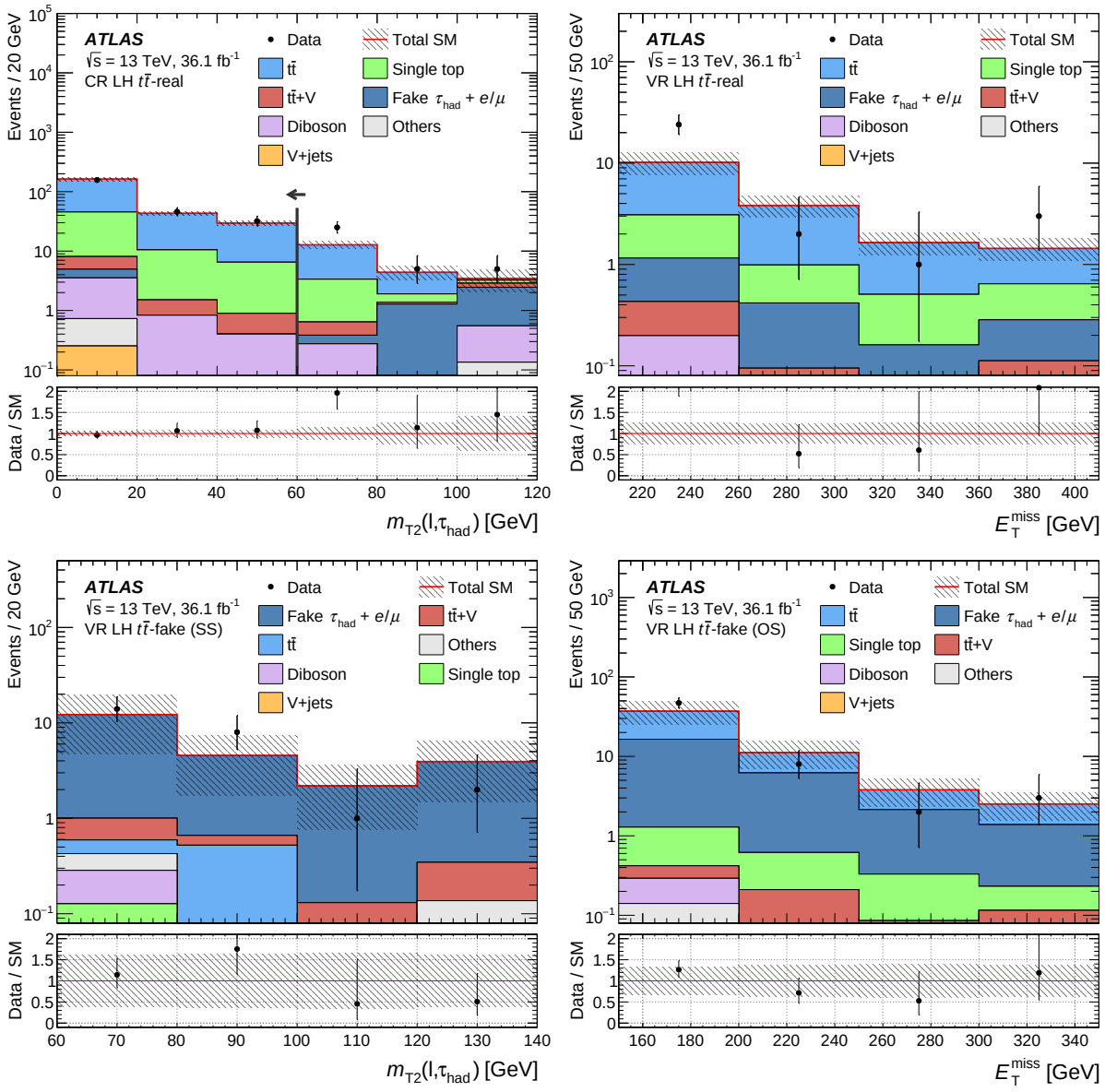

Figure 2: Distributions of $m_{\mathrm{T2}}(\ell, \tau_{\mathrm{had}})$ (left) and $E_{\mathrm{T}}^{\mathrm{miss}}$ (right) in the control region and the validation regions of the lep-had channel, CR LH $t\bar{t}$-real (top left), VR LH $t\bar{t}$-real (top right), VR LH $t\bar{t}$-fake (SS) (bottom left), and VR LH $t\bar{t}$-fake (OS) (bottom right). The vertical line and arrow in the top-left plot indicate the $m_{\mathrm{T2}}(\ell, \tau_{\mathrm{had}})$ requirement of CR LH $t\bar{t}$-real, which is not applied in this plot. (The range from 60 to 100 GeV in the top left plot corresponds to VR LH $t\bar{t}$-real.) The stacked histograms show the various SM background contributions. The hatched band indicates the total statistical and systematic uncertainty in the SM background. The total background from events with a fake tau lepton in the lep-had channel (fake τ_{had} + e/μ) is obtained from the fake-factor method. The rightmost bin includes the overflow.

Fake-factor method

The fake-factor method is used to estimate the contribution of events in the lep-had channel in which the reconstructed tau lepton is a fake. This estimate is obtained as the product of the number of events passing a selection based on looser tau identification requirements and the fake factor, which relates the number of events with looser tau-lepton candidates to the number where tau leptons meet the nominal identification criteria.

To compute the fake factor F, a looser set of criteria for the tau identification is used ("AntiID"), which is orthogonal to the default working point used in the analysis ("ID"), cf. Section 4. The value F is the ratio of the number of events with a tau lepton passing the ID requirements to the number passing the AntiID requirements in the measurement region (MR) in data; these numbers are denoted $N^{\star}(\text{data, MR})$, where $\star$ is ID or AntiID. It depends on the p_{T} and the number of tracks associated with the tau-lepton candidate. No strong dependence on the pseudorapidity is observed. As the contribution of electrons misidentified as tau leptons is small compared to that from jets, differences in the fake composition between the measurement region and the signal region are not expected to have significant impact on the estimate. The contamination from events with real tau leptons $N^{\star}_{\text{real}}(\text{MC, MR})$ is estimated from simulation and subtracted when taking the ratio,

$$F = \frac{N^{\text{ID}}(\text{data, MR}) - N^{\text{ID}}_{\text{real}}(\text{MC, MR})}{N^{\text{AntiID}}(\text{data, MR}) - N^{\text{AntiID}}_{\text{real}}(\text{MC, MR})}.$$

The measurement region is chosen such that this contamination is as small as possible. It is about 1% for AntiID and about 10% for ID tau leptons. The number of events with fake tau leptons passing the target selection (TR) is then estimated as

$$N_{\text{fakes}}(\text{TR}) = \left(N^{\text{AntiID}}(\text{data, TR}) - N^{\text{AntiID}}_{\text{real}}(\text{MC, TR})\right) \cdot F,$$

where again $N^{\text{AntiID}}_{\text{real}}(\text{MC, TR})$ is a correction that accounts for the contamination from events with real tau leptons and is estimated using simulation.

Both the number of events with looser tau identification in the target selection and the fake factor are obtained from data. The only inputs taken from simulation are small corrections that account for events with real tau leptons.

The measurement region in which the fake factors are determined is based on the lep-had preselection. Events are selected where the tau lepton has the same charge as the light lepton to increase the fraction of fake tau leptons. The largest contribution to the events with fake tau leptons in the signal region, which is estimated with the fake-factor method, is from $t\bar{t}$ production. Therefore, a requirement of $E_{\text{T}}^{\text{miss}} > 100\,\text{GeV}$ is applied and at least one b-tagged jet required to also obtain a high purity in $t\bar{t}$ events in the measurement region. Finally, $m_{\text{T2}}(\ell, \tau_{\text{had}}) < 60\,\text{GeV}$ is required to make the measurement region orthogonal to the same-charge validation region VR LH $t\bar{t}$-fake (SS). The fake factors determined in the measurement region vary between 0.22 (0.041) and 0.085 (0.009) for 1-prong (3-prong) tau leptons as a function of p_{T}.

6.2 Had-had channel

Two control and two validation regions are defined for the background with pair production of a top and an anti-top quark in the had-had channel. In all of these regions, the preselection requirements for the had-had channel from Table 2 are applied.

	CR HH $t\bar{t}$-fake	CR HH $t\bar{t}$-real	VR HH $t\bar{t}$-fake	VR HH $t\bar{t}$-real	SR HH
Charge(τ_1,τ_2)	—	opposite	—	opposite	opposite
$m_{\mathrm{T2}}(\tau_1, \tau_2)$	< 30 GeV	< 30 GeV	[30, 80] GeV	[30, 80] GeV	> 80 GeV
$E_{\mathrm{T}}^{\mathrm{miss}}$	> 120 GeV	> 120 GeV	> 160 GeV	> 160 GeV	> 200 GeV
$m_{\mathrm{T}}(\tau_1)$	< 70 GeV	> 70 GeV	< 100 GeV	> 100 GeV	—
$m(\tau_1, \tau_2)$	> 70 GeV	> 70 GeV	—	—	—

Table 4: Definitions of the $t\bar{t}$ control and validation regions and the signal region in the had-had channel. Here, τ_1 (τ_2) refers to the leading (subleading) τ_{had}. A dash means that no requirement on this variable is applied. The brackets indicate an allowed range for the variable. A common preselection as given in Table 2 for the had-had channel is applied.

As in the lep-had channel, the sequence of control regions, validation regions, and signal region is ordered by increasing m_{T2}, the main discriminating variable. The CRs are restricted to $m_{\mathrm{T2}} < 30$ GeV, and the SR requires $m_{\mathrm{T2}} > 80$ GeV. The VRs cover the intermediate phase-space region 30 GeV $< m_{\mathrm{T2}} < 80$ GeV, so that the extrapolation in m_{T2} from the CRs to the SR can be validated here. A separation between events with real and fake tau leptons is achieved using the transverse mass calculated from the leading tau lepton and the missing transverse momentum. Events with fake tau leptons dominate at low values of m_{T}; events with real tau leptons tend to have higher values of m_{T}. In the signal region, the two tau leptons are required to have opposite charge, but since in events with a fake tau lepton the relative sign of the electric charges of the tau leptons is random, the number of events with fake tau leptons in the fake CR and VRs is increased by not imposing this requirement. Also, the requirement on $E_{\mathrm{T}}^{\mathrm{miss}}$ is lowered to 120 GeV to increase the number of events in the CRs. A requirement on the invariant mass of the tau-lepton pair suppresses Z + jets events and increases the purity in $t\bar{t}$ events in the CRs. Table 4 summarizes the definitions of the CRs and VRs in the had-had channel.

Distributions of the main discriminating variables $m_{\mathrm{T2}}(\tau_1, \tau_2)$ and $E_{\mathrm{T}}^{\mathrm{miss}}$ in the two CRs and two VRs of the had-had channel are shown in Figure 3. The simulation-based estimates for $t\bar{t}$ production, separated into real and fake tau-lepton contributions, and for $t\bar{t} + V$ and diboson production are scaled with the normalization factors obtained from the background fit (cf. Table 8). The background process "$t\bar{t}$ (fake τ_{had})" includes both the events with one real and one fake tau lepton and events with two fake tau leptons.

The relative contributions of events selected by each of the two triggers used in the had-had channel (cf. Section 5.1) vary between the control and validation regions and the signal region, as the fraction of events selected by the $E_{\mathrm{T}}^{\mathrm{miss}}$ trigger becomes higher with an increasing $E_{\mathrm{T}}^{\mathrm{miss}}$ requirement. The normalization factors were therefore recomputed for the two sets of events selected exclusively by one of the two triggers. They are compatible within their statistical uncertainties, showing that there is no dependence of the normalization factors on the trigger selection. This is also confirmed by good agreement between data and predicted background yields in the validation regions when the normalization factors derived in the control regions are applied.

6.3 Common control regions

The definitions of the CR for events with $t\bar{t}$ production in association with a vector boson, CR $t\bar{t} + V$, and of the CR for events with diboson processes, CR VV, are given in Table 5. They do not use the common preselection described in Section 5.1 but select events with at least two signal leptons (e, μ or τ_{had}). These

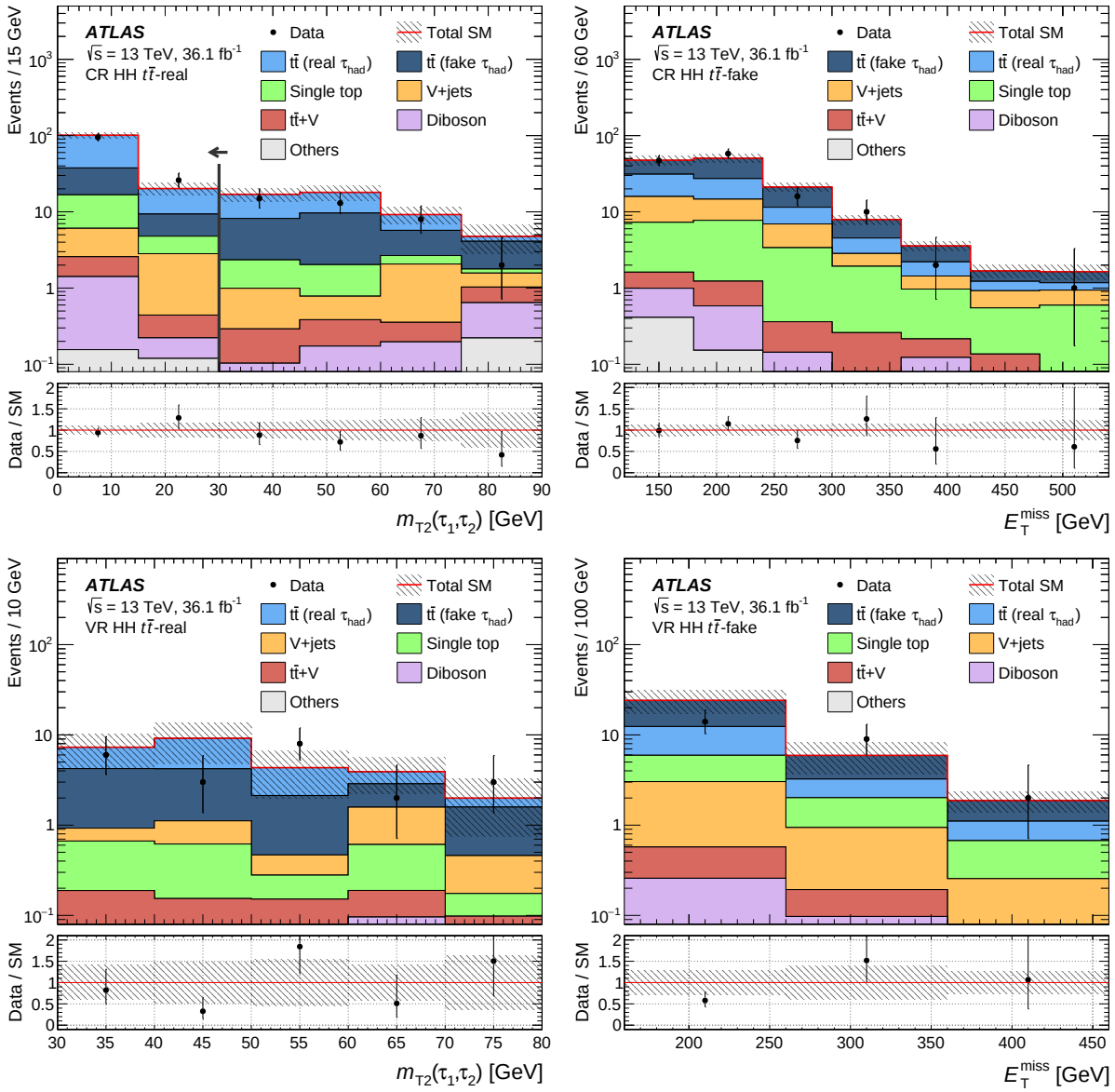

Figure 3: Distributions of $m_{\mathrm{T2}}(\tau_1, \tau_2)$ (left) and $E_{\mathrm{T}}^{\mathrm{miss}}$ (right) in two control and two validation regions in the had-had channel, CR HH $t\bar{t}$-real (top left), CR HH $t\bar{t}$-fake (top right), VR HH $t\bar{t}$-real (bottom left), and VR HH $t\bar{t}$-fake (bottom right). Here, τ_1 (τ_2) refers to the leading (subleading) τ_{had}. The vertical line and arrow in the top-left plot indicate the $m_{\mathrm{T2}}(\tau_1, \tau_2)$ requirement of CR HH $t\bar{t}$-real, which is not applied in this plot. The stacked histograms show the various SM background contributions. The hatched band indicates the total statistical and systematic uncertainty in the SM background. The rightmost bin includes the overflow. In the lower left plot, the overflow contribution is zero because VR HH $t\bar{t}$-real has an upper bound on m_{T2}.

	CR $t\bar{t}+V$	CR VV
$p_{\mathrm{T}}(\mathrm{jet}_2)$	$> 26\,\mathrm{GeV}$	$> 26\,\mathrm{GeV}$
n_{SFOS}	≥ 1	≥ 1
m_Z^{closest}	$[80, 100]\,\mathrm{GeV}$	$[80, 100]\,\mathrm{GeV}$
$n_{b\text{-jet}}$	≥ 2	0
n_{lepton}	≥ 3	≥ 2
$n_{\mathrm{lepton}} + n_{\mathrm{jet}}$	≥ 6	—
$E_{\mathrm{T}}^{\mathrm{miss}}/\sqrt{H_{\mathrm{T}}}$	—	$> 15\,\sqrt{\mathrm{GeV}}$
$m_{\mathrm{T2}}(\ell,\ell)$	—	$> 120\,\mathrm{GeV}$

Table 5: Definition of the $t\bar{t}+V$ and VV control regions. The total number of signal leptons (e, μ or τ_{had}) is given by n_{lepton}, and n_{SFOS} is the number of lepton pairs with the same flavor and opposite charge. Other variables are defined in the text. A dash means that no requirement on this variable is applied. The brackets indicate an allowed range for the variable.

events also need to have fired the single-lepton trigger and the respective trigger plateau requirement is applied as described in Section 5.1, so that at least one light lepton must be among the two leptons. Two jets must be present with $p_{\mathrm{T}} > 26\,\mathrm{GeV}$. No b-tagged jets are allowed in CR VV, whereas in CR $t\bar{t}+V$ at least two b-tagged jets are required to select events with top-quark decays.

The $t\bar{t}+V$ background in the signal region mostly consists of events in which a $t\bar{t}$ pair is produced in association with a Z boson that decays to two neutrinos providing large $E_{\mathrm{T}}^{\mathrm{miss}}$. This type of background cannot easily be separated from other backgrounds, in particular pure $t\bar{t}$ production, so that instead a CR enriched in $t\bar{t}+Z$ with $Z \to \ell\ell$ is used. It is then assumed that the normalization factor derived for this process is also valid for the Z boson decaying to neutrinos. Furthermore, as events with four or more leptons are too rare to make a CR, the CR $t\bar{t}+V$ also accepts events with only one additional, third signal lepton.

To select events with Z-boson decays, the invariant mass of each same-flavor, opposite-charge (SFOS) lepton pair in the event is calculated. The pair with invariant mass closest to the mass of the Z boson is selected and assumed to originate from the Z-boson decay. The invariant mass of this pair, m_Z^{closest}, is required to be within about 10 GeV of the Z-boson mass. As the invariant mass computed from the visible products of a Z-boson decay to hadronically decaying tau leptons is smaller than the Z-boson mass, this in effect removes most of the events with tau-lepton pairs. After applying these requirements, there is still a sizable contribution from Z + jets events, where the SFOS pair originates from the Z boson and one of the jets is misidentified as a tau lepton. Requiring the total number of leptons and jets to be at least six gives a small increase in the purity in $t\bar{t}+Z$ events in this region.

Events with diboson production entering the signal regions mostly have either two or three charged leptons. Events with four leptons are negligible in both channels. A CR for diboson production based on a pure tau-lepton selection would suffer from a high contamination from events in which a W boson is produced in association with jets, one of which is misidentified as a hadronically decaying tau lepton. Therefore, the CR selection includes all lepton flavors and makes use of m_{T2} and the significance of the $E_{\mathrm{T}}^{\mathrm{miss}}$, measured as $E_{\mathrm{T}}^{\mathrm{miss}}/\sqrt{H_{\mathrm{T}}}$, to suppress Z + jets events. The requirement on m_Z^{closest} is used to suppress signal contamination, which otherwise becomes non-negligible for small mass differences between the top squark and tau slepton in the simplified model. Figure 4 shows the distribution of $E_{\mathrm{T}}^{\mathrm{miss}}$ in CR $t\bar{t}+V$ and

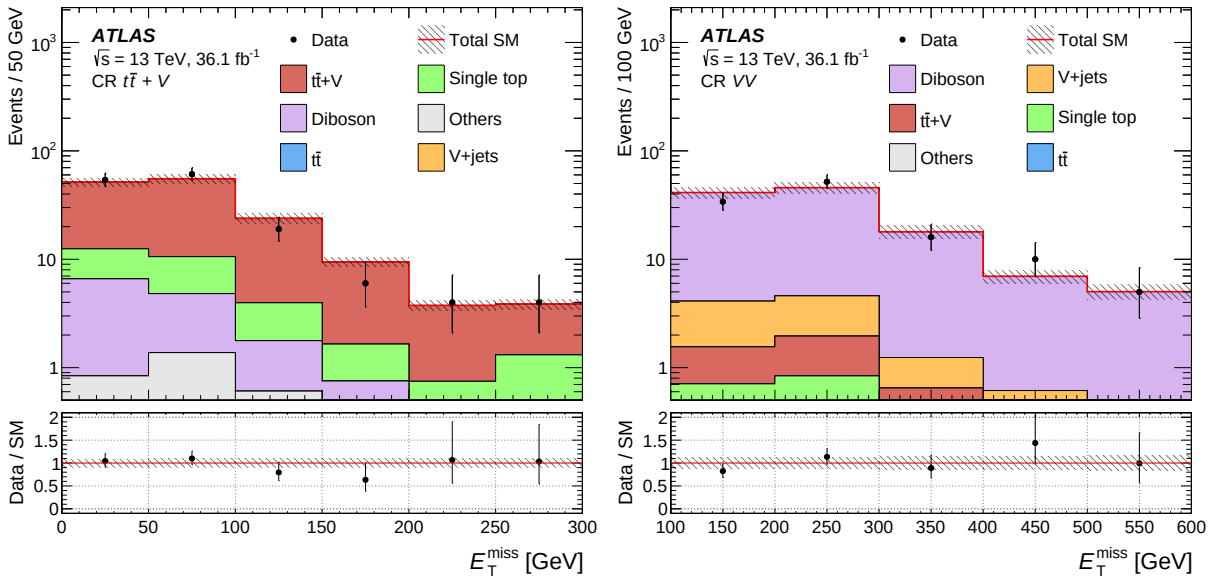

Figure 4: Distributions of $E_{\mathrm{T}}^{\mathrm{miss}}$ in CR $t\bar{t}+V$ (left) and CR VV (right). The hatched band indicates the total statistical and systematic uncertainty in the SM background. The rightmost bin includes the overflow. The lower bins of $E_{\mathrm{T}}^{\mathrm{miss}}$ in CR VV which are not shown in the right plot are empty due to the requirement on $E_{\mathrm{T}}^{\mathrm{miss}}/\sqrt{H_{\mathrm{T}}}$.

in CR VV with the normalization factors from the background fit (cf. Table 8) applied. The composition of different diboson processes in the signal region is similar to that of the control region.

7 Systematic uncertainties

Experimental systematic uncertainties are taken into account for all simulated background and signal samples. For leptons, experimental systematic uncertainties arise from the reconstruction and identification efficiencies, and for electrons and muons also from the isolation efficiency. For jets, additional uncertainties from the pileup subtraction, pseudorapidity intercalibration, flavor composition, and punch-through effects, as well as uncertainties in the flavor-tagging and jet-vertex tagging efficiencies are considered using a reduced set of nuisance parameters [93]. Uncertainties in the energy resolution and calibration are taken into account for all physics objects. The $E_{\mathrm{T}}^{\mathrm{miss}}$ has an additional uncertainty due to the contribution of the soft-track term. The fast detector simulation used for the signal samples brings additional uncertainties in jets and tau leptons. Further sources of experimental systematic uncertainty are the pileup reweighting of simulated events to cover the uncertainty in the ratio of the predicted and measured inelastic cross sections, and the measurement of the trigger scale factors.

Several sources of uncertainty are found to be important for the background estimate obtained from the fake-factor method. Statistical uncertainties in the fake factors from the number of events in the measurement region and the number of AntiID events in the respective target selection are propagated into the uncertainty in the final estimate. Further uncertainties in the fake factors arise from the contribution of multi-jet events, which enter the measurement region due to the softer requirement on $E_{\mathrm{T}}^{\mathrm{miss}}$ relative to the other lep-had selections, and the subtraction of events with real tau leptons. The former uncertainty is estimated by varying the $E_{\mathrm{T}}^{\mathrm{miss}}$ requirement of the measurement region, and the latter by scaling the

simulation-based estimate for these events by up to ±40%. An uncertainty from the choice of AntiID working point is derived by reevaluating and comparing the estimates obtained from the fake-factor method for different values of the AntiID working point. Finally, the impact of the extrapolation of the fake factor in m_{T2} is translated into an uncertainty by comparing fake factors obtained for different ranges of m_{T2} in the measurement region. This is the dominant source of uncertainty in the fake-factor method.

Uncertainties in the theoretical modeling are evaluated for the dominant processes selected in the analysis. For the hard-scatter modeling of the $t\bar{t}$ and single-top processes, systematic uncertainties are estimated by comparing the hard-process generation between Powheg and MadGraph5_aMC@NLO, both interfaced to Herwig++ for the parton showering. Uncertainties in the fragmentation and hadronization are estimated from a comparison of samples generated with Powheg for the hard scattering interfaced to Herwig++ or Pythia for the parton shower. Uncertainties in additional radiation are obtained through a variation of the generator settings, such as those for the produced shower radiation, the factorization and renormalization scales and the NLO radiation. An uncertainty in the treatment of the interference subtraction of single-top-quark production in the Wt channel and $t\bar{t}$ production at next-to-leading order is estimated as the difference between diagram-removal and diagram-subtraction schemes [94, 95].

For $t\bar{t}+V$ production, the uncertainty in the hard-scatter, fragmentation and hadronization modeling is assessed by comparing the nominal MadGraph5_aMC@NLO samples interfaced to Pythia to samples generated with Sherpa. For diboson and $V+$jets production, the nominal Sherpa samples are compared to samples generated with Powheg or MadGraph5_aMC@NLO, both interfaced to Pythia for the parton showering. For $t\bar{t}+V$, VV, and $V+$jets, the effects of additional variations of the internal parameters of the generators for the factorization and hadronization scales are evaluated.

An additional cross-section uncertainty of 5% is considered for $Z+$jets, $W+$jets [96], and single-top-quark production [91, 97, 98] because their yields are not normalized in control regions. The uncertainty in the integrated luminosity described in Section 3 is also applied to all backgrounds that are taken directly from simulation. In all regions, the statistical uncertainties in the MC simulations and the uncertainties in the normalization factors are taken into account.

The full set of systematic uncertainties in the total background yields is summarized in Table 6. The largest sources of experimental systematic uncertainty in both channels include the jet and tau energy calibration, the pileup reweighting and the $E_{\mathrm{T}}^{\mathrm{miss}}$ measurement. In the lep-had channel, the dominant contribution to the overall systematic uncertainty comes from the uncertainties in the fake-factor method. The advantage of using a data-driven method for the largest part of the background is the moderate total uncertainty in this channel compared to the had-had channel, where simulation is used to extrapolate from the control region. In the had-had channel, the uncertainty in the total background estimate is driven by the uncertainty in the estimate of $t\bar{t}$ events with fake tau leptons, the largest background contribution. The dominant effects arise from the systematic uncertainty in the tau energy scale and from jet mismodeling due to the simulation-based residual pileup correction, which significantly affect the extrapolation from the control to the signal region.

For the signal, in addition to the experimental uncertainties, theoretical uncertainties in the cross sections are taken from an envelope of cross-section predictions using different PDF sets and factorization and renormalization scales, as described in Ref. [99]. They vary between 13% and 20%, which is similar to the size of the experimental uncertainties in the signal.

	SR LH	SR HH
Total systematic uncertainty	± 29%	± 53%
Fake-factor method	± 23%	—
Jet-related	± 9.4%	± 36%
Tau-related	± 7.2%	± 32%
Other experimental	± 6.2%	± 12%
Theory modelling	± 8.4%	± 20%
MC statistics	± 7.5%	± 17%
Normalization factors	± 4.8%	± 14%
Luminosity	± 0.3%	± 0.8%

Table 6: Relative systematic uncertainties in the estimated number of background events in the signal regions (left: lep-had, right: had-had channel). In the lower part of the table, a breakdown into different categories is given: all jet- and tau-related systematics are added into a respective combined value, while the smaller experimental uncertainties from electrons, muons, flavor-tagging, $E_{\mathrm{T}}^{\mathrm{miss}}$, and pileup reweighting are combined into "Other experimental". The percentage values give the relative post-fit uncertainties in the total expected background yield. The individual contributions do not add up to the total given in the first row due to the correlations between the individual systematic uncertainties.

8 Results

The statistical interpretation of the results is performed using the HistFitter framework [100] that carries out the fitting procedure based on a maximum-likelihood approach and the hypothesis tests utilizing the profile-likelihood ratio as a test statistic with asymptotic formulae [101]. All regions are treated as single bins in the likelihood fits, i.e. no shape information is used. Systematic uncertainties are implemented as nuisance parameters, taking into account potential correlations. The background fit uses the three CRs of the lep-had and the had-had channels and the two common CRs simultaneously. The normalization factors from the background fit are extrapolated to the VRs and SRs in order to obtain the background estimates in these regions, again accounting for correlations between systematic uncertainties.

The results from the background fit for the individual expected contributions of the SM processes and for their sum in the two signal regions are shown in Table 7, together with the observed yields from the analysis dataset with an integrated luminosity of 36.1 fb^{-1}. Table 8 summarizes the four normalization factors obtained from the background fit. Overall, they are compatible with unity. The observed data yields in the signal regions in Table 7 are in agreement with the expected total background yields from SM processes in both the lep-had and the had-had channels. No significant excess is observed.

Figure 5 shows the distributions of m_{T2} and $E_{\mathrm{T}}^{\mathrm{miss}}$ in the signal regions of the lep-had channel and had-had channel. All selection requirements are applied, except that on the variable shown in the plot, which is instead indicated by the vertical line and arrow.

The analysis results are summarized in Figure 6, which shows the data yields (N_{obs}) and background expectations (N_{exp}) in all analysis regions, and the resulting pulls $(N_{\mathrm{obs}} - N_{\mathrm{exp}})/\sigma_{\mathrm{exp}}$ in the validation and signal regions, where σ_{exp} includes the total uncertainty in the background estimate and the Poisson uncertainty in the data yield. The pulls in all but one validation region are below one standard deviation. In the VR targeting $t\bar{t}$ events with a real tau lepton in the lep-had channel, an upwards fluctuation of

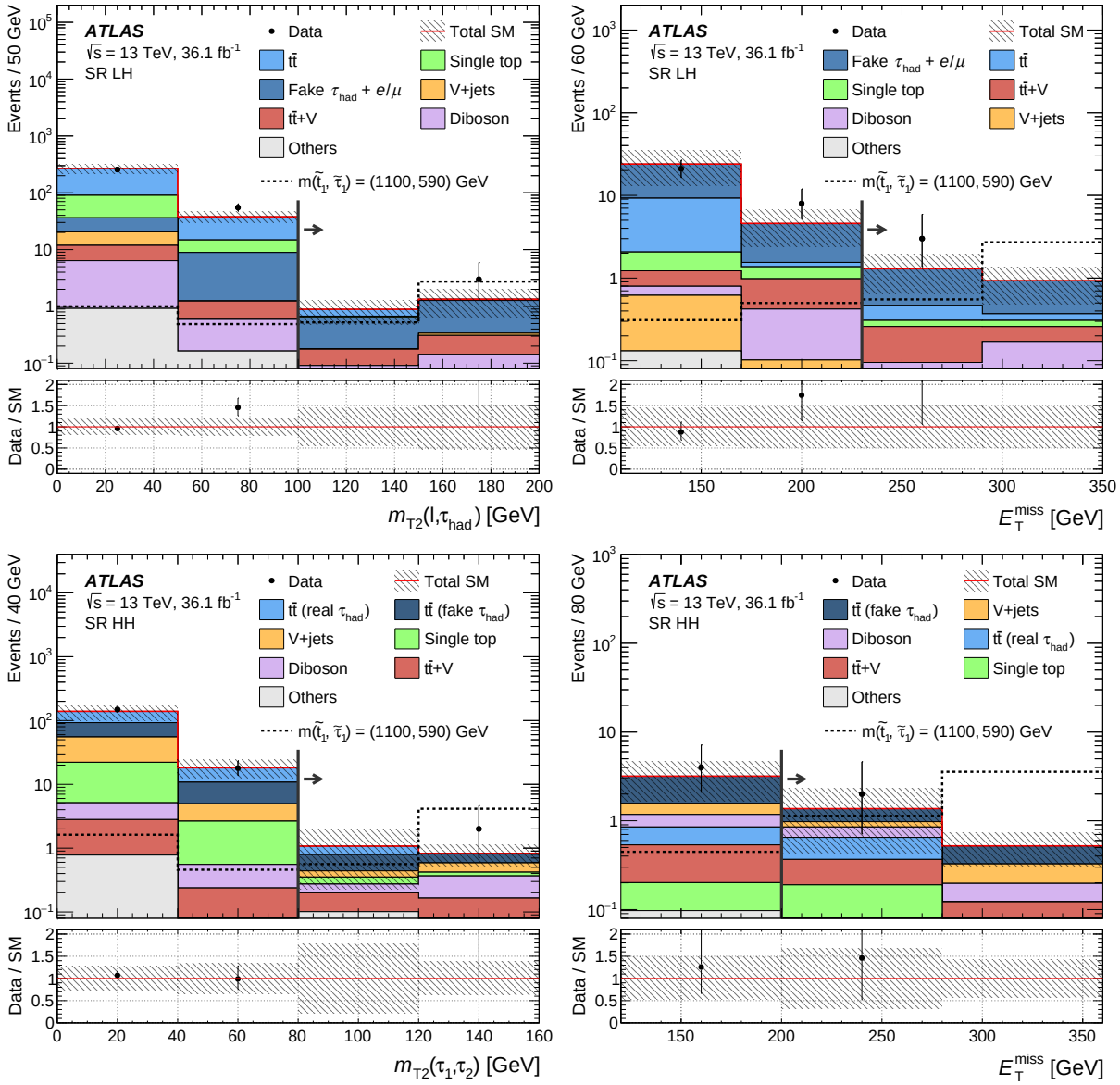

Figure 5: Distributions of m_{T2} (left) and $E_{\mathrm{T}}^{\mathrm{miss}}$ (right) in the signal regions of the lep-had channel (top) and had-had channel (bottom) before the respective selection requirements, indicated by the vertical line and arrow, are applied. Here, τ_1 (τ_2) refers to the leading (subleading) τ_{had}. The stacked histograms show the various SM background contributions. The total background from events with a fake tau lepton in the lep-had channel (fake τ_{had} + e/μ) is obtained from the fake-factor method. The hatched band indicates the total statistical and systematic uncertainty in the SM background. The error bars on the black data points represent the statistical uncertainty in the data yields. The dashed line shows the expected additional yields from a benchmark signal model. The rightmost bin includes the overflow.

	SR LH	SR HH
Observed events	3	2
Total background	2.2 ± 0.6	1.9 ± 1.0
Fake $\tau_{\text{had}} + e/\mu$	1.4 ± 0.5	—
$t\bar{t}$ (fake τ_{had})	—	$0.6 \pm {}^{0.7}_{0.6}$
$t\bar{t}$ (real τ_{had})	0.22 ± 0.12	$0.28 \pm {}^{0.30}_{0.28}$
$t\bar{t} + V$	0.25 ± 0.14	0.26 ± 0.12
Diboson	0.15 ± 0.11	0.28 ± 0.13
Single-top	$0.10 \pm {}^{0.24}_{0.10}$	0.13 ± 0.11
V + jets	0.032 ± 0.014	0.26 ± 0.09
Others	0.082 ± 0.022	0.09 ± 0.04
Signal ($m(\tilde{t}_1) = 1100$ GeV, $m(\tilde{\tau}_1) = 590$ GeV)	3.3 ± 0.7	4.7 ± 1.2

Table 7: Expected numbers of events from the SM background processes from the background fit and observed event yield in data for the signal regions in the lep-had and had-had channel, given for an integrated luminosity of 36.1 fb^{-1}. The expected yield for the signal model with $m(\tilde{t}_1) = 1100$ GeV and $m(\tilde{\tau}_1) = 590$ GeV is shown for comparison. The uncertainties include both the statistical and systematic uncertainties and are truncated at zero. The total background from events with a fake tau lepton in the lep-had channel (fake $\tau_{\text{had}} + e/\mu$) is obtained from the fake-factor method.

Process	Normalization factor
Diboson	$1.0 \, {}^{+0.6}_{-0.3}$
$t\bar{t} + V$	$1.39^{+0.23}_{-0.23}$
$t\bar{t}$ (fake τ_{had})	$1.2 \, {}^{+0.4}_{-0.4}$
$t\bar{t}$ (real τ_{had})	$0.81^{+0.20}_{-0.20}$

Table 8: Normalization factors obtained from the background-only fit. The normalization factor for $t\bar{t}$ events with fake tau leptons is only relevant for the had-had channel.

around 2.3 standard deviations is observed. However, the distribution of m_{T2} in this VR (top left plot in Figure 2) shows that the excess is confined to the single bin farthest away from the signal region ($60\,\text{GeV} < m_{\text{T2}}(\ell, \tau_{\text{had}}) < 80\,\text{GeV}$), and therefore inconsistent with a signal.

8.1 Interpretation

In the absence of a significant excess beyond the SM prediction in either signal region, an exclusion limit is derived on the masses of the particles in the simplified signal model. In contrast to the background fit, the combined likelihood fit that is performed to derive the model-dependent exclusion limits allows for signal contamination in the CRs and includes the signal region. The CL_s prescription [102] is used to derive the probability that the signal-plus-background hypothesis is compatible with the observation and to set lower limits on the masses of the supersymmetric particles.

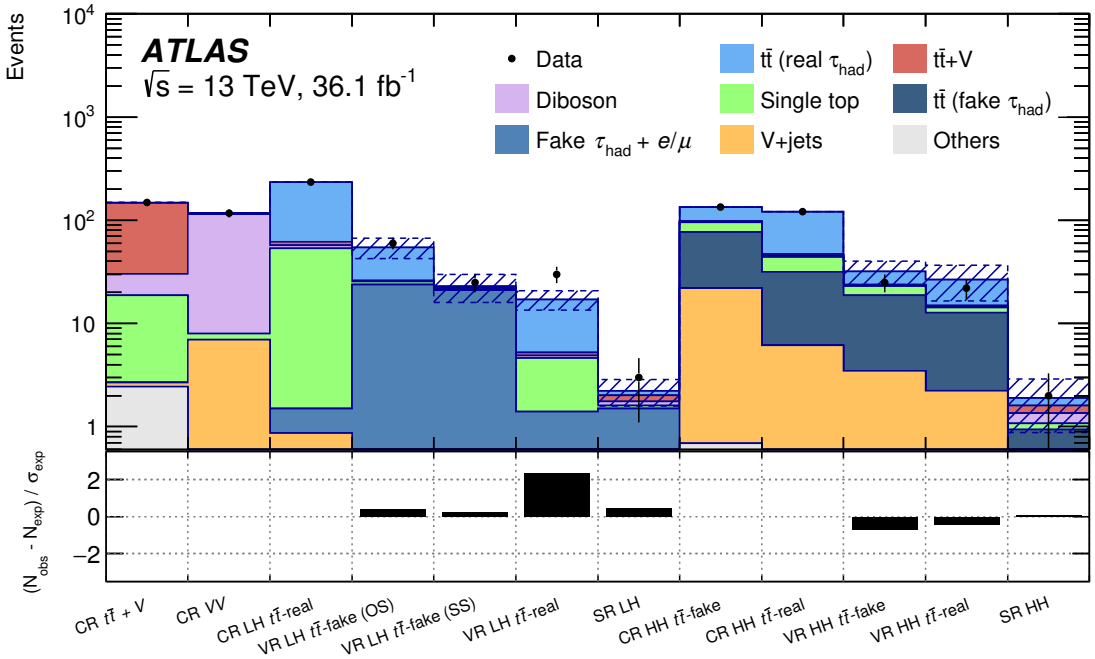

Figure 6: Data yield and background expectation in all analysis regions from the lep-had and had-had channel (top) and the resulting pulls in the validation and signal regions (bottom). The hatched band gives the total statistical and systematic uncertainty in the background estimate in each bin. The pulls in the control regions are small by construction as the normalization factors obtained from the fit are applied. The contribution of $t\bar{t}$ events to CR $t\bar{t}+V$ and CR VV is below a percent and not drawn here.

Figure 7 shows the expected and observed exclusion-limit contours at 95% confidence level (CL) obtained from the statistical combination of the lep-had and had-had channels with full experimental and theory systematic uncertainties. Top-squark masses up to 1.16 TeV and tau-slepton masses up to 1.00 TeV are excluded, which improves on the previous result from the ATLAS analysis of 20 fb^{-1} of LHC data at $\sqrt{s}$ = 8 TeV [22] by almost a factor of two in both mass parameters. The had-had channel has better sensitivity than the lep-had channel over the whole mass plane, but the combination helps to improve the sensitivity, in particular for large tau-slepton masses. For low tau-slepton masses, the sensitivity decreases and the limit on the top-squark mass is lower than at higher tau-slepton masses because the tau leptons from the tau-slepton decay become less energetic, which reduces the acceptance of the analysis selection. When evaluating the distribution of the test statistic used for the hypothesis tests with simulated pseudoexperiments instead of the asymptotic formulae, the observed excluded range of top-squark masses is reduced by up to 40 GeV.

In addition to the model-dependent limits above, the analysis results are also interpreted in terms of model-independent upper limits on the number of events from non-Standard-Model processes in the signal region, S^{95}_{obs}. Dividing this number by the integrated luminosity of the dataset gives an upper limit on the visible signal cross section, $\langle A\epsilon\sigma\rangle^{95}_{\text{obs}}$, defined as the product of acceptance, reconstruction efficiency and signal cross section. The model-independent limits are derived from a fit that is similar to the background fit, as it assumes no contamination by a potential signal in the CRs, but it includes the signal region with the extrapolated background contributions and a signal of variable strength. The model-independent limits are shown in Table 9 separately for the two channels, again computed using the CL$_s$ prescription. The lep-had channel yields a slightly lower expected limit on the number of signal

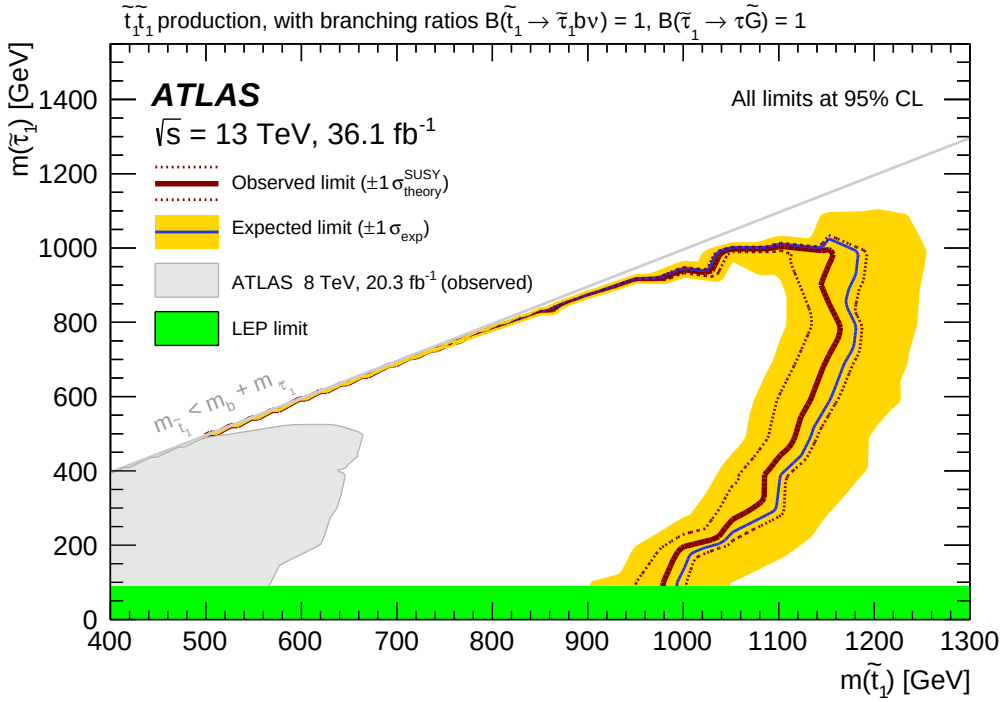

Figure 7: Expected (solid blue line) and observed (solid red line) exclusion-limit contours at 95% confidence level in the plane of top-squark and tau-slepton mass for the simplified model, obtained from the statistical combination of the lep-had and had-had channels, using full experimental and theory systematic uncertainties except the theoretical uncertainty in the signal cross section. The yellow band shows one-standard-deviation variations around the expected limit contour. The dotted red lines indicate how the observed limit moves when varying the signal cross section up or down by the corresponding uncertainty in the theoretical value. For comparison, the plot also shows the observed exclusion contour from the ATLAS Run-1 analysis [22] as the area shaded in gray and the limit on the mass of the tau slepton (for a massless LSP) from the LEP experiments [23] as a green band.

Signal channel	$\langle A\epsilon\sigma\rangle^{95}_{obs}$ [fb]	S^{95}_{obs}	S^{95}_{exp}	CL_b	$p(s=0)$ (Z)
SR LH	0.15	5.4	$4.5^{+2.6}_{-1.5}$	0.65	0.32 (0.47)
SR HH	0.13	4.7	$4.6^{+2.5}_{-1.5}$	0.52	0.48 (0.05)

Table 9: Left to right: observed 95% CL upper limits on the visible cross section ($\langle A\epsilon\sigma\rangle^{95}_{obs}$) and on the number of signal events (S^{95}_{obs}). The third column (S^{95}_{exp}) shows the expected 95% CL upper limit on the number of signal events, given the expected number (and $\pm 1\sigma$ excursions on the expectation) of background events. The last two columns indicate the CL_b value, i.e. the confidence level observed for the background-only hypothesis, and the discovery p-value ($p(s=0)$) and the corresponding significance (Z).

events than the had-had channel despite the larger expected SM background because the total uncertainty is smaller. On the other hand, the mild excess of observed events is larger in the lep-had channel, so that the observed model-independent limit is lower for the had-had channel than for the lep-had channel, and the p-value for the background-only hypothesis in the lep-had channel is smaller.

9 Conclusion

In this article, a search is presented for the direct pair production of supersymmetric top squarks in final states with two tau leptons, jets identified as originating from b-hadron decays, and missing transverse momentum.

The search uses a dataset with proton–proton collisions at a center-of-mass energy of $\sqrt{s} = 13\,\text{TeV}$, which was recorded with the ATLAS detector at the Large Hadron Collider in 2015 and 2016 and has a total integrated luminosity of $36.1\,\text{fb}^{-1}$. Two exclusive channels are considered, which select events with either two hadronically decaying tau leptons or one hadronically decaying tau lepton and one electron or muon. Good agreement between the Standard Model prediction and the event yield observed in data is found in the signal region of each channel. The analysis results are therefore interpreted in terms of upper limits on the production of supersymmetric particles. In a simplified model with production of two top squarks, each decaying via a tau slepton to a nearly massless gravitino as the lightest supersymmetric particle, masses up to $m(\tilde{t}_1) = 1.16\,\text{TeV}$ and $m(\tilde{\tau}_1) = 1.00\,\text{TeV}$ are excluded at 95% confidence level, improving on previous limits in this model by almost a factor of two. Model-independent limits allow the exclusion of visible cross sections of 0.15 (0.13) fb in the lep-had (had-had) channel for production of events beyond the Standard Model in this final state.

Acknowledgments

We thank CERN for the very successful operation of the LHC, as well as the support staff from our institutions without whom ATLAS could not be operated efficiently.

We acknowledge the support of ANPCyT, Argentina; YerPhI, Armenia; ARC, Australia; BMWFW and FWF, Austria; ANAS, Azerbaijan; SSTC, Belarus; CNPq and FAPESP, Brazil; NSERC, NRC and CFI, Canada; CERN; CONICYT, Chile; CAS, MOST and NSFC, China; COLCIENCIAS, Colombia; MSMT CR, MPO CR and VSC CR, Czech Republic; DNRF and DNSRC, Denmark; IN2P3-CNRS, CEA-DRF/IRFU, France; SRNSFG, Georgia; BMBF, HGF, and MPG, Germany; GSRT, Greece; RGC, Hong Kong SAR, China; ISF, I-CORE and Benoziyo Center, Israel; INFN, Italy; MEXT and JSPS, Japan; CNRST, Morocco; NWO, Netherlands; RCN, Norway; MNiSW and NCN, Poland; FCT, Portugal; MNE/IFA, Romania; MES of Russia and NRC KI, Russian Federation; JINR; MESTD, Serbia; MSSR, Slovakia; ARRS and MIZŠ, Slovenia; DST/NRF, South Africa; MINECO, Spain; SRC and Wallenberg Foundation, Sweden; SERI, SNSF and Cantons of Bern and Geneva, Switzerland; MOST, Taiwan; TAEK, Turkey; STFC, United Kingdom; DOE and NSF, United States of America. In addition, individual groups and members have received support from BCKDF, the Canada Council, CANARIE, CRC, Compute Canada, FQRNT, and the Ontario Innovation Trust, Canada; EPLANET, ERC, ERDF, FP7, Horizon 2020 and Marie Skłodowska-Curie Actions, European Union; Investissements d'Avenir Labex and Idex, ANR, Région Auvergne and Fondation Partager le Savoir, France; DFG and AvH Foundation, Germany; Herakleitos, Thales and Aristeia programmes co-financed by EU-ESF and the Greek NSRF; BSF, GIF and Minerva, Israel; BRF, Norway; CERCA Programme Generalitat de Catalunya, Generalitat Valenciana, Spain; the Royal Society and Leverhulme Trust, United Kingdom.

The crucial computing support from all WLCG partners is acknowledged gratefully, in particular from CERN, the ATLAS Tier-1 facilities at TRIUMF (Canada), NDGF (Denmark, Norway, Sweden), CC-IN2P3 (France), KIT/GridKA (Germany), INFN-CNAF (Italy), NL-T1 (Netherlands), PIC (Spain), ASGC (Taiwan), RAL (UK) and BNL (USA), the Tier-2 facilities worldwide and large non-WLCG resource providers. Major contributors of computing resources are listed in Ref. [103].

References

[1] Yu. A. Golfand and E. P. Likhtman,
Extension of the Algebra of Poincare Group Generators and Violation of p Invariance,
JETP Lett. **13** (1971) 323,
URL: http://www.jetpletters.ac.ru/ps/1584/article_24309.pdf.

[2] D. V. Volkov and V. P. Akulov, *Is the Neutrino a Goldstone Particle?*
Phys. Lett. B **46** (1973) 109.

[3] J. Wess and B. Zumino, *Supergauge Transformations in Four-Dimensions*,
Nucl. Phys. B **70** (1974) 39.

[4] J. Wess and B. Zumino, *Supergauge Invariant Extension of Quantum Electrodynamics*,
Nucl. Phys. B **78** (1974) 1.

[5] S. Ferrara and B. Zumino, *Supergauge Invariant Yang-Mills Theories*,
Nucl. Phys. B **79** (1974) 413.

[6] A. Salam and J. A. Strathdee, *Supersymmetry and Nonabelian Gauges*,
Phys. Lett. B **51** (1974) 353.

[7] S. P. Martin, *A Supersymmetry primer*, Adv. Ser. Direct. High Energy Phys. **21** (2010) 1,
arXiv: hep-ph/9709356.

[8] G. R. Farrar and P. Fayet, *Phenomenology of the Production, Decay, and Detection of New Hadronic States Associated with Supersymmetry*, Phys. Lett. B **76** (1978) 575.

[9] M. Dine and W. Fischler,
A Phenomenological Model of Particle Physics Based on Supersymmetry,
Phys. Lett. B **110** (1982) 227.

[10] L. Alvarez-Gaumé, M. Claudson, and M. B. Wise, *Low-Energy Supersymmetry*,
Nucl. Phys. B **207** (1982) 96.

[11] C. R. Nappi and B. A. Ovrut, *Supersymmetric Extension of the SU(3) x SU(2) x U(1) Model*,
Phys. Lett. B **113** (1982) 175.

[12] M. Asano, H. D. Kim, R. Kitano, and Y. Shimizu, *Natural supersymmetry at the LHC*,
JHEP **12** (2010) 019, arXiv: 1010.0692 [hep-ph].

[13] J. Alwall, P. C. Schuster, and N. Toro,
Simplified models for a first characterization of new physics at the LHC,
Phys. Rev. D **79** (2009) 075020, arXiv: 0810.3921 [hep-ph].

[14] D. Alves et al., *Simplified models for LHC new physics searches*,
J. Phys. G **39** (2012) 105005, ed. by R. Essig et al., arXiv: 1105.2838 [hep-ph].

[15] K. Inoue, A. Kakuto, H. Komatsu, and S. Takeshita,
Aspects of Grand Unified Models with Softly Broken Supersymmetry,
Prog. Theor. Phys. **68** (1982) 927, Erratum: Prog. Theor. Phys. **70** (1983) 330.

[16] J. R. Ellis and S. Rudaz, *Search for Supersymmetry in Toponium Decays*,
Phys. Lett. B **128** (1983) 248.

[17] ATLAS Collaboration, *ATLAS Run 1 searches for direct pair production of third-generation squarks at the Large Hadron Collider*, Eur. Phys. J. C **75** (2015) 510,
arXiv: 1506.08616 [hep-ex].

[18] ATLAS Collaboration, *Search for top squarks in final states with one isolated lepton, jets, and missing transverse momentum in $\sqrt{s}$ = 13 TeV pp collisions with the ATLAS detector*, Phys. Rev. D **94** (2016) 052009, arXiv: 1606.03903 [hep-ex].

[19] ATLAS Collaboration, *Search for direct top squark pair production in final states with two leptons in $\sqrt{s}$ = 13 TeV pp collisions with the ATLAS detector*, Eur. Phys. J. C **77** (2017) 898, arXiv: 1708.03247 [hep-ex].

[20] CMS Collaboration, *Search for direct production of supersymmetric partners of the top quark in the all-jets final state in proton-proton collisions at $\sqrt{s}$ = 13 TeV*, JHEP **10** (2017) 005, arXiv: 1707.03316 [hep-ex].

[21] CMS Collaboration, *Search for top squark pair production in pp collisions at $\sqrt{s}$ = 13 TeV using single lepton events*, JHEP **10** (2017) 019, arXiv: 1706.04402 [hep-ex].

[22] ATLAS Collaboration, *Search for direct top squark pair production in final states with two tau leptons in pp collisions at $\sqrt{s}$ = 8 TeV with the ATLAS detector*, Eur. Phys. J. C **76** (2016) 81, arXiv: 1509.04976 [hep-ex].

[23] The LEP2 SUSY Working Group and ALEPH, DELPHI, L3, OPAL Experiments, *Combined LEP Selectron/Smuon/Stau Results, 183-208 GeV*, http://lepsusy.web.cern.ch/lepsusy/www/sleptons_summer04/slep_final.html, 2004.

[24] ATLAS Collaboration, *Search for the direct production of charginos, neutralinos and staus in final states with at least two hadronically decaying taus and missing transverse momentum in pp collisions at $\sqrt{s}$ = 8 TeV with the ATLAS detector*, JHEP **10** (2014) 096, arXiv: 1407.0350 [hep-ex].

[25] ATLAS Collaboration, *Search for the electroweak production of supersymmetric particles in $\sqrt{s}$ = 8 TeV pp collisions with the ATLAS detector*, Phys. Rev. D **93** (2016) 052002, arXiv: 1509.07152 [hep-ex].

[26] ATLAS Collaboration, *The ATLAS Experiment at the CERN Large Hadron Collider*, JINST **3** (2008) S08003.

[27] ATLAS Collaboration, *ATLAS Insertable B-Layer Technical Design Report*, CERN-LHCC-2010-013. ATLAS-TDR-19, 2010, URL: https://cds.cern.ch/record/1291633.

[28] *ATLAS Insertable B-Layer Technical Design Report Addendum*, Addendum to CERN-LHCC-2010-013, ATLAS-TDR-019, 2012, URL: https://cds.cern.ch/record/1451888.

[29] ATLAS Collaboration, *Performance of the ATLAS trigger system in 2015*, Eur. Phys. J. C **77** (2017) 317, arXiv: 1611.09661 [hep-ex].

[30] E. Todesco and J. Wenninger, *Large Hadron Collider momentum calibration and accuracy*, Phys. Rev. Accel. Beams **20** (2017) 081003.

[31] ATLAS Collaboration, *Luminosity determination in pp collisions at $\sqrt{s}$ = 8 TeV using the ATLAS detector at the LHC*, Eur. Phys. J. C **76** (2016) 653, arXiv: 1608.03953 [hep-ex].

[32] J. Alwall et al., *The automated computation of tree-level and next-to-leading order differential cross sections, and their matching to parton shower simulations*, JHEP **07** (2014) 079, arXiv: 1405.0301 [hep-ph].

[33] T. Sjöstrand, S. Mrenna, and P. Skands, *A brief introduction to PYTHIA 8.1*, Comput. Phys. Commun. **178** (2008) 852, arXiv: 0710.3820 [hep-ph].

[34] T. Sjöstrand et al., *An introduction to PYTHIA 8.2*, Comput. Phys. Commun. **191** (2015) 159, arXiv: 1410.3012 [hep-ph].

[35] ATLAS Collaboration, *ATLAS Pythia 8 tunes to 7 TeV data*, ATL-PHYS-PUB-2014-021, 2014, URL: https://cds.cern.ch/record/1966419.

[36] R. D. Ball et al., *Parton distributions with LHC data*, Nucl. Phys. B **867** (2013) 244, arXiv: 1207.1303 [hep-ph].

[37] L. Lönnblad and S. Prestel, *Merging multi-leg NLO matrix elements with parton showers*, JHEP **03** (2013) 166, arXiv: 1211.7278 [hep-ph].

[38] W. Beenakker, M. Krämer, T. Plehn, M. Spira, and P. M. Zerwas, *Stop production at hadron colliders*, Nucl. Phys. B **515** (1998) 3, arXiv: hep-ph/9710451.

[39] W. Beenakker et al., *Supersymmetric top and bottom squark production at hadron colliders*, JHEP **08** (2010) 098, arXiv: 1006.4771 [hep-ph].

[40] W. Beenakker et al., *Squark and gluino hadroproduction*, Int. J. Mod. Phys. A **26** (2011) 2637, arXiv: 1105.1110 [hep-ph].

[41] S. Alioli, P. Nason, C. Oleari, and E. Re, *A general framework for implementing NLO calculations in shower Monte Carlo programs: the POWHEG BOX*, JHEP **06** (2010) 043, arXiv: 1002.2581 [hep-ph].

[42] E. Re, *Single-top Wt-channel production matched with parton showers using the POWHEG method*, Eur. Phys. J. C **71** (2011) 1547, arXiv: 1009.2450 [hep-ph].

[43] S. Frixione, P. Nason, and G. Ridolfi, *A Positive-weight next-to-leading-order Monte Carlo for heavy flavour hadroproduction*, JHEP **0709** (2007) 126, arXiv: 0707.3088 [hep-ph].

[44] R. Frederix, E. Re, and P. Torrielli, *Single-top t-channel hadroproduction in the four-flavour scheme with POWHEG and aMC@NLO*, JHEP **1209** (2012) 130, arXiv: 1207.5391 [hep-ph].

[45] S. Alioli, P. Nason, C. Oleari, and E. Re, *NLO single-top production matched with shower in POWHEG: s- and t-channel contributions*, JHEP **0909** (2009) 111, [Erratum: JHEP02,011(2010)], arXiv: 0907.4076 [hep-ph].

[46] T. Sjöstrand, S. Mrenna, and P. Skands, *PYTHIA 6.4 physics and manual*, JHEP **05** (2006) 026, arXiv: hep-ph/0603175 [hep-ph].

[47] H.-L. Lai et al., *New parton distributions for collider physics*, Phys. Rev. D **82** (2010) 074024, arXiv: 1007.2241 [hep-ph].

[48] J. Pumplin et al., *New generation of parton distributions with uncertainties from global QCD analysis*, JHEP **07** (2002) 012, arXiv: hep-ph/0201195 [hep-ph].

[49] P. Z. Skands, *Tuning Monte Carlo generators: The Perugia tunes*, Phys. Rev. D **82** (2010) 074018, arXiv: 1005.3457 [hep-ph].

[50] M. Bähr et al., *Herwig++ physics and manual*, Eur. Phys. J. C **58** (2008) 639, arXiv: 0803.0883 [hep-ph].

[51] J. Bellm et al., *Herwig++ 2.7 Release Note*, (2013), arXiv: 1310.6877 [hep-ph].

[52] S. Gieseke, C. Röhr, and A. Siódmok, *Colour reconnections in Herwig++*, Eur. Phys. J. C **72** (2012) 2225, arXiv: 1206.0041 [hep-ph].

[53] R. D. Ball et al., *Parton distributions for the LHC Run II*, JHEP **04** (2015) 040, arXiv: 1410.8849 [hep-ph].

[54] D. J. Lange, *The EvtGen particle decay simulation package*, Nucl. Instrum. Meth. A **462** (2001) 152 .

[55] ATLAS Collaboration, *ATLAS simulation of boson plus jets processes in Run 2*, ATL-PHYS-PUB-2017-006, 2017, URL: https://cds.cern.ch/record/2261937.

[56] T. Gleisberg et al., *Event generation with SHERPA 1.1*, JHEP **02** (2009) 007, arXiv: 0811.4622 [hep-ph].

[57] S. Schumann and F. Krauss, *A Parton shower algorithm based on Catani-Seymour dipole factorisation*, JHEP **03** (2008) 038, arXiv: 0709.1027 [hep-ph].

[58] ATLAS Collaboration, *Multi-Boson Simulation for* 13 *TeV ATLAS Analyses*, ATL-PHYS-PUB-2017-005, 2017, URL: https://cds.cern.ch/record/2261933.

[59] S. Agostinelli et al., *GEANT 4 — a simulation toolkit*, Nucl. Instrum. Meth. A **506** (2003) 250 .

[60] ATLAS Collaboration, *The ATLAS Simulation Infrastructure*, Eur. Phys. J. C **70** (2010) 823, arXiv: 1005.4568 [physics.ins-det].

[61] ATLAS Collaboration, *The simulation principle and performance of the ATLAS fast calorimeter simulation FastCaloSim*, ATL-PHYS-PUB-2010-013, 2010, URL: https://cds.cern.ch/record/1300517.

[62] ATLAS Collaboration, *Summary of ATLAS Pythia 8 tunes*, ATL-PHYS-PUB-2012-003, 2012, URL: https://cds.cern.ch/record/1474107.

[63] A. D. Martin, W. J. Stirling, R. S. Thorne, and G. Watt, *Parton distributions for the LHC*, Eur. Phys. J. C **63** (2009) 189, arXiv: 0901.0002 [hep-ph].

[64] ATLAS Collaboration, *Vertex Reconstruction Performance of the ATLAS Detector at* $\sqrt{s}$ = 13 *TeV*, ATL-PHYS-PUB-2015-026, 2015, URL: https://cds.cern.ch/record/2037717.

[65] ATLAS Collaboration, *Properties of jets and inputs to jet reconstruction and calibration with the ATLAS detector using proton–proton collisions at* $\sqrt{s}$ = 13 *TeV*, ATL-PHYS-PUB-2015-036, 2015, URL: https://cds.cern.ch/record/2044564.

[66] ATLAS Collaboration, *Topological cell clustering in the ATLAS calorimeters and its performance in LHC Run 1*, Eur. Phys. J. C **77** (2017) 490, arXiv: 1603.02934 [hep-ex].

[67] M. Cacciari, G. P. Salam, and G. Soyez, *The anti-k_t jet clustering algorithm*, JHEP **04** (2008) 063, arXiv: 0802.1189 [hep-ph].

[68] ATLAS Collaboration, *Jet energy scale measurements and their systematic uncertainties in proton-proton collisions at* $\sqrt{s}$ = 13 *TeV with the ATLAS detector*, Phys. Rev. D **96** (2017) 072002, arXiv: 1703.09665 [hep-ex].

[69] ATLAS Collaboration,
Selection of jets produced in 13 *TeV proton–proton collisions with the ATLAS detector*,
ATLAS-CONF-2015-029, 2015, URL: https://cds.cern.ch/record/2037702.

[70] ATLAS Collaboration, *Performance of pile-up mitigation techniques for jets in pp collisions at* $\sqrt{s}$ = 8 *TeV using the ATLAS detector*, Eur. Phys. J. C **76** (2016) 581,
arXiv: 1510.03823 [hep-ex].

[71] ATLAS Collaboration, *Performance of b-jet identification in the ATLAS experiment*,
JINST **11** (2016) P04008, arXiv: 1512.01094 [hep-ex].

[72] ATLAS Collaboration,
Optimisation of the ATLAS b-tagging performance for the 2016 LHC Run,
ATL-PHYS-PUB-2016-012, 2016, URL: https://cds.cern.ch/record/2160731.

[73] ATLAS Collaboration, *Reconstruction, Energy Calibration, and Identification of Hadronically Decaying Tau Leptons in the ATLAS Experiment for Run-2 of the LHC*,
ATL-PHYS-PUB-2015-045, 2015, URL: https://cds.cern.ch/record/2064383.

[74] ATLAS Collaboration, *Identification and energy calibration of hadronically decaying tau leptons with the ATLAS experiment in pp collisions at* $\sqrt{s}$ = 8 *TeV*, Eur. Phys. J. C **75** (2015) 303,
arXiv: 1412.7086 [hep-ex].

[75] ATLAS Collaboration, *Measurement of the tau lepton reconstruction and identification performance in the ATLAS experiment using pp collisions at* $\sqrt{s}$ = 13 *TeV*,
ATLAS-CONF-2017-029, 2017, URL: https://cds.cern.ch/record/2261772.

[76] ATLAS Collaboration, *Electron efficiency measurements with the ATLAS detector using the 2015 LHC proton–proton collision data*, ATLAS-CONF-2016-024, 2016,
URL: https://cds.cern.ch/record/2157687.

[77] ATLAS Collaboration, *Electron efficiency measurements with the ATLAS detector using 2012 LHC proton–proton collision data*, Eur. Phys. J. C **77** (2017) 195,
arXiv: 1612.01456 [hep-ex].

[78] ATLAS Collaboration, *Muon reconstruction performance of the ATLAS detector in proton–proton collision data at* $\sqrt{s}$ = 13 *TeV*, Eur. Phys. J. C **76** (2016) 292,
arXiv: 1603.05598 [hep-ex].

[79] ATLAS Collaboration, *Expected performance of missing transverse momentum reconstruction for the ATLAS detector at* $\sqrt{s}$ = 13 *TeV*, ATL-PHYS-PUB-2015-023, 2015,
URL: https://cds.cern.ch/record/2037700.

[80] ATLAS Collaboration, *Performance of missing transverse momentum reconstruction with the ATLAS detector in the first proton–proton collisions at* $\sqrt{s}$ = 13 *TeV*,
ATL-PHYS-PUB-2015-027, 2015, URL: https://cds.cern.ch/record/2037904.

[81] C. G. Lester and D. J. Summers,
Measuring masses of semi-invisibly decaying particles pair produced at hadron colliders,
Phys. Lett. B **463** (1999) 99, arXiv: hep-ph/9906349 [hep-ph].

[82] A. Barr, C. Lester, and P. Stephens, *A variable for measuring masses at hadron colliders when missing energy is expected; m_{T2}: the truth behind the glamour*, J. Phys. G **29** (2003) 2343,
arXiv: hep-ph/0304226.

[83] C. G. Lester and B. Nachman, *Bisection-based asymmetric M_{T2} computation: a higher precision calculator than existing symmetric methods*, JHEP **03** (2015) 100, arXiv: 1411.4312 [hep-ph].

[84] R. D. Cousins, J. T. Linnemann, and J. Tucker,
Evaluation of three methods for calculating statistical significance when incorporating a systematic uncertainty into a test of the background-only hypothesis for a Poisson process,
Nucl. Instrum. Meth. A **595** (2008) 480, arXiv: physics/0702156.

[85] R. D. Cousins, K. E. Hymes, and J. Tucker, *Frequentist evaluation of intervals estimated for a binomial parameter and for the ratio of Poisson means*, Nucl. Instrum. Meth. A **612** (2010) 388 , arXiv: 0905.3831 [physics.data-an].

[86] ATLAS Collaboration, *Multi-boson simulation for* 13 *TeV ATLAS analyses*,
ATL-PHYS-PUB-2016-002, 2016, URL: https://cds.cern.ch/record/2119986.

[87] ATLAS Collaboration, *Monte Carlo Generators for the Production of a W or Z/γ^* Boson in Association with Jets at ATLAS in Run 2*, ATL-PHYS-PUB-2016-003, 2016,
URL: https://cds.cern.ch/record/2120133.

[88] ATLAS Collaboration,
Modelling of the $t\bar{t}H$ and $t\bar{t}V(V = W, Z)$ processes for $\sqrt{s} = 13$ TeV ATLAS analyses,
ATL-PHYS-PUB-2016-005, 2016, URL: https://cds.cern.ch/record/2120826.

[89] M. Aliev et al., *HATHOR: HAdronic Top and Heavy quarks crOss section calculatoR*,
Comput. Phys. Commun. **182** (2011) 1034, arXiv: 1007.1327 [hep-ph].

[90] P. Kant et al., *HatHor for single top-quark production: Updated predictions and uncertainty estimates for single top-quark production in hadronic collisions*,
Comput. Phys. Commun. **191** (2015) 74, arXiv: 1406.4403 [hep-ph].

[91] N. Kidonakis, *Two-loop soft anomalous dimensions for single top quark associated production with a W^- or H^-*, Phys. Rev. D **82** (2010) 054018, arXiv: 1005.4451 [hep-ph].

[92] N. Kidonakis, "Top Quark Production," *Proceedings, Helmholtz International Summer School on Physics of Heavy Quarks and Hadrons (HQ 2013): JINR, Dubna, Russia, July 15-28, 2013*, 2014 139, arXiv: 1311.0283 [hep-ph].

[93] ATLAS Collaboration, *Jet Calibration and Systematic Uncertainties for Jets Reconstructed in the ATLAS Detector at $\sqrt{s} = 13$ TeV*, ATL-PHYS-PUB-2015-015, 2015,
URL: https://cds.cern.ch/record/2037613.

[94] ATLAS Collaboration,
Simulation of top-quark production for the ATLAS experiment at $\sqrt{s} = 13$ TeV,
ATL-PHYS-PUB-2016-004, 2016, URL: https://cds.cern.ch/record/2120417.

[95] S. Frixione, E. Laenen, P. Motylinski, B. R. Webber, and C. D. White,
Single-top hadroproduction in association with a W boson, JHEP **07** (2008) 029,
arXiv: 0805.3067 [hep-ph].

[96] ATLAS Collaboration, *Measurement of $W^\pm$ and Z-boson production cross sections in pp collisions at $\sqrt{s} = 13$ TeV with the ATLAS detector*, Phys. Lett. B **759** (2016) 601,
arXiv: 1603.09222 [hep-ex].

[97] N. Kidonakis, *NNLL resummation for s-channel single top quark production*,
Phys. Rev. D **81** (2010) 054028, arXiv: 1001.5034 [hep-ph].

[98] N. Kidonakis, *Next-to-next-to-leading-order collinear and soft gluon corrections for t-channel single top quark production*, Phys. Rev. D **83** (2011) 091503, arXiv: 1103.2792 [hep-ph].

[99] C. Borschensky et al.,
Squark and gluino production cross sections in pp collisions at $\sqrt{s}$ = 13, 14, 33 and 100 TeV,
Eur. Phys. J. C **74** (2014) 3174, arXiv: 1407.5066 [hep-ph].

[100] M. Baak et al., *HistFitter software framework for statistical data analysis*,
Eur. Phys. J. C **75** (2015) 153, arXiv: 1410.1280 [hep-ex].

[101] G. Cowan, K. Cranmer, E. Gross, and O. Vitells,
Asymptotic formulae for likelihood-based tests of new physics, Eur. Phys. J. C **71** (2011) 1554,
arXiv: 1007.1727 [physics.data-an], Erratum: Eur. Phys. J. C **73** (2013) 2501.

[102] A. L. Read, *Presentation of search results: the CL_s technique*, J. Phys. G **28** (2002) 2693.

[103] ATLAS Collaboration, *ATLAS Computing Acknowledgements*, ATL-GEN-PUB-2016-002,
URL: https://cds.cern.ch/record/2202407.

The ATLAS Collaboration

M. Aaboud[137d], G. Aad[88], B. Abbott[115], O. Abdinov[12,*], B. Abeloos[119], S.H. Abidi[161], O.S. AbouZeid[139], N.L. Abraham[151], H. Abramowicz[155], H. Abreu[154], Y. Abulaiti[6], B.S. Acharya[167a,167b,a], S. Adachi[157], L. Adamczyk[41a], J. Adelman[110], M. Adersberger[102], T. Adye[133], A.A. Affolder[139], Y. Afik[154], C. Agheorghiesei[28c], J.A. Aguilar-Saavedra[128a,128f], F. Ahmadov[68,b], G. Aielli[135a,135b], S. Akatsuka[71], T.P.A. Åkesson[84], E. Akilli[52], A.V. Akimov[98], G.L. Alberghi[22a,22b], J. Albert[172], P. Albicocco[50], M.J. Alconada Verzini[74], S. Alderweireldt[108], M. Aleksa[32], I.N. Aleksandrov[68], C. Alexa[28b], G. Alexander[155], T. Alexopoulos[10], M. Alhroob[115], B. Ali[130], M. Aliev[76a,76b], G. Alimonti[94a], J. Alison[33], S.P. Alkire[140], C. Allaire[119], B.M.M. Allbrooke[151], B.W. Allen[118], P.P. Allport[19], A. Aloisio[106a,106b], A. Alonso[39], F. Alonso[74], C. Alpigiani[140], A.A. Alshehri[56], M.I. Alstaty[88], B. Alvarez Gonzalez[32], D. Álvarez Piqueras[170], M.G. Alviggi[106a,106b], B.T. Amadio[16], Y. Amaral Coutinho[26a], L. Ambroz[122], C. Amelung[25], D. Amidei[92], S.P. Amor Dos Santos[128a,128c], S. Amoroso[32], C. Anastopoulos[141], L.S. Ancu[52], N. Andari[19], T. Andeen[11], C.F. Anders[60b], J.K. Anders[18], K.J. Anderson[33], A. Andreazza[94a,94b], V. Andrei[60a], S. Angelidakis[37], I. Angelozzi[109], A. Angerami[38], A.V. Anisenkov[111,c], A. Annovi[126a], C. Antel[60a], M.T. Anthony[141], M. Antonelli[50], A. Antonov[100,*], D.J.A. Antrim[166], F. Anulli[134a], M. Aoki[69], L. Aperio Bella[32], G. Arabidze[93], Y. Arai[69], J.P. Araque[128a], V. Araujo Ferraz[26a], R. Araujo Pereira[26a], A.T.H. Arce[48], R.E. Ardell[80], F.A. Arduh[74], J-F. Arguin[97], S. Argyropoulos[66], A.J. Armbruster[32], L.J. Armitage[79], O. Arnaez[161], H. Arnold[109], M. Arratia[30], O. Arslan[23], A. Artamonov[99,*], G. Artoni[122], S. Artz[86], S. Asai[157], N. Asbah[45], A. Ashkenazi[155], L. Asquith[151], K. Assamagan[27], R. Astalos[146a], R.J. Atkin[147a], M. Atkinson[169], N.B. Atlay[143], K. Augsten[130], G. Avolio[32], R. Avramidou[36a], B. Axen[16], M.K. Ayoub[35a], G. Azuelos[97,d], A.E. Baas[60a], M.J. Baca[19], H. Bachacou[138], K. Bachas[76a,76b], M. Backes[122], P. Bagnaia[134a,134b], M. Bahmani[42], H. Bahrasemani[144], J.T. Baines[133], M. Bajic[39], O.K. Baker[179], P.J. Bakker[109], D. Bakshi Gupta[82], E.M. Baldin[111,c], P. Balek[175], F. Balli[138], W.K. Balunas[124], E. Banas[42], A. Bandyopadhyay[23], Sw. Banerjee[176,e], A.A.E. Bannoura[177], L. Barak[155], W.M. Barbe[37], E.L. Barberio[91], D. Barberis[53a,53b], M. Barbero[88], T. Barillari[103], M-S Barisits[65], J.T. Barkeloo[118], T. Barklow[145], N. Barlow[30], R. Barnea[154], S.L. Barnes[36c], B.M. Barnett[133], R.M. Barnett[16], Z. Barnovska-Blenessy[36a], A. Baroncelli[136a], G. Barone[25], A.J. Barr[122], L. Barranco Navarro[170], F. Barreiro[85], J. Barreiro Guimarães da Costa[35a], R. Bartoldus[145], A.E. Barton[75], P. Bartos[146a], A. Basalaev[125], A. Bassalat[119], R.L. Bates[56], S.J. Batista[161], J.R. Batley[30], M. Battaglia[139], M. Bauce[134a,134b], F. Bauer[138], K.T. Bauer[166], H.S. Bawa[145,f], J.B. Beacham[113], M.D. Beattie[75], T. Beau[83], P.H. Beauchemin[165], P. Bechtle[23], H.P. Beck[18,g], H.C. Beck[58], K. Becker[122], M. Becker[86], C. Becot[112], A.J. Beddall[20e], A. Beddall[20b], V.A. Bednyakov[68], M. Bedognetti[109], C.P. Bee[150], T.A. Beermann[32], M. Begalli[26a], M. Begel[27], A. Behera[150], J.K. Behr[45], A.S. Bell[81], G. Bella[155], L. Bellagamba[22a], A. Bellerive[31], M. Bellomo[154], K. Belotskiy[100], N.L. Belyaev[100], O. Benary[155,*], D. Benchekroun[137a], M. Bender[102], N. Benekos[10], Y. Benhammou[155], E. Benhar Noccioli[179], J. Benitez[66], D.P. Benjamin[48], M. Benoit[52], J.R. Bensinger[25], S. Bentvelsen[109], L. Beresford[122], M. Beretta[50], D. Berge[45], E. Bergeaas Kuutmann[168], N. Berger[5], L.J. Bergsten[25], J. Beringer[16], S. Berlendis[57], N.R. Bernard[89], G. Bernardi[83], C. Bernius[145], F.U. Bernlochner[23], T. Berry[80], P. Berta[86], C. Bertella[35a], G. Bertoli[148a,148b], I.A. Bertram[75], C. Bertsche[45], G.J. Besjes[39], O. Bessidskaia Bylund[148a,148b], M. Bessner[45], N. Besson[138], A. Bethani[87], S. Bethke[103], A. Betti[23], A.J. Bevan[79], J. Beyer[103], R.M. Bianchi[127], O. Biebel[102], D. Biedermann[17], R. Bielski[87], K. Bierwagen[86], N.V. Biesuz[126a,126b], M. Biglietti[136a], T.R.V. Billoud[97], M. Bindi[58], A. Bingul[20b], C. Bini[134a,134b], S. Biondi[22a,22b], T. Bisanz[58], C. Bittrich[47], D.M. Bjergaard[48], J.E. Black[145], K.M. Black[24], R.E. Blair[6], T. Blazek[146a], I. Bloch[45], C. Blocker[25], A. Blue[56], U. Blumenschein[79],

Dr. Blunier[34a], G.J. Bobbink[109], V.S. Bobrovnikov[111,c], S.S. Bocchetta[84], A. Bocci[48], C. Bock[102], D. Boerner[177], D. Bogavac[102], A.G. Bogdanchikov[111], C. Bohm[148a], V. Boisvert[80], P. Bokan[168,h], T. Bold[41a], A.S. Boldyrev[101], A.E. Bolz[60b], M. Bomben[83], M. Bona[79], J.S. Bonilla[118], M. Boonekamp[138], A. Borisov[132], G. Borissov[75], J. Bortfeldt[32], D. Bortoletto[122], V. Bortolotto[62a], D. Boscherini[22a], M. Bosman[13], J.D. Bossio Sola[29], J. Boudreau[127], E.V. Bouhova-Thacker[75], D. Boumediene[37], C. Bourdarios[119], S.K. Boutle[56], A. Boveia[113], J. Boyd[32], I.R. Boyko[68], A.J. Bozson[80], J. Bracinik[19], A. Brandt[8], G. Brandt[177], O. Brandt[60a], F. Braren[45], U. Bratzler[158], B. Brau[89], J.E. Brau[118], W.D. Breaden Madden[56], K. Brendlinger[45], A.J. Brennan[91], L. Brenner[45], R. Brenner[168], S. Bressler[175], D.L. Briglin[19], T.M. Bristow[49], D. Britton[56], D. Britzger[60b], I. Brock[23], R. Brock[93], G. Brooijmans[38], T. Brooks[80], W.K. Brooks[34b], E. Brost[110], J.H Broughton[19], P.A. Bruckman de Renstrom[42], D. Bruncko[146b], A. Bruni[22a], G. Bruni[22a], L.S. Bruni[109], S. Bruno[135a,135b], B.H. Brunt[30], M. Bruschi[22a], N. Bruscino[127], P. Bryant[33], L. Bryngemark[45], T. Buanes[15], Q. Buat[32], P. Buchholz[143], A.G. Buckley[56], I.A. Budagov[68], F. Buehrer[51], M.K. Bugge[121], O. Bulekov[100], D. Bullock[8], T.J. Burch[110], S. Burdin[77], C.D. Burgard[109], A.M. Burger[5], B. Burghgrave[110], K. Burka[42], S. Burke[133], I. Burmeister[46], J.T.P. Burr[122], D. Büscher[51], V. Büscher[86], E. Buschmann[58], P. Bussey[56], J.M. Butler[24], C.M. Buttar[56], J.M. Butterworth[81], P. Butti[32], W. Buttinger[32], A. Buzatu[153], A.R. Buzykaev[111,c], G. Cabras[22a,22b], S. Cabrera Urbán[170], D. Caforio[130], H. Cai[169], V.M.M. Cairo[2], O. Cakir[4a], N. Calace[52], P. Calafiura[16], A. Calandri[88], G. Calderini[83], P. Calfayan[64], G. Callea[40a,40b], L.P. Caloba[26a], S. Calvente Lopez[85], D. Calvet[37], S. Calvet[37], T.P. Calvet[150], M. Calvetti[126a,126b], R. Camacho Toro[33], S. Camarda[32], P. Camarri[135a,135b], D. Cameron[121], R. Caminal Armadans[89], C. Camincher[57], S. Campana[32], M. Campanelli[81], A. Camplani[94a,94b], A. Campoverde[143], V. Canale[106a,106b], M. Cano Bret[36c], J. Cantero[116], T. Cao[155], Y. Cao[169], M.D.M. Capeans Garrido[32], I. Caprini[28b], M. Caprini[28b], M. Capua[40a,40b], R.M. Carbone[38], R. Cardarelli[135a], F. Cardillo[51], I. Carli[131], T. Carli[32], G. Carlino[106a], B.T. Carlson[127], L. Carminati[94a,94b], R.M.D. Carney[148a,148b], S. Caron[108], E. Carquin[34b], S. Carrá[94a,94b], G.D. Carrillo-Montoya[32], D. Casadei[19], M.P. Casado[13,i], A.F. Casha[161], M. Casolino[13], D.W. Casper[166], R. Castelijn[109], V. Castillo Gimenez[170], N.F. Castro[128a,128e], A. Catinaccio[32], J.R. Catmore[121], A. Cattai[32], J. Caudron[23], V. Cavaliere[27], E. Cavallaro[13], D. Cavalli[94a], M. Cavalli-Sforza[13], V. Cavasinni[126a,126b], E. Celebi[20d], F. Ceradini[136a,136b], L. Cerda Alberich[170], A.S. Cerqueira[26b], A. Cerri[151], L. Cerrito[135a,135b], F. Cerutti[16], A. Cervelli[22a,22b], S.A. Cetin[20d], A. Chafaq[137a], DC Chakraborty[110], S.K. Chan[59], W.S. Chan[109], Y.L. Chan[62a], P. Chang[169], J.D. Chapman[30], D.G. Charlton[19], C.C. Chau[31], C.A. Chavez Barajas[151], S. Che[113], A. Chegwidden[93], S. Chekanov[6], S.V. Chekulaev[163a], G.A. Chelkov[68,j], M.A. Chelstowska[32], C. Chen[36a], C. Chen[67], H. Chen[27], J. Chen[36a], J. Chen[38], S. Chen[35b], S. Chen[124], X. Chen[35c,k], Y. Chen[70], Y.-H. Chen[45], H.C. Cheng[92], H.J. Cheng[35a,35d], A. Cheplakov[68], E. Cheremushkina[132], R. Cherkaoui El Moursli[137e], E. Cheu[7], K. Cheung[63], L. Chevalier[138], V. Chiarella[50], G. Chiarelli[126a], G. Chiodini[76a], A.S. Chisholm[32], A. Chitan[28b], I. Chiu[157], Y.H. Chiu[172], M.V. Chizhov[68], K. Choi[64], A.R. Chomont[37], S. Chouridou[156], Y.S. Chow[109], V. Christodoulou[81], M.C. Chu[62a], J. Chudoba[129], A.J. Chuinard[90], J.J. Chwastowski[42], L. Chytka[117], D. Cinca[46], V. Cindro[78], I.A. Cioară[23], A. Ciocio[16], F. Cirotto[106a,106b], Z.H. Citron[175], M. Citterio[94a], A. Clark[52], M.R. Clark[38], P.J. Clark[49], R.N. Clarke[16], C. Clement[148a,148b], Y. Coadou[88], M. Cobal[167a,167c], A. Coccaro[53a,53b], J. Cochran[67], L. Colasurdo[108], B. Cole[38], A.P. Colijn[109], J. Collot[57], P. Conde Muiño[128a,128b], E. Coniavitis[51], S.H. Connell[147b], I.A. Connelly[87], S. Constantinescu[28b], G. Conti[32], F. Conventi[106a,l], A.M. Cooper-Sarkar[122], F. Cormier[171], K.J.R. Cormier[161], M. Corradi[134a,134b], E.E. Corrigan[84], F. Corriveau[90,m], A. Cortes-Gonzalez[32], M.J. Costa[170], D. Costanzo[141], G. Cottin[30], G. Cowan[80], B.E. Cox[87], J. Crane[87], K. Cranmer[112], S.J. Crawley[56], R.A. Creager[124], G. Cree[31], S. Crépé-Renaudin[57], F. Crescioli[83], M. Cristinziani[23], V. Croft[112], G. Crosetti[40a,40b], A. Cueto[85], T. Cuhadar Donszelmann[141], A.R. Cukierman[145], M. Curatolo[50], J. Cúth[86], S. Czekierda[42], P. Czodrowski[32], G. D'amen[22a,22b],

S. D'Auria[56], L. D'Eramo[83], M. D'Onofrio[77], M.J. Da Cunha Sargedas De Sousa[128a,128b], C. Da Via[87], W. Dabrowski[41a], T. Dado[146a,h], S. Dahbi[137e], T. Dai[92], O. Dale[15], F. Dallaire[97], C. Dallapiccola[89], M. Dam[39], J.R. Dandoy[124], M.F. Daneri[29], N.P. Dang[176,e], N.D Dann[87], M. Danninger[171], M. Dano Hoffmann[138], V. Dao[32], G. Darbo[53a], S. Darmora[8], O. Dartsi[5], A. Dattagupta[118], T. Daubney[45], W. Davey[23], C. David[45], T. Davidek[131], D.R. Davis[48], E. Dawe[91], I. Dawson[141], K. De[8], R. de Asmundis[106a], A. De Benedetti[115], S. De Castro[22a,22b], S. De Cecco[83], N. De Groot[108], P. de Jong[109], H. De la Torre[93], F. De Lorenzi[67], A. De Maria[58,n], D. De Pedis[134a], A. De Salvo[134a], U. De Sanctis[135a,135b], A. De Santo[151], K. De Vasconcelos Corga[88], J.B. De Vivie De Regie[119], C. Debenedetti[139], D.V. Dedovich[68], N. Dehghanian[3], I. Deigaard[109], M. Del Gaudio[40a,40b], J. Del Peso[85], D. Delgove[119], F. Deliot[138], C.M. Delitzsch[7], A. Dell'Acqua[32], L. Dell'Asta[24], M. Della Pietra[106a,106b], D. della Volpe[52], M. Delmastro[5], C. Delporte[119], P.A. Delsart[57], D.A. DeMarco[161], S. Demers[179], M. Demichev[68], S.P. Denisov[132], D. Denysiuk[109], D. Derendarz[42], J.E. Derkaoui[137d], F. Derue[83], P. Dervan[77], K. Desch[23], C. Deterre[45], K. Dette[161], M.R. Devesa[29], P.O. Deviveiros[32], A. Dewhurst[133], S. Dhaliwal[25], F.A. Di Bello[52], A. Di Ciaccio[135a,135b], L. Di Ciaccio[5], W.K. Di Clemente[124], C. Di Donato[106a,106b], A. Di Girolamo[32], B. Di Micco[136a,136b], R. Di Nardo[32], K.F. Di Petrillo[59], A. Di Simone[51], R. Di Sipio[161], D. Di Valentino[31], C. Diaconu[88], M. Diamond[161], F.A. Dias[39], T. Dias do Vale[128a], M.A. Diaz[34a], J. Dickinson[16], E.B. Diehl[92], J. Dietrich[17], S. Díez Cornell[45], A. Dimitrievska[16], J. Dingfelder[23], P. Dita[28b], S. Dita[28b], F. Dittus[32], F. Djama[88], T. Djobava[54b], J.I. Djuvsland[60a], M.A.B. do Vale[26c], M. Dobre[28b], D. Dodsworth[25], C. Doglioni[84], J. Dolejsi[131], Z. Dolezal[131], M. Donadelli[26d], J. Donini[37], J. Dopke[133], A. Doria[106a], M.T. Dova[74], A.T. Doyle[56], E. Drechsler[58], E. Dreyer[144], M. Dris[10], Y. Du[36b], J. Duarte-Campderros[155], F. Dubinin[98], A. Dubreuil[52], E. Duchovni[175], G. Duckeck[102], A. Ducourthial[83], O.A. Ducu[97,o], D. Duda[109], A. Dudarev[32], A.Chr. Dudder[86], E.M. Duffield[16], L. Duflot[119], M. Dührssen[32], C. Dülsen[177], M. Dumancic[175], A.E. Dumitriu[28b,p], A.K. Duncan[56], M. Dunford[60a], A. Duperrin[88], H. Duran Yildiz[4a], M. Düren[55], A. Durglishvili[54b], D. Duschinger[47], B. Dutta[45], D. Duvnjak[1], M. Dyndal[45], B.S. Dziedzic[42], C. Eckardt[45], K.M. Ecker[103], R.C. Edgar[92], T. Eifert[32], G. Eigen[15], K. Einsweiler[16], T. Ekelof[168], M. El Kacimi[137c], R. El Kosseifi[88], V. Ellajosyula[88], M. Ellert[168], F. Ellinghaus[177], A.A. Elliot[172], N. Ellis[32], J. Elmsheuser[27], M. Elsing[32], D. Emeliyanov[133], Y. Enari[157], J.S. Ennis[173], M.B. Epland[48], J. Erdmann[46], A. Ereditato[18], S. Errede[169], M. Escalier[119], C. Escobar[170], B. Esposito[50], O. Estrada Pastor[170], A.I. Etienvre[138], E. Etzion[155], H. Evans[64], A. Ezhilov[125], M. Ezzi[137e], F. Fabbri[22a,22b], L. Fabbri[22a,22b], V. Fabiani[108], G. Facini[81], R.M. Fakhrutdinov[132], S. Falciano[134a], J. Faltova[131], Y. Fang[35a], M. Fanti[94a,94b], A. Farbin[8], A. Farilla[136a], E.M. Farina[123a,123b], T. Farooque[93], S. Farrell[16], S.M. Farrington[173], P. Farthouat[32], F. Fassi[137e], P. Fassnacht[32], D. Fassouliotis[9], M. Faucci Giannelli[49], A. Favareto[53a,53b], W.J. Fawcett[52], L. Fayard[119], O.L. Fedin[125,q], W. Fedorko[171], M. Feickert[43], S. Feigl[121], L. Feligioni[88], C. Feng[36b], E.J. Feng[32], M. Feng[48], M.J. Fenton[56], A.B. Fenyuk[132], L. Feremenga[8], J. Ferrando[45], A. Ferrari[168], P. Ferrari[109], R. Ferrari[123a], D.E. Ferreira de Lima[60b], A. Ferrer[170], D. Ferrere[52], C. Ferretti[92], F. Fiedler[86], A. Filipčič[78], F. Filthaut[108], M. Fincke-Keeler[172], K.D. Finelli[24], M.C.N. Fiolhais[128a,128c,r], L. Fiorini[170], C. Fischer[13], J. Fischer[177], W.C. Fisher[93], N. Flaschel[45], I. Fleck[143], P. Fleischmann[92], R.R.M. Fletcher[124], T. Flick[177], B.M. Flierl[102], L.M. Flores[124], L.R. Flores Castillo[62a], N. Fomin[15], G.T. Forcolin[87], A. Formica[138], F.A. Förster[13], A.C. Forti[87], A.G. Foster[19], D. Fournier[119], H. Fox[75], S. Fracchia[141], P. Francavilla[126a,126b], M. Franchini[22a,22b], S. Franchino[60a], D. Francis[32], L. Franconi[121], M. Franklin[59], M. Frate[166], M. Fraternali[123a,123b], D. Freeborn[81], S.M. Fressard-Batraneanu[32], B. Freund[97], W.S. Freund[26a], D. Froidevaux[32], J.A. Frost[122], C. Fukunaga[158], T. Fusayasu[104], J. Fuster[170], O. Gabizon[154], A. Gabrielli[22a,22b], A. Gabrielli[16], G.P. Gach[41a], S. Gadatsch[52], S. Gadomski[80], P. Gadow[103], G. Gagliardi[53a,53b], L.G. Gagnon[97], C. Galea[108], B. Galhardo[128a,128c], E.J. Gallas[122], B.J. Gallop[133], P. Gallus[130], G. Galster[39], R. Gamboa Goni[79], K.K. Gan[113], S. Ganguly[175], Y. Gao[77],

Y.S. Gao[145,f], F.M. Garay Walls[34a], C. García[170], J.E. García Navarro[170], J.A. García Pascual[35a], M. Garcia-Sciveres[16], R.W. Gardner[33], N. Garelli[145], V. Garonne[121], K. Gasnikova[45], A. Gaudiello[53a,53b], G. Gaudio[123a], I.L. Gavrilenko[98], A. Gavrilyuk[99], C. Gay[171], G. Gaycken[23], E.N. Gazis[10], C.N.P. Gee[133], J. Geisen[58], M. Geisen[86], M.P. Geisler[60a], K. Gellerstedt[148a,148b], C. Gemme[53a], M.H. Genest[57], C. Geng[92], S. Gentile[134a,134b], C. Gentsos[156], S. George[80], D. Gerbaudo[13], G. Gessner[46], S. Ghasemi[143], M. Ghneimat[23], B. Giacobbe[22a], S. Giagu[134a,134b], N. Giangiacomi[22a,22b], P. Giannetti[126a], S.M. Gibson[80], M. Gignac[139], M. Gilchriese[16], D. Gillberg[31], G. Gilles[177], D.M. Gingrich[3,d], M.P. Giordani[167a,167c], F.M. Giorgi[22a], P.F. Giraud[138], P. Giromini[59], G. Giugliarelli[167a,167c], D. Giugni[94a], F. Giuli[122], M. Giulini[60b], S. Gkaitatzis[156], I. Gkialas[9,s], E.L. Gkougkousis[13], P. Gkountoumis[10], L.K. Gladilin[101], C. Glasman[85], J. Glatzer[13], P.C.F. Glaysher[45], A. Glazov[45], M. Goblirsch-Kolb[25], J. Godlewski[42], S. Goldfarb[91], T. Golling[52], D. Golubkov[132], A. Gomes[128a,128b,128d], R. Gonçalo[128a], R. Goncalves Gama[26b], G. Gonella[51], L. Gonella[19], A. Gongadze[68], F. Gonnella[19], J.L. Gonski[59], S. González de la Hoz[170], S. Gonzalez-Sevilla[52], L. Goossens[32], P.A. Gorbounov[99], H.A. Gordon[27], B. Gorini[32], E. Gorini[76a,76b], A. Gorišek[78], A.T. Goshaw[48], C. Gössling[46], M.I. Gostkin[68], C.A. Gottardo[23], C.R. Goudet[119], D. Goujdami[137c], A.G. Goussiou[140], N. Govender[147b,t], C. Goy[5], E. Gozani[154], I. Grabowska-Bold[41a], P.O.J. Gradin[168], E.C. Graham[77], J. Gramling[166], E. Gramstad[121], S. Grancagnolo[17], V. Gratchev[125], P.M. Gravila[28f], C. Gray[56], H.M. Gray[16], Z.D. Greenwood[82,u], C. Grefe[23], K. Gregersen[81], I.M. Gregor[45], P. Grenier[145], K. Grevtsov[45], J. Griffiths[8], A.A. Grillo[139], K. Grimm[145], S. Grinstein[13,v], Ph. Gris[37], J.-F. Grivaz[119], S. Groh[86], E. Gross[175], J. Grosse-Knetter[58], G.C. Grossi[82], Z.J. Grout[81], A. Grummer[107], L. Guan[92], W. Guan[176], J. Guenther[32], A. Guerguichon[119], F. Guescini[163a], D. Guest[166], O. Gueta[155], R. Gugel[51], B. Gui[113], T. Guillemin[5], S. Guindon[32], U. Gul[56], C. Gumpert[32], J. Guo[36c], W. Guo[92], Y. Guo[36a,w], R. Gupta[43], S. Gurbuz[20a], G. Gustavino[115], B.J. Gutelman[154], P. Gutierrez[115], N.G. Gutierrez Ortiz[81], C. Gutschow[81], C. Guyot[138], M.P. Guzik[41a], C. Gwenlan[122], C.B. Gwilliam[77], A. Haas[112], C. Haber[16], H.K. Hadavand[8], N. Haddad[137e], A. Hadef[88], S. Hageböck[23], M. Hagihara[164], H. Hakobyan[180,*], M. Haleem[178], J. Haley[116], G. Halladjian[93], G.D. Hallewell[88], K. Hamacher[177], P. Hamal[117], K. Hamano[172], A. Hamilton[147a], G.N. Hamity[141], K. Han[36a,x], L. Han[36a], S. Han[35a,35d], K. Hanagaki[69,y], M. Hance[139], D.M. Handl[102], B. Haney[124], R. Hankache[83], P. Hanke[60a], E. Hansen[84], J.B. Hansen[39], J.D. Hansen[39], M.C. Hansen[23], P.H. Hansen[39], K. Hara[164], A.S. Hard[176], T. Harenberg[177], S. Harkusha[95], P.F. Harrison[173], N.M. Hartmann[102], Y. Hasegawa[142], A. Hasib[49], S. Hassani[138], S. Haug[18], R. Hauser[93], L. Hauswald[47], L.B. Havener[38], M. Havranek[130], C.M. Hawkes[19], R.J. Hawkings[32], D. Hayden[93], C.P. Hays[122], J.M. Hays[79], H.S. Hayward[77], S.J. Haywood[133], M.P. Heath[49], T. Heck[86], V. Hedberg[84], L. Heelan[8], S. Heer[23], K.K. Heidegger[51], S. Heim[45], T. Heim[16], B. Heinemann[45,z], J.J. Heinrich[102], L. Heinrich[112], C. Heinz[55], J. Hejbal[129], L. Helary[32], A. Held[171], S. Hellesund[121], S. Hellman[148a,148b], C. Helsens[32], R.C.W. Henderson[75], Y. Heng[176], S. Henkelmann[171], A.M. Henriques Correia[32], G.H. Herbert[17], H. Herde[25], V. Herget[178], Y. Hernández Jiménez[147c], H. Herr[86], G. Herten[51], R. Hertenberger[102], L. Hervas[32], T.C. Herwig[124], G.G. Hesketh[81], N.P. Hessey[163a], J.W. Hetherly[43], S. Higashino[69], E. Higón-Rodriguez[170], K. Hildebrand[33], E. Hill[172], J.C. Hill[30], K.H. Hiller[45], S.J. Hillier[19], M. Hils[47], I. Hinchliffe[16], M. Hirose[120], D. Hirschbuehl[177], B. Hiti[78], O. Hladik[129], D.R. Hlaluku[147c], X. Hoad[49], J. Hobbs[150], N. Hod[163a], M.C. Hodgkinson[141], A. Hoecker[32], M.R. Hoeferkamp[107], F. Hoenig[102], D. Hohn[23], D. Hohov[119], T.R. Holmes[33], M. Holzbock[102], M. Homann[46], S. Honda[164], T. Honda[69], T.M. Hong[127], B.H. Hooberman[169], W.H. Hopkins[118], Y. Horii[105], A.J. Horton[144], L.A. Horyn[33], J-Y. Hostachy[57], A. Hostiuc[140], S. Hou[153], A. Hoummada[137a], J. Howarth[87], J. Hoya[74], M. Hrabovsky[117], J. Hrdinka[32], I. Hristova[17], J. Hrivnac[119], T. Hryn'ova[5], A. Hrynevich[96], P.J. Hsu[63], S.-C. Hsu[140], Q. Hu[27], S. Hu[36c], Y. Huang[35a], Z. Hubacek[130], F. Hubaut[88], F. Huegging[23], T.B. Huffman[122], E.W. Hughes[38], M. Huhtinen[32], R.F.H. Hunter[31], P. Huo[150], A.M. Hupe[31], N. Huseynov[68,b], J. Huston[93], J. Huth[59], R. Hyneman[92], G. Iacobucci[52],

G. Iakovidis[27], I. Ibragimov[143], L. Iconomidou-Fayard[119], Z. Idrissi[137e], P. Iengo[32], R. Ignazzi[39], O. Igonkina[109,aa], R. Iguchi[157], T. Iizawa[174], Y. Ikegami[69], M. Ikeno[69], D. Iliadis[156], N. Ilic[145], F. Iltzsche[47], G. Introzzi[123a,123b], M. Iodice[136a], K. Iordanidou[38], V. Ippolito[134a,134b], M.F. Isacson[168], N. Ishijima[120], M. Ishino[157], M. Ishitsuka[159], C. Issever[122], S. Istin[20a,ab], F. Ito[164], J.M. Iturbe Ponce[62a], R. Iuppa[162a,162b], H. Iwasaki[69], J.M. Izen[44], V. Izzo[106a], S. Jabbar[3], P. Jacka[129], P. Jackson[1], R.M. Jacobs[23], V. Jain[2], G. Jäkel[177], K.B. Jakobi[86], K. Jakobs[51], S. Jakobsen[65], T. Jakoubek[129], D.O. Jamin[116], D.K. Jana[82], R. Jansky[52], J. Janssen[23], M. Janus[58], P.A. Janus[41a], G. Jarlskog[84], N. Javadov[68,b], T. Javůrek[51], M. Javurkova[51], F. Jeanneau[138], L. Jeanty[16], J. Jejelava[54a,ac], A. Jelinskas[173], P. Jenni[51,ad], C. Jeske[173], S. Jézéquel[5], H. Ji[176], J. Jia[150], H. Jiang[67], Y. Jiang[36a], Z. Jiang[145], S. Jiggins[81], J. Jimenez Pena[170], S. Jin[35b], A. Jinaru[28b], O. Jinnouchi[159], H. Jivan[147c], P. Johansson[141], K.A. Johns[7], C.A. Johnson[64], W.J. Johnson[140], K. Jon-And[148a,148b], R.W.L. Jones[75], S.D. Jones[151], S. Jones[7], T.J. Jones[77], J. Jongmanns[60a], P.M. Jorge[128a,128b], J. Jovicevic[163a], X. Ju[176], J.J. Junggeburth[103], A. Juste Rozas[13,v], A. Kaczmarska[42], M. Kado[119], H. Kagan[113], M. Kagan[145], T. Kaji[174], E. Kajomovitz[154], C.W. Kalderon[84], A. Kaluza[86], S. Kama[43], A. Kamenshchikov[132], L. Kanjir[78], Y. Kano[157], V.A. Kantserov[100], J. Kanzaki[69], B. Kaplan[112], L.S. Kaplan[176], D. Kar[147c], K. Karakostas[10], N. Karastathis[10], M.J. Kareem[163b], E. Karentzos[10], S.N. Karpov[68], Z.M. Karpova[68], V. Kartvelishvili[75], A.N. Karyukhin[132], K. Kasahara[164], L. Kashif[176], R.D. Kass[113], A. Kastanas[149], Y. Kataoka[157], C. Kato[157], A. Katre[52], J. Katzy[45], K. Kawade[70], K. Kawagoe[73], T. Kawamoto[157], G. Kawamura[58], E.F. Kay[77], V.F. Kazanin[111,c], R. Keeler[172], R. Kehoe[43], J.S. Keller[31], E. Kellermann[84], J.J. Kempster[19], J. Kendrick[19], O. Kepka[129], B.P. Kerševan[78], S. Kersten[177], R.A. Keyes[90], M. Khader[169], F. Khalil-zada[12], A. Khanov[116], A.G. Kharlamov[111,c], T. Kharlamova[111], A. Khodinov[160], T.J. Khoo[52], V. Khovanskiy[99,*], E. Khramov[68], J. Khubua[54b,ae], S. Kido[70], M. Kiehn[52], C.R. Kilby[80], H.Y. Kim[8], S.H. Kim[164], Y.K. Kim[33], N. Kimura[167a,167c], O.M. Kind[17], B.T. King[77], D. Kirchmeier[47], J. Kirk[133], A.E. Kiryunin[103], T. Kishimoto[157], D. Kisielewska[41a], V. Kitali[45], O. Kivernyk[5], E. Kladiva[146b], T. Klapdor-Kleingrothaus[51], M.H. Klein[92], M. Klein[77], U. Klein[77], K. Kleinknecht[86], P. Klimek[110], A. Klimentov[27], R. Klingenberg[46,*], T. Klingl[23], T. Klioutchnikova[32], F.F. Klitzner[102], P. Kluit[109], S. Kluth[103], E. Kneringer[65], E.B.F.G. Knoops[88], A. Knue[51], A. Kobayashi[157], D. Kobayashi[73], T. Kobayashi[157], M. Kobel[47], M. Kocian[145], P. Kodys[131], T. Koffas[31], E. Koffeman[109], N.M. Köhler[103], T. Koi[145], M. Kolb[60b], I. Koletsou[5], T. Kondo[69], N. Kondrashova[36c], K. Köneke[51], A.C. König[108], T. Kono[69,af], R. Konoplich[112,ag], N. Konstantinidis[81], B. Konya[84], R. Kopeliansky[64], S. Koperny[41a], K. Korcyl[42], K. Kordas[156], A. Korn[81], I. Korolkov[13], E.V. Korolkova[141], O. Kortner[103], S. Kortner[103], T. Kosek[131], V.V. Kostyukhin[23], A. Kotwal[48], A. Koulouris[10], A. Kourkoumeli-Charalampidi[123a,123b], C. Kourkoumelis[9], E. Kourlitis[141], V. Kouskoura[27], A.B. Kowalewska[42], R. Kowalewski[172], T.Z. Kowalski[41a], C. Kozakai[157], W. Kozanecki[138], A.S. Kozhin[132], V.A. Kramarenko[101], G. Kramberger[78], D. Krasnopevtsev[100], M.W. Krasny[83], A. Krasznahorkay[32], D. Krauss[103], J.A. Kremer[41a], J. Kretzschmar[77], K. Kreutzfeldt[55], P. Krieger[161], F. Krieter[102], K. Krizka[16], K. Kroeninger[46], H. Kroha[103], J. Kroll[129], J. Kroll[124], J. Kroseberg[23], J. Krstic[14], U. Kruchonak[68], H. Krüger[23], N. Krumnack[67], M.C. Kruse[48], T. Kubota[91], S. Kuday[4b], J.T. Kuechler[177], S. Kuehn[32], A. Kugel[60a], F. Kuger[178], T. Kuhl[45], V. Kukhtin[68], R. Kukla[88], Y. Kulchitsky[95], S. Kuleshov[34b], Y.P. Kulinich[169], M. Kuna[57], T. Kunigo[71], A. Kupco[129], T. Kupfer[46], O. Kuprash[155], H. Kurashige[70], L.L. Kurchaninov[163a], Y.A. Kurochkin[95], M.G. Kurth[35a,35d], E.S. Kuwertz[172], M. Kuze[159], J. Kvita[117], T. Kwan[172], A. La Rosa[103], J.L. La Rosa Navarro[26d], L. La Rotonda[40a,40b], F. La Ruffa[40a,40b], C. Lacasta[170], F. Lacava[134a,134b], J. Lacey[45], D.P.J. Lack[87], H. Lacker[17], D. Lacour[83], E. Ladygin[68], R. Lafaye[5], B. Laforge[83], S. Lai[58], S. Lammers[64], W. Lampl[7], E. Lançon[27], U. Landgraf[51], M.P.J. Landon[79], M.C. Lanfermann[52], V.S. Lang[45], J.C. Lange[13], R.J. Langenberg[32], A.J. Lankford[166], F. Lanni[27], K. Lantzsch[23], A. Lanza[123a], A. Lapertosa[53a,53b], S. Laplace[83], J.F. Laporte[138], T. Lari[94a], F. Lasagni Manghi[22a,22b], M. Lassnig[32], T.S. Lau[62a],

A. Laudrain[119], A.T. Law[139], P. Laycock[77], M. Lazzaroni[94a,94b], B. Le[91], O. Le Dortz[83], E. Le Guirriec[88], E.P. Le Quilleuc[138], M. LeBlanc[7], T. LeCompte[6], F. Ledroit-Guillon[57], C.A. Lee[27], G.R. Lee[34a], S.C. Lee[153], L. Lee[59], B. Lefebvre[90], M. Lefebvre[172], F. Legger[102], C. Leggett[16], G. Lehmann Miotto[32], W.A. Leight[45], A. Leisos[156,ah], M.A.L. Leite[26d], R. Leitner[131], D. Lellouch[175], B. Lemmer[58], K.J.C. Leney[81], T. Lenz[23], B. Lenzi[32], R. Leone[7], S. Leone[126a], C. Leonidopoulos[49], G. Lerner[151], C. Leroy[97], R. Les[161], A.A.J. Lesage[138], C.G. Lester[30], M. Levchenko[125], J. Levêque[5], D. Levin[92], L.J. Levinson[175], M. Levy[19], D. Lewis[79], B. Li[36a,w], C.-Q. Li[36a], H. Li[36b], L. Li[36c], Q. Li[35a,35d], Q. Li[36a], S. Li[36c,36d], X. Li[36c], Y. Li[143], Z. Liang[35a], B. Liberti[135a], A. Liblong[161], K. Lie[62c], A. Limosani[152], C.Y. Lin[30], K. Lin[93], S.C. Lin[182], T.H. Lin[86], R.A. Linck[64], B.E. Lindquist[150], A.L. Lionti[52], E. Lipeles[124], A. Lipniacka[15], M. Lisovyi[60b], T.M. Liss[169,ai], A. Lister[171], A.M. Litke[139], J.D. Little[8], B.L Liu[6], B. Liu[67], H. Liu[92], H. Liu[27], J.K.K. Liu[122], J.B. Liu[36a], kliu Liu[83], M. Liu[36a], P. Liu[16], Y.L. Liu[36a], Y. Liu[36a], M. Livan[123a,123b], A. Lleres[57], J. Llorente Merino[35a], S.L. Lloyd[79], C.Y. Lo[62b], F. Lo Sterzo[43], E.M. Lobodzinska[45], P. Loch[7], F.K. Loebinger[87], A. Loesle[51], K.M. Loew[25], T. Lohse[17], K. Lohwasser[141], M. Lokajicek[129], B.A. Long[24], J.D. Long[169], R.E. Long[75], L. Longo[76a,76b], K.A. Looper[113], J.A. Lopez[34b], I. Lopez Paz[13], A. Lopez Solis[83], J. Lorenz[102], N. Lorenzo Martinez[5], M. Losada[21], P.J. Lösel[102], X. Lou[35a], X. Lou[45], A. Lounis[119], J. Love[6], P.A. Love[75], H. Lu[62a], N. Lu[92], Y.J. Lu[63], H.J. Lubatti[140], C. Luci[134a,134b], A. Lucotte[57], C. Luedtke[51], F. Luehring[64], I. Luise[83], W. Lukas[65], L. Luminari[134a], B. Lund-Jensen[149], M.S. Lutz[89], P.M. Luzi[83], D. Lynn[27], R. Lysak[129], E. Lytken[84], F. Lyu[35a], V. Lyubushkin[68], H. Ma[27], L.L. Ma[36b], Y. Ma[36b], G. Maccarrone[50], A. Macchiolo[103], C.M. Macdonald[141], B. Maček[78], J. Machado Miguens[124], D. Madaffari[170], R. Madar[37], W.F. Mader[47], A. Madsen[45], N. Madysa[47], J. Maeda[70], S. Maeland[15], T. Maeno[27], A.S. Maevskiy[101], V. Magerl[51], C. Maidantchik[26a], T. Maier[102], A. Maio[128a,128b,128d], O. Majersky[146a], S. Majewski[118], Y. Makida[69], N. Makovec[119], B. Malaescu[83], Pa. Malecki[42], V.P. Maleev[125], F. Malek[57], U. Mallik[66], D. Malon[6], C. Malone[30], S. Maltezos[10], S. Malyukov[32], J. Mamuzic[170], G. Mancini[50], I. Mandić[78], J. Maneira[128a,128b], L. Manhaes de Andrade Filho[26b], J. Manjarres Ramos[47], K.H. Mankinen[84], A. Mann[102], A. Manousos[65], B. Mansoulie[138], J.D. Mansour[35a], R. Mantifel[90], M. Mantoani[58], S. Manzoni[94a,94b], G. Marceca[29], L. March[52], L. Marchese[122], G. Marchiori[83], M. Marcisovsky[129], C.A. Marin Tobon[32], M. Marjanovic[37], D.E. Marley[92], F. Marroquim[26a], Z. Marshall[16], M.U.F Martensson[168], S. Marti-Garcia[170], C.B. Martin[113], T.A. Martin[173], V.J. Martin[49], B. Martin dit Latour[15], M. Martinez[13,v], V.I. Martinez Outschoorn[89], S. Martin-Haugh[133], V.S. Martoiu[28b], A.C. Martyniuk[81], A. Marzin[32], L. Masetti[86], T. Mashimo[157], R. Mashinistov[98], J. Masik[87], A.L. Maslennikov[111,c], L.H. Mason[91], L. Massa[135a,135b], P. Mastrandrea[5], A. Mastroberardino[40a,40b], T. Masubuchi[157], P. Mättig[177], J. Maurer[28b], S.J. Maxfield[77], D.A. Maximov[111,c], R. Mazini[153], I. Maznas[156], S.M. Mazza[139], N.C. Mc Fadden[107], G. Mc Goldrick[161], S.P. Mc Kee[92], A. McCarn[92], T.G. McCarthy[103], L.I. McClymont[81], E.F. McDonald[91], J.A. Mcfayden[32], G. Mchedlidze[58], M.A. McKay[43], S.J. McMahon[133], P.C. McNamara[91], C.J. McNicol[173], R.A. McPherson[172,m], Z.A. Meadows[89], S. Meehan[140], T. Megy[51], S. Mehlhase[102], A. Mehta[77], T. Meideck[57], B. Meirose[44], D. Melini[170,aj], B.R. Mellado Garcia[147c], J.D. Mellenthin[58], M. Melo[146a], F. Meloni[18], A. Melzer[23], S.B. Menary[87], L. Meng[77], X.T. Meng[92], A. Mengarelli[22a,22b], S. Menke[103], E. Meoni[40a,40b], S. Mergelmeyer[17], C. Merlassino[18], P. Mermod[52], L. Merola[106a,106b], C. Meroni[94a], F.S. Merritt[33], A. Messina[134a,134b], J. Metcalfe[6], A.S. Mete[166], C. Meyer[124], J-P. Meyer[138], J. Meyer[154], H. Meyer Zu Theenhausen[60a], F. Miano[151], R.P. Middleton[133], S. Miglioranzi[53a,53b], L. Mijović[49], G. Mikenberg[175], M. Mikestikova[129], M. Mikuž[78], M. Milesi[91], A. Milic[161], D.A. Millar[79], D.W. Miller[33], A. Milov[175], D.A. Milstead[148a,148b], A.A. Minaenko[132], I.A. Minashvili[54b], A.I. Mincer[112], B. Mindur[41a], M. Mineev[68], Y. Minegishi[157], Y. Ming[176], L.M. Mir[13], A. Mirto[76a,76b], K.P. Mistry[124], T. Mitani[174], J. Mitrevski[102], V.A. Mitsou[170], A. Miucci[18], P.S. Miyagawa[141], A. Mizukami[69], J.U. Mjörnmark[84], T. Mkrtchyan[180], M. Mlynarikova[131], T. Moa[148a,148b],

K. Mochizuki[97], P. Mogg[51], S. Mohapatra[38], S. Molander[148a,148b], R. Moles-Valls[23], M.C. Mondragon[93], K. Mönig[45], J. Monk[39], E. Monnier[88], A. Montalbano[144], J. Montejo Berlingen[32], F. Monticelli[74], S. Monzani[94a], R.W. Moore[3], N. Morange[119], D. Moreno[21], M. Moreno Llácer[32], P. Morettini[53a], M. Morgenstern[109], S. Morgenstern[32], D. Mori[144], T. Mori[157], M. Morii[59], M. Morinaga[174], V. Morisbak[121], A.K. Morley[32], G. Mornacchi[32], J.D. Morris[79], L. Morvaj[150], P. Moschovakos[10], M. Mosidze[54b], H.J. Moss[141], J. Moss[145,ak], K. Motohashi[159], R. Mount[145], E. Mountricha[27], E.J.W. Moyse[89], S. Muanza[88], F. Mueller[103], J. Mueller[127], R.S.P. Mueller[102], D. Muenstermann[75], P. Mullen[56], G.A. Mullier[18], F.J. Munoz Sanchez[87], P. Murin[146b], W.J. Murray[173,133], A. Murrone[94a,94b], M. Muškinja[78], C. Mwewa[147a], A.G. Myagkov[132,al], J. Myers[118], M. Myska[130], B.P. Nachman[16], O. Nackenhorst[46], K. Nagai[122], R. Nagai[69,af], K. Nagano[69], Y. Nagasaka[61], K. Nagata[164], M. Nagel[51], E. Nagy[88], A.M. Nairz[32], Y. Nakahama[105], K. Nakamura[69], T. Nakamura[157], I. Nakano[114], R.F. Naranjo Garcia[45], R. Narayan[11], D.I. Narrias Villar[60a], I. Naryshkin[125], T. Naumann[45], G. Navarro[21], R. Nayyar[7], H.A. Neal[92], P.Yu. Nechaeva[98], T.J. Neep[138], A. Negri[123a,123b], M. Negrini[22a], S. Nektarijevic[108], C. Nellist[58], M.E. Nelson[122], S. Nemecek[129], P. Nemethy[112], M. Nessi[32,am], M.S. Neubauer[169], M. Neumann[177], P.R. Newman[19], T.Y. Ng[62c], Y.S. Ng[17], H.D.N. Nguyen[88], T. Nguyen Manh[97], E. Nibigira[37], R.B. Nickerson[122], R. Nicolaidou[138], J. Nielsen[139], N. Nikiforou[11], V. Nikolaenko[132,al], I. Nikolic-Audit[83], K. Nikolopoulos[19], P. Nilsson[27], Y. Ninomiya[69], A. Nisati[134a], N. Nishu[36c], R. Nisius[103], I. Nitsche[46], T. Nitta[174], T. Nobe[157], Y. Noguchi[71], M. Nomachi[120], I. Nomidis[31], M.A. Nomura[27], T. Nooney[79], M. Nordberg[32], N. Norjoharuddeen[122], T. Novak[78], O. Novgorodova[47], R. Novotny[130], M. Nozaki[69], L. Nozka[117], K. Ntekas[166], E. Nurse[81], F. Nuti[91], K. O'Connor[25], D.C. O'Neil[144], A.A. O'Rourke[45], V. O'Shea[56], F.G. Oakham[31,d], H. Oberlack[103], T. Obermann[23], J. Ocariz[83], A. Ochi[70], I. Ochoa[38], J.P. Ochoa-Ricoux[34a], S. Oda[73], S. Odaka[69], A. Oh[87], S.H. Oh[48], C.C. Ohm[149], H. Ohman[168], H. Oide[53a,53b], H. Okawa[164], Y. Okumura[157], T. Okuyama[69], A. Olariu[28b], L.F. Oleiro Seabra[128a], S.A. Olivares Pino[34a], D. Oliveira Damazio[27], J.L. Oliver[1], M.J.R. Olsson[33], A. Olszewski[42], J. Olszowska[42], A. Onofre[128a,128e], K. Onogi[105], P.U.E. Onyisi[11,an], H. Oppen[121], M.J. Oreglia[33], Y. Oren[155], D. Orestano[136a,136b], E.C. Orgill[87], N. Orlando[62b], R.S. Orr[161], B. Osculati[53a,53b,*], R. Ospanov[36a], G. Otero y Garzon[29], H. Otono[73], M. Ouchrif[137d], F. Ould-Saada[121], A. Ouraou[138], K.P. Oussoren[109], Q. Ouyang[35a], M. Owen[56], R.E. Owen[19], V.E. Ozcan[20a], N. Ozturk[8], K. Pachal[144], A. Pacheco Pages[13], L. Pacheco Rodriguez[138], C. Padilla Aranda[13], S. Pagan Griso[16], M. Paganini[179], G. Palacino[64], S. Palazzo[40a,40b], S. Palestini[32], M. Palka[41b], D. Pallin[37], E.St. Panagiotopoulou[10], I. Panagoulias[10], C.E. Pandini[52], J.G. Panduro Vazquez[80], P. Pani[32], D. Pantea[28b], L. Paolozzi[52], Th.D. Papadopoulou[10], K. Papageorgiou[9,s], A. Paramonov[6], D. Paredes Hernandez[62b], B. Parida[36c], A.J. Parker[75], M.A. Parker[30], K.A. Parker[45], F. Parodi[53a,53b], J.A. Parsons[38], U. Parzefall[51], V.R. Pascuzzi[161], J.M.P Pasner[139], E. Pasqualucci[134a], S. Passaggio[53a], Fr. Pastore[80], P. Pasuwan[148a,148b], S. Pataraia[86], J.R. Pater[87], A. Pathak[176,e], T. Pauly[32], B. Pearson[103], S. Pedraza Lopez[170], R. Pedro[128a,128b], S.V. Peleganchuk[111,c], O. Penc[129], C. Peng[35a,35d], H. Peng[36a], J. Penwell[64], B.S. Peralva[26b], M.M. Perego[138], A.P. Pereira Peixoto[128a], D.V. Perepelitsa[27], F. Peri[17], L. Perini[94a,94b], H. Pernegger[32], S. Perrella[106a,106b], V.D. Peshekhonov[68,*], K. Peters[45], R.F.Y. Peters[87], B.A. Petersen[32], T.C. Petersen[39], E. Petit[57], A. Petridis[1], C. Petridou[156], P. Petroff[119], E. Petrolo[134a], M. Petrov[122], F. Petrucci[136a,136b], N.E. Pettersson[89], A. Peyaud[138], R. Pezoa[34b], T. Pham[91], F.H. Phillips[93], P.W. Phillips[133], G. Piacquadio[150], E. Pianori[173], A. Picazio[89], M.A. Pickering[122], R. Piegaia[29], J.E. Pilcher[33], A.D. Pilkington[87], M. Pinamonti[135a,135b], J.L. Pinfold[3], M. Pitt[175], M.-A. Pleier[27], V. Pleskot[131], E. Plotnikova[68], D. Pluth[67], P. Podberezko[111], R. Poettgen[84], R. Poggi[123a,123b], L. Poggioli[119], I. Pogrebnyak[93], D. Pohl[23], I. Pokharel[58], G. Polesello[123a], A. Poley[45], A. Policicchio[40a,40b], R. Polifka[32], A. Polini[22a], C.S. Pollard[45], V. Polychronakos[27], D. Ponomarenko[100], L. Pontecorvo[134a], G.A. Popeneciu[28d], D.M. Portillo Quintero[83], S. Pospisil[130], K. Potamianos[45], I.N. Potrap[68], C.J. Potter[30], H. Potti[11], T. Poulsen[84], J. Poveda[32], M.E. Pozo Astigarraga[32],

P. Pralavorio[88], S. Prell[67], D. Price[87], M. Primavera[76a], S. Prince[90], N. Proklova[100], K. Prokofiev[62c], F. Prokoshin[34b], S. Protopopescu[27], J. Proudfoot[6], M. Przybycien[41a], A. Puri[169], P. Puzo[119], J. Qian[92], Y. Qin[87], A. Quadt[58], M. Queitsch-Maitland[45], A. Qureshi[1], S.K. Radhakrishnan[150], P. Rados[91], F. Ragusa[94a,94b], G. Rahal[181], J.A. Raine[87], S. Rajagopalan[27], T. Rashid[119], S. Raspopov[5], M.G. Ratti[94a,94b], D.M. Rauch[45], F. Rauscher[102], S. Rave[86], B. Ravina[141], I. Ravinovich[175], J.H. Rawling[87], M. Raymond[32], A.L. Read[121], N.P. Readioff[57], M. Reale[76a,76b], D.M. Rebuzzi[123a,123b], A. Redelbach[178], G. Redlinger[27], R. Reece[139], R.G. Reed[147c], K. Reeves[44], L. Rehnisch[17], J. Reichert[124], A. Reiss[86], C. Rembser[32], H. Ren[35a,35d], M. Rescigno[134a], S. Resconi[94a], E.D. Resseguie[124], S. Rettie[171], E. Reynolds[19], O.L. Rezanova[111,c], P. Reznicek[131], R. Richter[103], S. Richter[81], E. Richter-Was[41b], O. Ricken[23], M. Ridel[83], P. Rieck[103], C.J. Riegel[177], O. Rifki[45], M. Rijssenbeek[150], A. Rimoldi[123a,123b], M. Rimoldi[18], L. Rinaldi[22a], G. Ripellino[149], B. Ristić[32], E. Ritsch[32], I. Riu[13], J.C. Rivera Vergara[34a], F. Rizatdinova[116], E. Rizvi[79], C. Rizzi[13], R.T. Roberts[87], S.H. Robertson[90,m], A. Robichaud-Veronneau[90], D. Robinson[30], J.E.M. Robinson[45], A. Robson[56], E. Rocco[86], C. Roda[126a,126b], Y. Rodina[88,ao], S. Rodriguez Bosca[170], A. Rodriguez Perez[13], D. Rodriguez Rodriguez[170], A.M. Rodríguez Vera[163b], S. Roe[32], C.S. Rogan[59], O. Røhne[121], R. Röhrig[103], J. Roloff[59], A. Romaniouk[100], M. Romano[22a,22b], E. Romero Adam[170], N. Rompotis[77], M. Ronzani[112], L. Roos[83], S. Rosati[134a], K. Rosbach[51], P. Rose[139], N.-A. Rosien[58], E. Rossi[106a,106b], L.P. Rossi[53a], L. Rossini[94a,94b], J.H.N. Rosten[30], R. Rosten[140], M. Rotaru[28b], J. Rothberg[140], D. Rousseau[119], D. Roy[147c], A. Rozanov[88], Y. Rozen[154], X. Ruan[147c], F. Rubbo[145], F. Rühr[51], A. Ruiz-Martinez[31], Z. Rurikova[51], N.A. Rusakovich[68], H.L. Russell[90], J.P. Rutherfoord[7], N. Ruthmann[32], E.M. Rüttinger[45], Y.F. Ryabov[125], M. Rybar[169], G. Rybkin[119], S. Ryu[6], A. Ryzhov[132], G.F. Rzehorz[58], P. Sabatini[58], G. Sabato[109], S. Sacerdoti[119], H.F-W. Sadrozinski[139], R. Sadykov[68], F. Safai Tehrani[134a], P. Saha[110], M. Sahinsoy[60a], M. Saimpert[45], M. Saito[157], T. Saito[157], H. Sakamoto[157], A. Sakharov[112], D. Salamani[52], G. Salamanna[136a,136b], J.E. Salazar Loyola[34b], D. Salek[109], P.H. Sales De Bruin[168], D. Salihagic[103], A. Salnikov[145], J. Salt[170], D. Salvatore[40a,40b], F. Salvatore[151], A. Salvucci[62a,62b,62c], A. Salzburger[32], D. Sammel[51], D. Sampsonidis[156], D. Sampsonidou[156], J. Sánchez[170], A. Sanchez Pineda[167a,167c], H. Sandaker[121], C.O. Sander[45], M. Sandhoff[177], C. Sandoval[21], D.P.C. Sankey[133], M. Sannino[53a,53b], Y. Sano[105], A. Sansoni[50], C. Santoni[37], H. Santos[128a], I. Santoyo Castillo[151], A. Sapronov[68], J.G. Saraiva[128a,128d], O. Sasaki[69], K. Sato[164], E. Sauvan[5], P. Savard[161,d], N. Savic[103], R. Sawada[157], C. Sawyer[133], L. Sawyer[82,u], C. Sbarra[22a], A. Sbrizzi[22a,22b], T. Scanlon[81], D.A. Scannicchio[166], J. Schaarschmidt[140], P. Schacht[103], B.M. Schachtner[102], D. Schaefer[33], L. Schaefer[124], J. Schaeffer[86], S. Schaepe[32], U. Schäfer[86], A.C. Schaffer[119], D. Schaile[102], R.D. Schamberger[150], V.A. Schegelsky[125], D. Scheirich[131], F. Schenck[17], M. Schernau[166], C. Schiavi[53a,53b], S. Schier[139], L.K. Schildgen[23], Z.M. Schillaci[25], E.J. Schioppa[32], M. Schioppa[40a,40b], K.E. Schleicher[51], S. Schlenker[32], K.R. Schmidt-Sommerfeld[103], K. Schmieden[32], C. Schmitt[86], S. Schmitt[45], S. Schmitz[86], U. Schnoor[51], L. Schoeffel[138], A. Schoening[60b], E. Schopf[23], M. Schott[86], J.F.P. Schouwenberg[108], J. Schovancova[32], S. Schramm[52], N. Schuh[86], A. Schulte[86], H.-C. Schultz-Coulon[60a], M. Schumacher[51], B.A. Schumm[139], Ph. Schune[138], A. Schwartzman[145], T.A. Schwarz[92], H. Schweiger[87], Ph. Schwemling[138], R. Schwienhorst[93], A. Sciandra[23], G. Sciolla[25], M. Scornajenghi[40a,40b], F. Scuri[126a], F. Scutti[91], L.M. Scyboz[103], J. Searcy[92], P. Seema[23], S.C. Seidel[107], A. Seiden[139], J.M. Seixas[26a], G. Sekhniaidze[106a], K. Sekhon[92], S.J. Sekula[43], N. Semprini-Cesari[22a,22b], S. Senkin[37], C. Serfon[121], L. Serin[119], L. Serkin[167a,167b], M. Sessa[136a,136b], H. Severini[115], T. Šfiligoj[78], F. Sforza[165], A. Sfyrla[52], E. Shabalina[58], J.D. Shahinian[139], N.W. Shaikh[148a,148b], L.Y. Shan[35a], R. Shang[169], J.T. Shank[24], M. Shapiro[16], A. Sharma[122], A.S. Sharma[1], P.B. Shatalov[99], K. Shaw[167a,167b], S.M. Shaw[87], A. Shcherbakova[148a,148b], C.Y. Shehu[151], Y. Shen[115], N. Sherafati[31], A.D. Sherman[24], P. Sherwood[81], L. Shi[153,ap], S. Shimizu[70], C.O. Shimmin[179], M. Shimojima[104], I.P.J. Shipsey[122], S. Shirabe[73], M. Shiyakova[68,aq], J. Shlomi[175], A. Shmeleva[98], D. Shoaleh Saadi[97], M.J. Shochet[33], S. Shojaii[91], D.R. Shope[115], S. Shrestha[113],

E. Shulga[100], P. Sicho[129], A.M. Sickles[169], P.E. Sidebo[149], E. Sideras Haddad[147c], O. Sidiropoulou[178], A. Sidoti[22a,22b], F. Siegert[47], Dj. Sijacki[14], J. Silva[128a,128d], M. Silva Jr.[176], S.B. Silverstein[148a], L. Simic[68], S. Simion[119], E. Simioni[86], B. Simmons[81], M. Simon[86], P. Sinervo[161], N.B. Sinev[118], M. Sioli[22a,22b], G. Siragusa[178], I. Siral[92], S.Yu. Sivoklokov[101], J. Sjölin[148a,148b], M.B. Skinner[75], P. Skubic[115], M. Slater[19], T. Slavicek[130], M. Slawinska[42], K. Sliwa[165], R. Slovak[131], V. Smakhtin[175], B.H. Smart[5], J. Smiesko[146a], N. Smirnov[100], S.Yu. Smirnov[100], Y. Smirnov[100], L.N. Smirnova[101,ar], O. Smirnova[84], J.W. Smith[58], M.N.K. Smith[38], R.W. Smith[38], M. Smizanska[75], K. Smolek[130], A.A. Snesarev[98], I.M. Snyder[118], S. Snyder[27], R. Sobie[172,m], F. Socher[47], A.M. Soffa[166], A. Soffer[155], A. Søgaard[49], D.A. Soh[153], G. Sokhrannyi[78], C.A. Solans Sanchez[32], M. Solar[130], E.Yu. Soldatov[100], U. Soldevila[170], A.A. Solodkov[132], A. Soloshenko[68], O.V. Solovyanov[132], V. Solovyev[125], P. Sommer[141], H. Son[165], W. Song[133], A. Sopczak[130], F. Sopkova[146b], D. Sosa[60b], C.L. Sotiropoulou[126a,126b], S. Sottocornola[123a,123b], R. Soualah[167a,167c], A.M. Soukharev[111,c], D. South[45], B.C. Sowden[80], S. Spagnolo[76a,76b], M. Spalla[103], M. Spangenberg[173], F. Spanò[80], D. Sperlich[17], F. Spettel[103], T.M. Spieker[60a], R. Spighi[22a], G. Spigo[32], L.A. Spiller[91], M. Spousta[131], R.D. St. Denis[56,*], A. Stabile[94a,94b], R. Stamen[60a], S. Stamm[17], E. Stanecka[42], R.W. Stanek[6], C. Stanescu[136a], M.M. Stanitzki[45], B.S. Stapf[109], S. Stapnes[121], E.A. Starchenko[132], G.H. Stark[33], J. Stark[57], S.H Stark[39], P. Staroba[129], P. Starovoitov[60a], S. Stärz[32], R. Staszewski[42], M. Stegler[45], P. Steinberg[27], B. Stelzer[144], H.J. Stelzer[32], O. Stelzer-Chilton[163a], H. Stenzel[55], T.J. Stevenson[79], G.A. Stewart[32], M.C. Stockton[118], G. Stoicea[28b], P. Stolte[58], S. Stonjek[103], A. Straessner[47], M.E. Stramaglia[18], J. Strandberg[149], S. Strandberg[148a,148b], M. Strauss[115], P. Strizenec[146b], R. Ströhmer[178], D.M. Strom[118], R. Stroynowski[43], A. Strubig[49], S.A. Stucci[27], B. Stugu[15], N.A. Styles[45], D. Su[145], J. Su[127], S. Suchek[60a], Y. Sugaya[120], M. Suk[130], V.V. Sulin[98], D.M.S. Sultan[52], S. Sultansoy[4c], T. Sumida[71], S. Sun[92], X. Sun[3], K. Suruliz[151], C.J.E. Suster[152], M.R. Sutton[151], S. Suzuki[69], M. Svatos[129], M. Swiatlowski[33], S.P. Swift[2], A. Sydorenko[86], I. Sykora[146a], T. Sykora[131], D. Ta[86], K. Tackmann[45], J. Taenzer[155], A. Taffard[166], R. Tafirout[163a], E. Tahirovic[79], N. Taiblum[155], H. Takai[27], R. Takashima[72], E.H. Takasugi[103], K. Takeda[70], T. Takeshita[142], Y. Takubo[69], M. Talby[88], A.A. Talyshev[111,c], J. Tanaka[157], M. Tanaka[159], R. Tanaka[119], R. Tanioka[70], B.B. Tannenwald[113], S. Tapia Araya[34b], S. Tapprogge[86], A. Tarek Abouelfadl Mohamed[83], S. Tarem[154], G. Tarna[28b,p], G.F. Tartarelli[94a], P. Tas[131], M. Tasevsky[129], T. Tashiro[71], E. Tassi[40a,40b], A. Tavares Delgado[128a,128b], Y. Tayalati[137e], A.C. Taylor[107], A.J. Taylor[49], G.N. Taylor[91], P.T.E. Taylor[91], W. Taylor[163b], P. Teixeira-Dias[80], D. Temple[144], H. Ten Kate[32], P.K. Teng[153], J.J. Teoh[120], F. Tepel[177], S. Terada[69], K. Terashi[157], J. Terron[85], S. Terzo[13], M. Testa[50], R.J. Teuscher[161,m], S.J. Thais[179], T. Theveneaux-Pelzer[45], F. Thiele[39], J.P. Thomas[19], P.D. Thompson[19], A.S. Thompson[56], L.A. Thomsen[179], E. Thomson[124], Y. Tian[38], R.E. Ticse Torres[58], V.O. Tikhomirov[98,as], Yu.A. Tikhonov[111,c], S. Timoshenko[100], P. Tipton[179], S. Tisserant[88], K. Todome[159], S. Todorova-Nova[5], S. Todt[47], J. Tojo[73], S. Tokár[146a], K. Tokushuku[69], E. Tolley[113], M. Tomoto[105], L. Tompkins[145,at], K. Toms[107], B. Tong[59], P. Tornambe[51], E. Torrence[118], H. Torres[47], E. Torró Pastor[140], C. Tosciri[122], J. Toth[88,au], F. Touchard[88], D.R. Tovey[141], C.J. Treado[112], T. Trefzger[178], F. Tresoldi[151], A. Tricoli[27], I.M. Trigger[163a], S. Trincaz-Duvoid[83], M.F. Tripiana[13], W. Trischuk[161], B. Trocmé[57], A. Trofymov[45], C. Troncon[94a], M. Trovatelli[172], L. Truong[147b], M. Trzebinski[42], A. Trzupek[42], F. Tsai[45], K.W. Tsang[62a], J.C-L. Tseng[122], P.V. Tsiareshka[95], N. Tsirintanis[9], S. Tsiskaridze[13], V. Tsiskaridze[150], E.G. Tskhadadze[54a], I.I. Tsukerman[99], V. Tsulaia[16], S. Tsuno[69], D. Tsybychev[150], Y. Tu[62b], A. Tudorache[28b], V. Tudorache[28b], T.T. Tulbure[28a], A.N. Tuna[59], S. Turchikhin[68], D. Turgeman[175], I. Turk Cakir[4b,av], R. Turra[94a], P.M. Tuts[38], G. Ucchielli[22a,22b], I. Ueda[69], M. Ughetto[148a,148b], F. Ukegawa[164], G. Unal[32], A. Undrus[27], G. Unel[166], F.C. Ungaro[91], Y. Unno[69], K. Uno[157], J. Urban[146b], P. Urquijo[91], P. Urrejola[86], G. Usai[8], J. Usui[69], L. Vacavant[88], V. Vacek[130], B. Vachon[90], K.O.H. Vadla[121], A. Vaidya[81], C. Valderanis[102], E. Valdes Santurio[148a,148b], M. Valente[52], S. Valentinetti[22a,22b], A. Valero[170], L. Valéry[45], R.A. Vallance[19], A. Vallier[5],

J.A. Valls Ferrer[170], T.R. Van Daalen[13], W. Van Den Wollenberg[109], H. van der Graaf[109], P. van Gemmeren[6], J. Van Nieuwkoop[144], I. van Vulpen[109], M.C. van Woerden[109], M. Vanadia[135a,135b], W. Vandelli[32], A. Vaniachine[160], P. Vankov[109], R. Vari[134a], E.W. Varnes[7], C. Varni[53a,53b], T. Varol[43], D. Varouchas[119], A. Vartapetian[8], K.E. Varvell[152], J.G. Vasquez[179], G.A. Vasquez[34b], F. Vazeille[37], D. Vazquez Furelos[13], T. Vazquez Schroeder[90], J. Veatch[58], L.M. Veloce[161], F. Veloso[128a,128c], S. Veneziano[134a], A. Ventura[76a,76b], M. Venturi[172], N. Venturi[32], V. Vercesi[123a], M. Verducci[136a,136b], W. Verkerke[109], A.T. Vermeulen[109], J.C. Vermeulen[109], M.C. Vetterli[144,d], N. Viaux Maira[34b], O. Viazlo[84], I. Vichou[169,*], T. Vickey[141], O.E. Vickey Boeriu[141], G.H.A. Viehhauser[122], S. Viel[16], L. Vigani[122], M. Villa[22a,22b], M. Villaplana Perez[94a,94b], E. Vilucchi[50], M.G. Vincter[31], V.B. Vinogradov[68], A. Vishwakarma[45], C. Vittori[22a,22b], I. Vivarelli[151], S. Vlachos[10], M. Vogel[177], P. Vokac[130], G. Volpi[13], S.E. von Buddenbrock[147c], E. von Toerne[23], V. Vorobel[131], K. Vorobev[100], M. Vos[170], J.H. Vossebeld[77], N. Vranjes[14], M. Vranjes Milosavljevic[14], V. Vrba[130], M. Vreeswijk[109], R. Vuillermet[32], I. Vukotic[33], P. Wagner[23], W. Wagner[177], J. Wagner-Kuhr[102], H. Wahlberg[74], S. Wahrmund[47], K. Wakamiya[70], J. Walder[75], R. Walker[102], W. Walkowiak[143], V. Wallangen[148a,148b], A.M. Wang[59], C. Wang[36b,p], F. Wang[176], H. Wang[16], H. Wang[3], J. Wang[60b], J. Wang[152], Q. Wang[115], R.-J. Wang[83], R. Wang[36a], R. Wang[6], S.M. Wang[153], T. Wang[38], W. Wang[153,aw], W. Wang[36a,ax], Z. Wang[36c], C. Wanotayaroj[45], A. Warburton[90], C.P. Ward[30], D.R. Wardrope[81], A. Washbrook[49], P.M. Watkins[19], A.T. Watson[19], M.F. Watson[19], G. Watts[140], S. Watts[87], B.M. Waugh[81], A.F. Webb[11], S. Webb[86], M.S. Weber[18], S.M. Weber[60a], S.A. Weber[31], J.S. Webster[6], A.R. Weidberg[122], B. Weinert[64], J. Weingarten[58], M. Weirich[86], C. Weiser[51], P.S. Wells[32], T. Wenaus[27], T. Wengler[32], S. Wenig[32], N. Wermes[23], M.D. Werner[67], P. Werner[32], M. Wessels[60a], T.D. Weston[18], K. Whalen[118], N.L. Whallon[140], A.M. Wharton[75], A.S. White[92], A. White[8], M.J. White[1], R. White[34b], D. Whiteson[166], B.W. Whitmore[75], F.J. Wickens[133], W. Wiedenmann[176], M. Wielers[133], C. Wiglesworth[39], L.A.M. Wiik-Fuchs[51], A. Wildauer[103], F. Wilk[87], H.G. Wilkens[32], H.H. Williams[124], S. Williams[30], C. Willis[93], S. Willocq[89], J.A. Wilson[19], I. Wingerter-Seez[5], E. Winkels[151], F. Winklmeier[118], O.J. Winston[151], B.T. Winter[23], M. Wittgen[145], M. Wobisch[82,u], A. Wolf[86], T.M.H. Wolf[109], R. Wolff[88], M.W. Wolter[42], H. Wolters[128a,128c], V.W.S. Wong[171], N.L. Woods[139], S.D. Worm[19], B.K. Wosiek[42], K.W. Woźniak[42], K. Wraight[56], M. Wu[33], S.L. Wu[176], X. Wu[52], Y. Wu[36a], T.R. Wyatt[87], B.M. Wynne[49], S. Xella[39], Z. Xi[92], L. Xia[35c], D. Xu[35a], H. Xu[36a], L. Xu[27], T. Xu[138], W. Xu[92], B. Yabsley[152], S. Yacoob[147a], K. Yajima[120], D.P. Yallup[81], D. Yamaguchi[159], Y. Yamaguchi[159], A. Yamamoto[69], T. Yamanaka[157], F. Yamane[70], M. Yamatani[157], T. Yamazaki[157], Y. Yamazaki[70], Z. Yan[24], H. Yang[36c,36d], H. Yang[16], S. Yang[66], Y. Yang[153], Y. Yang[157], Z. Yang[15], W-M. Yao[16], Y.C. Yap[45], Y. Yasu[69], E. Yatsenko[5], K.H. Yau Wong[23], J. Ye[43], S. Ye[27], I. Yeletskikh[68], E. Yigitbasi[24], E. Yildirim[86], K. Yorita[174], K. Yoshihara[124], C. Young[145], C.J.S. Young[32], J. Yu[8], J. Yu[67], X. Yue[60a], S.P.Y. Yuen[23], I. Yusuff[30,ay], B. Zabinski[42], G. Zacharis[10], R. Zaidan[13], A.M. Zaitsev[132,al], N. Zakharchuk[45], J. Zalieckas[15], S. Zambito[59], D. Zanzi[32], C. Zeitnitz[177], G. Zemaityte[122], J.C. Zeng[169], Q. Zeng[145], O. Zenin[132], T. Ženiš[146a], D. Zerwas[119], M. Zgubič[122], D. Zhang[36b], D. Zhang[92], F. Zhang[176], G. Zhang[36a,ax], H. Zhang[35b], J. Zhang[6], L. Zhang[51], L. Zhang[36a], M. Zhang[169], P. Zhang[35b], R. Zhang[23], R. Zhang[36a,p], X. Zhang[36b], Y. Zhang[35a,35d], Z. Zhang[119], X. Zhao[43], Y. Zhao[36b,x], Z. Zhao[36a], A. Zhemchugov[68], B. Zhou[92], C. Zhou[176], L. Zhou[43], M. Zhou[35a,35d], M. Zhou[150], N. Zhou[36c], Y. Zhou[7], C.G. Zhu[36b], H. Zhu[35a], J. Zhu[92], Y. Zhu[36a], X. Zhuang[35a], K. Zhukov[98], V. Zhulanov[111,az], A. Zibell[178], D. Zieminska[64], N.I. Zimine[68], S. Zimmermann[51], Z. Zinonos[103], M. Zinser[86], M. Ziolkowski[143], L. Živković[14], G. Zobernig[176], A. Zoccoli[22a,22b], T.G. Zorbas[141], R. Zou[33], M. zur Nedden[17], L. Zwalinski[32].

[1] Department of Physics, University of Adelaide, Adelaide, Australia

[2] Physics Department, SUNY Albany, Albany NY, United States of America

[3] Department of Physics, University of Alberta, Edmonton AB, Canada
[4] [(a)] Department of Physics, Ankara University, Ankara; [(b)] Istanbul Aydin University, Istanbul; [(c)] Division of Physics, TOBB University of Economics and Technology, Ankara, Turkey
[5] LAPP, Univ. Grenoble Alpes, Univ. Savoie Mont Blanc, CNRS/IN2P3, Annecy, France
[6] High Energy Physics Division, Argonne National Laboratory, Argonne IL, United States of America
[7] Department of Physics, University of Arizona, Tucson AZ, United States of America
[8] Department of Physics, The University of Texas at Arlington, Arlington TX, United States of America
[9] Physics Department, National and Kapodistrian University of Athens, Athens, Greece
[10] Physics Department, National Technical University of Athens, Zografou, Greece
[11] Department of Physics, The University of Texas at Austin, Austin TX, United States of America
[12] Institute of Physics, Azerbaijan Academy of Sciences, Baku, Azerbaijan
[13] Institut de Física d'Altes Energies (IFAE), The Barcelona Institute of Science and Technology, Barcelona, Spain
[14] Institute of Physics, University of Belgrade, Belgrade, Serbia
[15] Department for Physics and Technology, University of Bergen, Bergen, Norway
[16] Physics Division, Lawrence Berkeley National Laboratory and University of California, Berkeley CA, United States of America
[17] Department of Physics, Humboldt University, Berlin, Germany
[18] Albert Einstein Center for Fundamental Physics and Laboratory for High Energy Physics, University of Bern, Bern, Switzerland
[19] School of Physics and Astronomy, University of Birmingham, Birmingham, United Kingdom
[20] [(a)] Department of Physics, Bogazici University, Istanbul; [(b)] Department of Physics Engineering, Gaziantep University, Gaziantep; [(d)] Istanbul Bilgi University, Faculty of Engineering and Natural Sciences, Istanbul; [(e)] Bahcesehir University, Faculty of Engineering and Natural Sciences, Istanbul, Turkey
[21] Centro de Investigaciones, Universidad Antonio Narino, Bogota, Colombia
[22] [(a)] INFN Sezione di Bologna; [(b)] Dipartimento di Fisica e Astronomia, Università di Bologna, Bologna, Italy
[23] Physikalisches Institut, University of Bonn, Bonn, Germany
[24] Department of Physics, Boston University, Boston MA, United States of America
[25] Department of Physics, Brandeis University, Waltham MA, United States of America
[26] [(a)] Universidade Federal do Rio De Janeiro COPPE/EE/IF, Rio de Janeiro; [(b)] Electrical Circuits Department, Federal University of Juiz de Fora (UFJF), Juiz de Fora; [(c)] Federal University of Sao Joao del Rei (UFSJ), Sao Joao del Rei; [(d)] Instituto de Fisica, Universidade de Sao Paulo, Sao Paulo, Brazil
[27] Physics Department, Brookhaven National Laboratory, Upton NY, United States of America
[28] [(a)] Transilvania University of Brasov, Brasov; [(b)] Horia Hulubei National Institute of Physics and Nuclear Engineering; [(c)] Department of Physics, Alexandru Ioan Cuza University of Iasi, Iasi; [(d)] National Institute for Research and Development of Isotopic and Molecular Technologies, Physics Department, Cluj Napoca; [(e)] University Politehnica Bucharest, Bucharest; [(f)] West University in Timisoara, Timisoara, Romania
[29] Departamento de Física, Universidad de Buenos Aires, Buenos Aires, Argentina
[30] Cavendish Laboratory, University of Cambridge, Cambridge, United Kingdom
[31] Department of Physics, Carleton University, Ottawa ON, Canada
[32] CERN, Geneva, Switzerland
[33] Enrico Fermi Institute, University of Chicago, Chicago IL, United States of America
[34] [(a)] Departamento de Física, Pontificia Universidad Católica de Chile, Santiago; [(b)] Departamento de Física, Universidad Técnica Federico Santa María, Valparaíso, Chile

[35] [(a)] Institute of High Energy Physics, Chinese Academy of Sciences, Beijing; [(b)] Department of Physics, Nanjing University, Jiangsu; [(c)] Physics Department, Tsinghua University, Beijing; [(d)] University of Chinese Academy of Science (UCAS), Beijing, China
[36] [(a)] Department of Modern Physics and State Key Laboratory of Particle Detection and Electronics, University of Science and Technology of China, Anhui; [(b)] School of Physics, Shandong University, Shandong; [(c)] School of Physics and Astronomy, Key Laboratory for Particle Physics, Astrophysics and Cosmology, Ministry of Education; Shanghai Key Laboratory for Particle Physics and Cosmology, Shanghai Jiao Tong University; [(d)] Tsung-Dao Lee Institute, Shanghai, China
[37] Université Clermont Auvergne, CNRS/IN2P3, LPC, Clermont-Ferrand, France
[38] Nevis Laboratory, Columbia University, Irvington NY, United States of America
[39] Niels Bohr Institute, University of Copenhagen, Kobenhavn, Denmark
[40] [(a)] INFN Gruppo Collegato di Cosenza, Laboratori Nazionali di Frascati; [(b)] Dipartimento di Fisica, Università della Calabria, Rende, Italy
[41] [(a)] AGH University of Science and Technology, Faculty of Physics and Applied Computer Science, Krakow; [(b)] Marian Smoluchowski Institute of Physics, Jagiellonian University, Krakow, Poland
[42] Institute of Nuclear Physics Polish Academy of Sciences, Krakow, Poland
[43] Physics Department, Southern Methodist University, Dallas TX, United States of America
[44] Physics Department, University of Texas at Dallas, Richardson TX, United States of America
[45] DESY, Hamburg and Zeuthen, Germany
[46] Lehrstuhl für Experimentelle Physik IV, Technische Universität Dortmund, Dortmund, Germany
[47] Institut für Kern- und Teilchenphysik, Technische Universität Dresden, Dresden, Germany
[48] Department of Physics, Duke University, Durham NC, United States of America
[49] SUPA - School of Physics and Astronomy, University of Edinburgh, Edinburgh, United Kingdom
[50] INFN e Laboratori Nazionali di Frascati, Frascati, Italy
[51] Fakultät für Mathematik und Physik, Albert-Ludwigs-Universität, Freiburg, Germany
[52] Departement de Physique Nucleaire et Corpusculaire, Université de Genève, Geneva, Switzerland
[53] [(a)] INFN Sezione di Genova; [(b)] Dipartimento di Fisica, Università di Genova, Genova, Italy
[54] [(a)] E. Andronikashvili Institute of Physics, Iv. Javakhishvili Tbilisi State University, Tbilisi; [(b)] High Energy Physics Institute, Tbilisi State University, Tbilisi, Georgia
[55] II. Physikalisches Institut, Justus-Liebig-Universit Germany
[56] SUPA - School of Physics and Astronomy, University of Glasgow, Glasgow, United Kingdom
[57] LPSC, Université Grenoble Alpes, CNRS-IN2P3, Grenoble INP, Grenoble, France
[58] II Physikalisches Institut, Georg-August-Universität, Göttingen, Germany
[59] Laboratory for Particle Physics and Cosmology, Harvard University, Cambridge MA, United States of America
[60] [(a)] Kirchhoff-Institut für Physik, Ruprecht-Karls-Universität Heidelberg, Heidelberg; [(b)] Physikalisches Institut, Ruprecht-Karls-Universität Heidelberg, Heidelberg, Germany
[61] Faculty of Applied Information Science, Hiroshima Institute of Technology, Hiroshima, Japan
[62] [(a)] Department of Physics, The Chinese University of Hong Kong, Shatin, N.T., Hong Kong; [(b)] Department of Physics, The University of Hong Kong, Hong Kong; [(c)] Department of Physics and Institute for Advanced Study, The Hong Kong University of Science and Technology, Clear Water Bay, Kowloon, Hong Kong, China
[63] Department of Physics, National Tsing Hua University, Hsinchu, Taiwan
[64] Department of Physics, Indiana University, Bloomington IN, United States of America
[65] Institut für Astro- und Teilchenphysik, Leopold-Franzens-Universität, Innsbruck, Austria
[66] University of Iowa, Iowa City IA, United States of America
[67] Department of Physics and Astronomy, Iowa State University, Ames IA, United States of America

[68] Joint Institute for Nuclear Research, JINR Dubna, Dubna, Russia
[69] KEK, High Energy Accelerator Research Organization, Tsukuba, Japan
[70] Graduate School of Science, Kobe University, Kobe, Japan
[71] Faculty of Science, Kyoto University, Kyoto, Japan
[72] Kyoto University of Education, Kyoto, Japan
[73] Research Center for Advanced Particle Physics and Department of Physics, Kyushu University, Fukuoka, Japan
[74] Instituto de Física La Plata, Universidad Nacional de La Plata and CONICET, La Plata, Argentina
[75] Physics Department, Lancaster University, Lancaster, United Kingdom
[76] [(a)] INFN Sezione di Lecce; [(b)] Dipartimento di Matematica e Fisica, Università del Salento, Lecce, Italy
[77] Oliver Lodge Laboratory, University of Liverpool, Liverpool, United Kingdom
[78] Department of Experimental Particle Physics, Jožef Stefan Institute and Department of Physics, University of Ljubljana, Ljubljana, Slovenia
[79] School of Physics and Astronomy, Queen Mary University of London, London, United Kingdom
[80] Department of Physics, Royal Holloway University of London, Surrey, United Kingdom
[81] Department of Physics and Astronomy, University College London, London, United Kingdom
[82] Louisiana Tech University, Ruston LA, United States of America
[83] Laboratoire de Physique Nucléaire et de Hautes Energies, UPMC and Université Paris-Diderot and CNRS/IN2P3, Paris, France
[84] Fysiska institutionen, Lunds universitet, Lund, Sweden
[85] Departamento de Fisica Teorica C-15 and CIAFF, Universidad Autonoma de Madrid, Madrid, Spain
[86] Institut für Physik, Universität Mainz, Mainz, Germany
[87] School of Physics and Astronomy, University of Manchester, Manchester, United Kingdom
[88] CPPM, Aix-Marseille Université and CNRS/IN2P3, Marseille, France
[89] Department of Physics, University of Massachusetts, Amherst MA, United States of America
[90] Department of Physics, McGill University, Montreal QC, Canada
[91] School of Physics, University of Melbourne, Victoria, Australia
[92] Department of Physics, The University of Michigan, Ann Arbor MI, United States of America
[93] Department of Physics and Astronomy, Michigan State University, East Lansing MI, United States of America
[94] [(a)] INFN Sezione di Milano; [(b)] Dipartimento di Fisica, Università di Milano, Milano, Italy
[95] B.I. Stepanov Institute of Physics, National Academy of Sciences of Belarus, Minsk, Republic of Belarus
[96] Research Institute for Nuclear Problems of Byelorussian State University, Minsk, Republic of Belarus
[97] Group of Particle Physics, University of Montreal, Montreal QC, Canada
[98] P.N. Lebedev Physical Institute of the Russian Academy of Sciences, Moscow, Russia
[99] Institute for Theoretical and Experimental Physics (ITEP), Moscow, Russia
[100] National Research Nuclear University MEPhI, Moscow, Russia
[101] D.V. Skobeltsyn Institute of Nuclear Physics, M.V. Lomonosov Moscow State University, Moscow, Russia
[102] Fakultät für Physik, Ludwig-Maximilians-Universität München, München, Germany
[103] Max-Planck-Institut für Physik (Werner-Heisenberg-Institut), München, Germany
[104] Nagasaki Institute of Applied Science, Nagasaki, Japan
[105] Graduate School of Science and Kobayashi-Maskawa Institute, Nagoya University, Nagoya, Japan
[106] [(a)] INFN Sezione di Napoli; [(b)] Dipartimento di Fisica, Università di Napoli, Napoli, Italy
[107] Department of Physics and Astronomy, University of New Mexico, Albuquerque NM, United States

of America
[108] Institute for Mathematics, Astrophysics and Particle Physics, Radboud University Nijmegen/Nikhef, Nijmegen, Netherlands
[109] Nikhef National Institute for Subatomic Physics and University of Amsterdam, Amsterdam, Netherlands
[110] Department of Physics, Northern Illinois University, DeKalb IL, United States of America
[111] Budker Institute of Nuclear Physics, SB RAS, Novosibirsk, Russia
[112] Department of Physics, New York University, New York NY, United States of America
[113] Ohio State University, Columbus OH, United States of America
[114] Faculty of Science, Okayama University, Okayama, Japan
[115] Homer L. Dodge Department of Physics and Astronomy, University of Oklahoma, Norman OK, United States of America
[116] Department of Physics, Oklahoma State University, Stillwater OK, United States of America
[117] Palacký University, RCPTM, Olomouc, Czech Republic
[118] Center for High Energy Physics, University of Oregon, Eugene OR, United States of America
[119] LAL, Univ. Paris-Sud, CNRS/IN2P3, Université Paris-Saclay, Orsay, France
[120] Graduate School of Science, Osaka University, Osaka, Japan
[121] Department of Physics, University of Oslo, Oslo, Norway
[122] Department of Physics, Oxford University, Oxford, United Kingdom
[123] [(a)] INFN Sezione di Pavia; [(b)] Dipartimento di Fisica, Università di Pavia, Pavia, Italy
[124] Department of Physics, University of Pennsylvania, Philadelphia PA, United States of America
[125] National Research Centre "Kurchatov Institute" B.P.Konstantinov Petersburg Nuclear Physics Institute, St. Petersburg, Russia
[126] [(a)] INFN Sezione di Pisa; [(b)] Dipartimento di Fisica E. Fermi, Università di Pisa, Pisa, Italy
[127] Department of Physics and Astronomy, University of Pittsburgh, Pittsburgh PA, United States of America
[128] [(a)] Laboratório de Instrumentação e Física Experimental de Partículas - LIP, Lisboa; [(b)] Faculdade de Ciências, Universidade de Lisboa, Lisboa; [(c)] Department of Physics, University of Coimbra, Coimbra; [(d)] Centro de Física Nuclear da Universidade de Lisboa, Lisboa; [(e)] Departamento de Fisica, Universidade do Minho, Braga, Portugal; [(f)] Departamento de Fisica Teorica y del Cosmos, Universidad de Granada, Granada (Spain), Spain; [(g)] Dep Fisica and CEFITEC of Faculdade de Ciencias e Tecnologia, Universidade Nova de Lisboa, Caparica, Portugal
[129] Institute of Physics, Academy of Sciences of the Czech Republic, Praha, Czech Republic
[130] Czech Technical University in Prague, Praha, Czech Republic
[131] Charles University, Faculty of Mathematics and Physics, Prague, Czech Republic
[132] State Research Center Institute for High Energy Physics (Protvino), NRC KI, Russia
[133] Particle Physics Department, Rutherford Appleton Laboratory, Didcot, United Kingdom
[134] [(a)] INFN Sezione di Roma; [(b)] Dipartimento di Fisica, Sapienza Università di Roma, Roma, Italy
[135] [(a)] INFN Sezione di Roma Tor Vergata; [(b)] Dipartimento di Fisica, Università di Roma Tor Vergata, Roma, Italy
[136] [(a)] INFN Sezione di Roma Tre; [(b)] Dipartimento di Matematica e Fisica, Università Roma Tre, Roma, Italy
[137] [(a)] Faculté des Sciences Ain Chock, Réseau Universitaire de Physique des Hautes Energies - Université Hassan II, Casablanca; [(b)] Centre National de l'Energie des Sciences Techniques Nucleaires, Rabat; [(c)] Faculté des Sciences Semlalia, Université Cadi Ayyad, LPHEA-Marrakech; [(d)] Faculté des Sciences, Université Mohamed Premier and LPTPM, Oujda; [(e)] Faculté des sciences, Université Mohammed V, Rabat, Morocco

[138] Institut de Recherches sur les Lois Fondamentales de l'Univers, DSM/IRFU, CEA Saclay, Gif-sur-Yvette, France
[139] Santa Cruz Institute for Particle Physics, University of California Santa Cruz, Santa Cruz CA, United States of America
[140] Department of Physics, University of Washington, Seattle WA, United States of America
[141] Department of Physics and Astronomy, University of Sheffield, Sheffield, United Kingdom
[142] Department of Physics, Shinshu University, Nagano, Japan
[143] Department Physik, Universität Siegen, Siegen, Germany
[144] Department of Physics, Simon Fraser University, Burnaby BC, Canada
[145] SLAC National Accelerator Laboratory, Stanford CA, United States of America
[146] [(a)] Faculty of Mathematics, Physics and Informatics, Comenius University, Bratislava; [(b)] Department of Subnuclear Physics, Institute of Experimental Physics of the Slovak Academy of Sciences, Kosice, Slovak Republic
[147] [(a)] Department of Physics, University of Cape Town, Cape Town; [(b)] Department of Mechanical Engineering Science, University of Johannesburg, Johannesburg; [(c)] School of Physics, University of the Witwatersrand, Johannesburg, South Africa
[148] [(a)] Department of Physics, Stockholm University; [(b)] The Oskar Klein Centre, Stockholm, Sweden
[149] Physics Department, Royal Institute of Technology, Stockholm, Sweden
[150] Departments of Physics and Astronomy, Stony Brook University, Stony Brook NY, United States of America
[151] Department of Physics and Astronomy, University of Sussex, Brighton, United Kingdom
[152] School of Physics, University of Sydney, Sydney, Australia
[153] Institute of Physics, Academia Sinica, Taipei, Taiwan
[154] Department of Physics, Technion: Israel Institute of Technology, Haifa, Israel
[155] Raymond and Beverly Sackler School of Physics and Astronomy, Tel Aviv University, Tel Aviv, Israel
[156] Department of Physics, Aristotle University of Thessaloniki, Thessaloniki, Greece
[157] International Center for Elementary Particle Physics and Department of Physics, The University of Tokyo, Tokyo, Japan
[158] Graduate School of Science and Technology, Tokyo Metropolitan University, Tokyo, Japan
[159] Department of Physics, Tokyo Institute of Technology, Tokyo, Japan
[160] Tomsk State University, Tomsk, Russia
[161] Department of Physics, University of Toronto, Toronto ON, Canada
[162] [(a)] INFN-TIFPA; [(b)] University of Trento, Trento, Italy
[163] [(a)] TRIUMF, Vancouver BC; [(b)] Department of Physics and Astronomy, York University, Toronto ON, Canada
[164] Division of Physics and Tomonaga Center for the History of the Universe, Faculty of Pure and Applied Sciences, University of Tsukuba, Tsukuba, Japan
[165] Department of Physics and Astronomy, Tufts University, Medford MA, United States of America
[166] Department of Physics and Astronomy, University of California Irvine, Irvine CA, United States of America
[167] [(a)] INFN Gruppo Collegato di Udine, Sezione di Trieste, Udine; [(b)] ICTP, Trieste; [(c)] Dipartimento di Chimica, Fisica e Ambiente, Università di Udine, Udine, Italy
[168] Department of Physics and Astronomy, University of Uppsala, Uppsala, Sweden
[169] Department of Physics, University of Illinois, Urbana IL, United States of America
[170] Instituto de Fisica Corpuscular (IFIC), Centro Mixto Universidad de Valencia - CSIC, Spain
[171] Department of Physics, University of British Columbia, Vancouver BC, Canada
[172] Department of Physics and Astronomy, University of Victoria, Victoria BC, Canada

[173] Department of Physics, University of Warwick, Coventry, United Kingdom
[174] Waseda University, Tokyo, Japan
[175] Department of Particle Physics, The Weizmann Institute of Science, Rehovot, Israel
[176] Department of Physics, University of Wisconsin, Madison WI, United States of America
[177] Fakultät für Mathematik und Naturwissenschaften, Fachgruppe Physik, Bergische Universität Wuppertal, Wuppertal, Germany
[178] Fakultät für Physik und Astronomie, Julius-Maximilians-Universität, Würzburg, Germany
[179] Department of Physics, Yale University, New Haven CT, United States of America
[180] Yerevan Physics Institute, Yerevan, Armenia
[181] Centre de Calcul de l'Institut National de Physique Nucléaire et de Physique des Particules (IN2P3), Villeurbanne, France
[182] Academia Sinica Grid Computing, Institute of Physics, Academia Sinica, Taipei, Taiwan
[a] Also at Department of Physics, King's College London, London, United Kingdom
[b] Also at Institute of Physics, Azerbaijan Academy of Sciences, Baku, Azerbaijan
[c] Also at Novosibirsk State University, Novosibirsk, Russia
[d] Also at TRIUMF, Vancouver BC, Canada
[e] Also at Department of Physics and Astronomy, University of Louisville, Louisville, KY, United States of America
[f] Also at Department of Physics, California State University, Fresno CA, United States of America
[g] Also at Department of Physics, University of Fribourg, Fribourg, Switzerland
[h] Also at II Physikalisches Institut, Georg-August-Universität, Göttingen, Germany
[i] Also at Departament de Fisica de la Universitat Autonoma de Barcelona, Barcelona, Spain
[j] Also at Tomsk State University, Tomsk, and Moscow Institute of Physics and Technology State University, Dolgoprudny, Russia
[k] Also at The Collaborative Innovation Center of Quantum Matter (CICQM), Beijing, China
[l] Also at Universita di Napoli Parthenope, Napoli, Italy
[m] Also at Institute of Particle Physics (IPP), Canada
[n] Also at Dipartimento di Fisica E. Fermi, Università di Pisa, Pisa, Italy
[o] Also at Horia Hulubei National Institute of Physics and Nuclear Engineering, Romania
[p] Also at CPPM, Aix-Marseille Université and CNRS/IN2P3, Marseille, France
[q] Also at Department of Physics, St. Petersburg State Polytechnical University, St. Petersburg, Russia
[r] Also at Borough of Manhattan Community College, City University of New York, New York City, United States of America
[s] Also at Department of Financial and Management Engineering, University of the Aegean, Chios, Greece
[t] Also at Centre for High Performance Computing, CSIR Campus, Rosebank, Cape Town, South Africa
[u] Also at Louisiana Tech University, Ruston LA, United States of America
[v] Also at Institucio Catalana de Recerca i Estudis Avancats, ICREA, Barcelona, Spain
[w] Also at Department of Physics, The University of Michigan, Ann Arbor MI, United States of America
[x] Also at LAL, Univ. Paris-Sud, CNRS/IN2P3, Université Paris-Saclay, Orsay, France
[y] Also at Graduate School of Science, Osaka University, Osaka, Japan
[z] Also at Fakultät für Mathematik und Physik, Albert-Ludwigs-Universität, Freiburg, Germany
[aa] Also at Institute for Mathematics, Astrophysics and Particle Physics, Radboud University Nijmegen/Nikhef, Nijmegen, Netherlands
[ab] Also at Near East University, Nicosia, North Cyprus, Mersin 10, Turkey
[ac] Also at Institute of Theoretical Physics, Ilia State University, Tbilisi, Georgia
[ad] Also at CERN, Geneva, Switzerland

[ae] Also at Georgian Technical University (GTU),Tbilisi, Georgia
[af] Also at Ochadai Academic Production, Ochanomizu University, Tokyo, Japan
[ag] Also at Manhattan College, New York NY, United States of America
[ah] Also at Hellenic Open University, Patras, Greece
[ai] Also at The City College of New York, New York NY, United States of America
[aj] Also at Departamento de Fisica Teorica y del Cosmos, Universidad de Granada, Granada (Spain), Spain
[ak] Also at Department of Physics, California State University, Sacramento CA, United States of America
[al] Also at Moscow Institute of Physics and Technology State University, Dolgoprudny, Russia
[am] Also at Departement de Physique Nucleaire et Corpusculaire, Université de Genève, Geneva, Switzerland
[an] Also at Department of Physics, The University of Texas at Austin, Austin TX, United States of America
[ao] Also at Institut de Física d'Altes Energies (IFAE), The Barcelona Institute of Science and Technology, Barcelona, Spain
[ap] Also at School of Physics, Sun Yat-sen University, Guangzhou, China
[aq] Also at Institute for Nuclear Research and Nuclear Energy (INRNE) of the Bulgarian Academy of Sciences, Sofia, Bulgaria
[ar] Also at Faculty of Physics, M.V.Lomonosov Moscow State University, Moscow, Russia
[as] Also at National Research Nuclear University MEPhI, Moscow, Russia
[at] Also at Department of Physics, Stanford University, Stanford CA, United States of America
[au] Also at Institute for Particle and Nuclear Physics, Wigner Research Centre for Physics, Budapest, Hungary
[av] Also at Giresun University, Faculty of Engineering, Turkey
[aw] Also at Department of Physics, Nanjing University, Jiangsu, China
[ax] Also at Institute of Physics, Academia Sinica, Taipei, Taiwan
[ay] Also at University of Malaya, Department of Physics, Kuala Lumpur, Malaysia
[az] Also at Budker Institute of Nuclear Physics, SB RAS, Novosibirsk, Russia
[*] Deceased